Aus der

Universitätsklinik für Allgemeine, Viszeral- und

Transplantationschirurgie Tübingen

Acidic ascites inhibits gastric and ovarian cancer cell proliferation and correlate with the metabolomic, lipidomic, and inflammatory phenotype of human patients

Inaugural-Dissertation
zur Erlangung des Doktorgrades
der Medizin

der Medizinischen Fakultät
der Eberhard-Karls-Universität
zu Tübingen

vorgelegt von

Yang, Qianlu

2024

Dekan: Professor Dr. rer. nat. Bernd Pichler

1. Berichterstatter: Professor Dr. med. A. Königsrainer

2. Berichterstatter: Professor Dr. U. Lauer

Tag der Disputation: 02.09.2024

Contents

List of Tables

List of Figures

Abbreviations

ATP	adenosine triphosphate
ASCT2	alanine-serine-cysteine transporter 2
ACS	acetyl-CoA synthetases
BSA	bovine serum albumin
BCCAs	branched-chain amino acids
CAFs	cancer-associated fibroblasts
CAs	carbonic anhydrases
CA2	carbonic anhydrase 2
CA9	carbonic anhydrase 9
CA12	carbonic anhydrase 12
CXCL8	C-X-C motif chemokine ligand 8
CPMG	Carr-Purcell-Meiboom-Gill pulse programs
CPT1	carnitine palmitoyl transferase 1
CKB	creatine kinase B
CDK1	cyclin-dependent kinase 1
DR5	death receptor 5
DNA	deoxyribonucleic acid
EMT	epithelial-to-mesenchymal transition
ECE	electronic current exclusion
ECM	extracellular matrix
FGF	fibroblast growth factors
FIGO	Fédération Internationale de Gynécologie et d'Obstétrique
FC	fold change
FABP4	fatty acid-binding protein 4
GC	gastric cancer
GLUT	glucose transporter
GEO	Gene Expression Omnibus
GSEA	Gene set enrichment analysis
GO	gene ontology
GPLC	high-performance liquid chromatography
GPNA	L-g-glutamyl-p-nitroanilide
HGF	hepatocyte growth factor
HSP	hexosamine synthesis pathway
HIF-1α	hypoxia-inducible factor 1α
IL-6	Interleukin 6
IL-8	Interleukin 8
KRAS	Kirsten rat sarcoma virus
LDH	lactate dehydrogenase
MMP-1	matrix metalloproteinase-1
MDSCs	myeloid-derived suppressor cells
MTT	3-(4,5-dimethylthiazol-2-yl)-2,5- diphenyltetrazolium bromide
MTBE	tert-butyl methyl ether
NMR	nuclear magnetic resonance
NADPH	nicotinamide adenine dinucleotide phosphate
NADH	nicotinamide adenine dinucleotide hydrogen
NES	normalized enrichment score
NEAA	non-essential amino acid

NOESY1D	Nuclear Overhauser Spectroscopy
OC	ovarian cancer
OPLS-DA	orthogonal projections to latent structures discriminant analysis
OS	overall survival
PM	peritoneal metastasis
PPP	pentose phosphate pathway
PIK3CA	phosphatidylinositol-4,5-bisphosphate 3-kinase catalytic subunit alpha
pHi	intracellular milieu
pHe	extracellular tumor microenvironment
PQN	probabilistic quotient normalization
PCA	Principle component analysis
PUFA	polyunsaturated fatty acid
PMCs	peritoneal mesothelial cells
QOL	quality of life
ROS	reactive oxygen species
SDF-1	stromal cell-derived factor-1
SEM	scanning electron microscopy
SNR	signal-to-noise ratio
TGF-β	transforming growth factor beta
TAMs	tumor-associated macrophages
TIL	tumor-infiltrating lymphocytes
Tregs	regulatory T cells
TCA	tricarboxylic acid cycle
TRAIL	tumor necrosis factor-related apoptosis-inducing ligand
TSP	3-(trimethylsilyl) propionic-2,2,3,3 acid sodium salt D4 (TSP-D4)
TMS	tetramethylsilane
VAT	visceral adipose tissue
VEGF	vascular endothelial growth factor
αSMA	α-smooth muscle actin

Introduction

Peritoneal metastasis (PM) is the spread of tumor cells from primary cancer onto the peritoneum's visceral and parietal surfaces. Various types of tumors, particularly those originating from the ovary and gastrointestinal tract, display a strong predilection for the peritoneal cavity as the site of metastasis (Mikuła-Pietrasik et al., 2018). For example, 32% of patients with gastric cancer develop peritoneal metastasis during the disease (Riihimäki et al., 2016).

Peritoneal metastasis is usually diagnosed at an advanced stage (Yonemura et al., 2010, Lengyel, 2010). Cancer cells detach from their primary tumor, gain motility, develop resistance to anoikis, adhere to the peritoneum, and invade and proliferate (Sluiter et al., 2016). Despite recent advances in surgery, radiotherapy, chemotherapy, and biological therapy, the five-year survival of patients remains poor (Rau et al., 2020, van Baal et al., 2018). The resting metabolism rises in tandem with the progression of peritoneal metastasis, resulting in the development of cachexia, anorexia, and ultimately, the demise of patients (Archid et al., 2019, Hilal et al., 2017).

With its recognition as a multifunctional organ, the peritoneum is the object of active translational research (Neelakantan et al., 2019). Anatomically, the peritoneal membrane consists of five layers: the first layer is endothelial cells, combined with the intravascular space of capillaries. The endothelial basement membrane separates the endothelial cells from the third layer, interstitial space. They are followed by the sub-mesothelial basement membrane and the final layer of mesothelial cells (Kipps et al., 2013). Functionally, the peritoneum regulates the interactions between the abdominal cavity and the rest of the body, remarkably fluid and protein homeostasis. In physiological conditions, the peritoneum limits the capillary fluid filtration into the peritoneal cavity, with only a few milliliters of free liquid in this cavity. The peritoneum has a potent innate and adaptive immune function and harbors a comprehensive set of immune cells, including macrophages, B, and T cells (Ray and Dittel, 2010b).

Ascites assumes a central role in the pathophysiology of peritoneal metastasis. Cancer cells invade the peritoneum and disturb peritoneal homeostasis when they spread into the abdomen. The tumor secretome (in particular VEGF and inflammatory cytokines) affects the permeability of the microvessels and increases the proteins exudate through the capillary wall. Moreover, angiogenesis induces leaky neovessels lacking a basal membrane. These combined mechanisms give rise to ascites in many peritoneal metastasis patients (Nagy et al., 1993). The most common primary cancer associated with ascites is OC (38%) (Parsons et al., 1996), followed by GC (21%) (Ayantunde and Parsons, 2007).

Ascites plays both passive (transport) and active (energy metabolism, neoangiogenesis, immunotolerance) roles in the progression of peritoneal metastasis. Ascites transports the exfoliated tumor cells within the abdominal cavity and contribute to their dissemination (Ray and Dittel, 2010a). Ascites provides tumor cells with critical nutrients and energy sources, particularly lactate (Ray and Dittel, 2010a). Advites is rich in VEGF and stimulates neoangiogenesis throughout the abdominal cavity (Lawler, 2022). In addition, ascites facilitates tumor immune escape (Tian et al., 2022). Therefore, clarifying the role of ascites in metastasizing tumor cells is particularly important for developing translational approaches in peritoneal metastasis research.

Hundreds of thousands of cancer cells are left in the abdomen after cancer surgery (Steinert et al., 2008). Fortunately, only some of them give rise to peritoneal metastasis. Cancer cells shed into the peritoneal cavity have lost contact with their tumor microenvironment (TME). They are hypoxic (without vascular supply) and have less nutrient access. Thus, most of these cells undergo a particular type of apoptosis, termed “*anoikis*” (a Greek word meaning “homelessness”), and cannot thrive in the adverse peritoneal environment.

To survive, detached tumor cells must adapt and gain a competitive advantage by:

- modifying their surface integrins during oncogenic transformation, enabling

metastatic colonization,

- modulating their energy metabolism, using extramitochondrial aerobic glycolysis (Warburg effect) and autophagy,
- resisting oxidative stress from the increasingly hypoxic intraperitoneal environment,
- preparing the peritoneum for tumor cell invasion by inducing Mesothelial-Mesenchymal Transition (MMT).

MMT is a form of Epithelial-to-mesenchymal transition (EMT) particular to the Peritoneal Mesothelial cells (PMCs). PMCs are mesothelial cells with several epithelial characteristics, including orientation, microvilli, intercellular junctions, etc. MMT. is a cellular process in which cells lose their epithelial characteristics and acquire mesenchymal features. This change is associated with malignant phenotype, including tumor initiation, malignant progression, stem-like, migratory, invasive behavior, and chemoresistance (Nieto et al., 2016, De Craene and Berx, 2013, Brabletz, 2012).

The cascade of metabolic adaptations leading to the adaptation of tumor cells to their new environment includes, in particular (Simpson et al., 2008, Warburg et al., 1927b):

- a switch from mitochondrial phosphorylation to cytoplasmic aerobic glycolysis (Warburg et al., 1927b),
- a decrease in the flux of the pentose phosphate pathway (PPP),
- the use of intermediates of the glycolytic pathway for anabolic reactions,
- an elevation in reactive oxygen species (ROS) generated by mitochondria (Hawk and Schafer, 2018).

To ensures the cell's antioxidant defenses against a hostile microenvironment and chemotherapeutic agents.

Normal cells produce their energy by metabolizing glucose via the mitochondrial tricarboxylic acid (TCA) cycle. The TCA cycle is a highly effective pathway producing 32 to 34 ATP molecules per glucose molecule. However, as described by Otto Warburg (Warburg et al., 1927a), cancer cells prefer aerobic glycolysis to mitochondrial

phosphorylation to satisfy their metabolic needs. Energy production is accelerated (by a factor 18 vs. TCA cycle), providing a rapid energy supply to the cancer cells. However, under anoxia conditions, the yield of glycolysis is severely impaired, with only two ATP per glucose molecule (Cooper et al., 2007). This low yield results in a massive energy need and consumption from the tumor tissue.

- *Metabolic switch in metastatic units*

Oncogenic mutations in growth signaling proteins such as PIK3CA, Akt, and KRas (Hosios et al., 2016, Keibler et al., 2016) result in the activation of glycolytic enzymes in cancer cells (Cox et al., 2018). Many studies on cancer cell metabolism found that glucose is the key source of metabolic carbon in cancer cells (Vander Heiden et al., 2009). The enormous amounts of glucose needed to meet rapid growth demands are sustained by aerobic glycolysis and oxidative phosphorylation in oxygen-rich environments. In hypoxic environments, such as in the tumor core, anaerobic glycolysis overtakes oxidative phosphorylation as the primary source of energy (Hay, 2016). In anaerobic glycolysis, pyruvate is catalyzed to lactate instead of acetyl-CoA (Valvona et al., 2016).

Aerobic glycolysis is a cytoplasmic process. Glucose enters the cell via glucose transporter (GLUT) proteins, mutated c-MYC, KRAS, and YAP upregulate GLUT1 expression and turn off function mutations in p53, increasing GLUT3 expression, which can increase glucose trapped in the cell (Kawauchi et al., 2008). In the glycolytic pathway, glucose is metabolized to pyruvate, supplied carbon intermediates, generating ATP and nicotinamide adenine dinucleotide hydrogen (NADH).

- *The competitive advantage of metastatic units*

Cancer cells detached into the peritoneal cavity gain a competitive advantage and increase their chances of survival by forming conglomerates (spheroids or metastatic units) with normal resident cells and by creating synergies with these cells. Detached cancer cells enlist normal cells from the host to construct their tumor microenvironment. In particular, they recruit the host`s fibroblasts to create cancer-associated fibroblasts

(CAFs). CAFs are defined as cells (Gao et al., 2019a):

- containing a high level of α-smooth muscle actin (αSMA)-positive myofibroblasts,
- with increased angiogenetic activity, as compared to isolated CAFs,
- with increased secretion of SDF-1 (stromal cell-derived factor-1). SDF-1 is a proangiogenic cytokine stimulating tumor growth,
- keeping a stable capacity to promote tumors and exert myo-fibroblastic features even without cancer cells (Orimo and Weinberg, 2006).

CAFs sustain the energy metabolism of cancer cells by providing lactate and amino acids. glucose and glutamine, the two nutrients with the highest consumption rates, are not the major contributors of carbon to cell mass. However, the most significant contributors to cell tumor mass are amino acids, which comprise proteins. Amino acids (excluding glutamine) collectively constitute the highest proportion of carbon atoms in neo-carcinoma cells, representing 20% to 40% of the total mass (Hosios et al., 2016).

Moreover, the CAF`s secretome (cytokine IL-6; chemokines CXCL8/IL-8; growth factors FGF, HGF, TGF-β, VEGF), extracellular matrix proteins; and remodeling enzymes (collagen I, tenascin C periostin, fibronectin, and MMP-1) support tumor progression (Augsten, 2014). Chemokines secreted by CAFs facilitate the infiltration of tumor-associated immune cells into peritoneal metastasis. These cells encompass tumor-associated macrophages (TAMs), tumor-infiltrating lymphocytes (TILs), immunosuppressive regulatory T cells (Tregs), and myeloid-derived suppressor cells (MDSCs) (Liao et al., 2019). This infiltrate associated immune cells results in the development of immunotolerance during the progression of peritoneal metastasis.

- Role of the intracellular and extracellular pH

In normal cells, intracellular pH (pHi) is generally around 7.2 and lower than the extracellular pH (pHe) of approximately 7.4. However, cancer cells have a higher pHi of >7.4 and a lower pHe of 6.7–7.1 (Gillies et al., 2002, Stüwe et al., 2007). Membrane

ion pumps and transporters, particularly acid extruders and carbonic anhydrases (CAs), facilitate H^+ efflux from cancer cells (Lee et al., 2014, Hinton et al., 2009). Various types of proton pumps and intracellular buffer systems regulate the extracellular pH and intracellular pH within the tumor (Silva et al., 2009). The carbonic anhydrase enzymes CA2, CA9, and CA12 play a role in maintaining the balance of the $HCO3^-/CO3^{2-}$ buffer system in tumors, and Na+/H+ exchangers are responsible for regulating the Na+/H+ buffer system (Călinescu et al., 2014). The regulation of extracellular pH and intracellular pH relies on the synergistic effects of these pumps and buffer systems.

The metabolic switch and increased expression and activity of plasma membrane ion pumps and transporters can maintain an alkaline intracellular milieu (pHi) within an acidic extracellular tumor microenvironment (pHe). An alkaline pHi promotes glycolysis, inhibits gluconeogenesis, and may depend on several pH-sensitive glycolytic enzymes, such as lactate dehydrogenase (LDH) (Dietl et al., 2010). This reversed pH gradient is recognized as a hallmark of cancer (Gallagher et al., 2008, Webb et al., 2011). Moreover, an acidic pHe is also characteristic of multi-drug resistance (Thews et al., 2006).

The cancer cell phenotype is pH-dependent (Denker et al., 2000): an increased pHi is an established permissive signal for cell proliferation and promotes survival by limiting apoptosis (Lagadic-Gossmann et al., 2004, Matsuyama et al., 2000). Furthermore, an increased pHi facilitates cell proliferation, resistance to anoikis, and permissive metabolic adaptation and is obligatory for efficient directed cell migration (Wilson et al., 2019). Finally, an acidic pHe is an essential factor in tumor cells' ability to degrade the ECM and to survive outside the ECM. It promotes cell invasion and transformation, induces angiogenesis, and maintains the metastatic process (Pouysségur et al., 2001, Gillies, 2001, Rich et al., 2000).

Insufficient perfusion, uncontrolled proliferation, and deregulated energy metabolism alter tumor microenvironments' physicochemical composition (Boedtkjer et al., 2012). As with the interstitium in normal tissue, the tumor microenvironment is characterized

by acidity, hypoxia, elevated lactate, reduced glucose concentrations, and secretome changes (Huber et al., 2017, Stock and Pedersen, 2017).

Cancer cells may exhibit a more intricate interplay of proteins and buffer systems, as they typically maintain an alkaline pHi and an acidic pHe compared to normal cells. Therefore, extracellular pH may influence cell growth and function in two ways. One aspect is that the ratio of pHe to pHi can impact several crucial biochemical processes in the cell metabolism system. These processes include ATP synthesis, cell proliferation, aggressiveness, migration, diffusion, and the functioning of numerous membrane proteins (Fang et al., 2008). Another consideration is that even a minor disturbance in pHe may trigger alternative splicing of components within the extracellular matrix, resulting in the production of tenascin and fibronectin forms specific to cancer cells (Borsi et al., 1995).

The pH of the tumor microenvironment plays a crucial role in cancer development and treatment in clinical applications. Even a minor alteration in the ratio of extracellular pH to intracellular pH can impact numerous biological and chemical processes within cells, ultimately contributing to the proliferation and aggressiveness of cancer cells (Fang et al., 2008). For instance, when melanoma is cultured in a slightly acidic environment (pH 6.8), there is a notable increase in its metastatic potential, aggressiveness, and migratory activity in vitro (Moellering et al., 2008). Moreover, other types of cancer, like breast cancer, are also shown to lower the pH of its extracellular environment slightly, potentially promoting its invasiveness and metastasis (Montcourrier et al., 1997).

While an acidic extracellular microenvironment promotes cancer development, an highly acidic pHe restricts cancer cells' growth ability. Cancer cells usually have a higher pHi than normal cells under similar environmental conditions, promoting cancer progression et al. pHe declines, the pHi of cancer cells drops substantially; opposite proteins exudate provide a local tumor microenvironment composed of cellular and acellular factors, which modulate cancer cell behavior and contribute to tumor heterogeneity in cancer (Kim et al., 2016). Ascites contain tumor cells, either as single

cells or as spheroids, and a variety of stromal cells, including fibroblasts, mesothelial cells, and stromal cells derived from adipose tissue (ASC/MSC), endothelial cells, and adipocytes (Wels et al., 2008, Bhowmick et al., 2004). Cytokines, proteins, exosomes, and metabolites are some of the acellular factors that link these cellular components (Matte et al., 2012, Shender et al., 2014).

Several studies have demonstrated that normoxic acidosis enhances cell invasion, stem cell phenotypes, immunotherapy resistance, and chemotherapy in various cancer cell models (Estrella et al., 2013, Hjelmeland et al., 2011). However, the growth rate of gastric and ovarian cancer cells was inversely proportional to the medium acidity in-vitro. Extracellular acidity inhibited gastric cancer cell growth by arresting the cell cycle and sensitizing tumor necrosis factor-related apoptosis-inducing ligand (TRAIL)-mediated apoptosis partially via DR5 in GCs while confers resistance to various types of chemotherapeutic drugs (Hong and Han, 2018). Chemotherapy drugs, including lovastatin and cantharidin, have increased efficacy in the mildly acidic environment in ovarian, mesothelioma, and pancreatic tumor cells (Fukamachi et al., 2010).

Previous research has mainly focused on describing metastatic cell behavior regulated by a reversed pH gradient in solid tumors and their microenvironment. In most experiments examining acidic extracellular influence on tumors, cancer cells were only exposed to a slightly acidic environment, the extracellular pH being only lowered to 6.5-6.8. However, few studies show clastogenic events can happen in a strongly acidic pHe and cause double-stranded DNA breaks (Morita et al., 1992, Massonneau et al., 2018). Potential mechanisms are acid-induced effects on topoisomerase II and direct genotoxicity of reactive oxygen species.

In the context of peritoneal metastasis, whether the intra-peritoneal environment (ascites pH) affects abdominal tumor proliferation remains unclear. Another unresolved question revolves around how the production of ascites in the peritoneal cavity influences tumor immunity, metabolism, and recurrence in human patients.

In the current study, we employed an exploratory approach to comprehensively characterize the metabolome of malignant ascites and investigate the impact of ascites on the phenotype of cancer cells. The ascites samples underwent thorough phenotyping through three distinct methods:

1) peritoneal pH and different physical-chemical parameters of malignant ascites vs. benign lavages were measured by the blood-gas analyzer in OC patients;

2) cytokines in malignant ascites were measured by flow cytometry based on a 13-plex cytokine panel;

3) nuclear magnetic resonance (NMR) measured metabolites in malignant ascites.

Then, functional assays were used to verify the influence of pHe on several cancer hallmarks of human gastric and ovarian cancer cell lines.

Material and Methods

Portions of the material and methods section have been published in the following publication: Yang Q, Bae G, Nadiradze G, Castagna A, Berezhnoy G, Zizmare L, Kulkarni A, Singh Y, Weinreich FJ, Kommoss S, Reymond MA, Trautwein C. Acidic ascites inhibits ovarian cancer cell proliferation and correlates with the metabolomic, lipidomic and inflammatory phenotype of human patients. J Transl Med. 2022 Dec 12;20(1):581. doi: 10.1186/s12967-022-03763-3. PMID: 36503580; PMCID: PMC9743551.

This study comprises two parts; the first is an observational study measuring the pH, physical-chemical parameters, cytokines, and different metabolites in malignant ascites in human patients in-vivo. The second part is functional research in-vitro using 2D and 3D cell models. The 2D experiments verify the influence of pHe on several hallmarks (metabolic change, metabolic activity, resistance to apoptosis, adhesion, and migration ability) in human gastric and ovarian cancer cell lines. Subsequently, the morphology and aggregation of tumor cells, dependent on pH, were assessed in a 3D spheroid model.

Ethical background

The Ethics Committee approved this study, Faculty of Medicine, University of Tübingen, Germany (Ref. Nr. 696/2016BO2 and 117/2020BO1). All patients provided written informed consent, and the sampling process did not impact their treatment. All identifying data were anonymized, per the European General Data Protection Regulation (GDPR 2016) and German law.

Collection of patient specimens

Malignant ascites were obtained from patients undergoing cytoreductive surgery for confirmed cancer, including ovarian and gastrointestinal cancers, both with peritoneal metastasis and without peritoneal metastasis; Peritoneal lavage was collected from patients with benign diseases (inflammatory bowel disease, hernia, or gastric sleeve

resection) at the Dept. of General and Transplant Surgery and the Women's Hospital, University Hospital Tübingen, Germany.

Surgeons and gynecologists sampled ascites and lavage fluid in a sterile, closed syringe in the operating room. The samples were promptly placed on ice and transferred to the laboratory within a few minutes for further processing. In the laboratory, the ascites and lavage were aliquoted into two parts. The first aliquot (3ml) was immediately frozen at -80 °C. The remaining portion was centrifuged at 2000 rpm at 4°C for 30 minutes; the supernatant was aliquoted to 2ml tubes and frozen at -80 °C.

Anonymized clinical data, including the time, the amount of fluid, standard demographics data, cancer historiography, and extent of peritoneal lesions, were collected.

Functional characterization of the tumor phenotype in-vitro under various pH conditions

Various hallmarks of aggressive tumor phenotypes were characterized in-vitro using 2D and 3D models. The metabolic parameters of the culture medium were determined with an industry-standard blood gas analyzer, and changes were monitored. The cellular metabolic activity was determined by MTT assay. Resistance to apoptosis was tested by flow cytometry; adhesion ability was measured by adhesion ECM assay, and migration ability by scratch assay. Further details are given below.

2D-model

Cell culture

- Cell lines

Human gastric cancer cells (MKN45, DSMZ, Heidelberg, Germany) were established from the poorly differentiated adenocarcinoma of the stomach (medullary type) of a 62-year-old woman, both spindle-shaped or oval cells growing in monolayers and single round cells or clumps in suspension. The cell culture medium of MKN45 is 90% RPMI 1640 Medium (ThermoFisher, Erlangen, Germany) and 10% fetal bovine serum (FBS) (ThermoFisher, USA).

Human ovarian cancer cells (OAW42, DKFZ, Heidelberg, Germany) were established from the ascites of a patient with ovarian cystadenocarcinoma. The cells have retained the ability to form free-floating cysts in vitro, produce an extracellular matrix, and show a defined chemosensitivity pattern. The cell culture medium of OAW42 is 90% DMEM with GlutaMAX™ Supplement (ThermoFisher, USA) and 10% fetal bovine serum (FBS) (ThermoFisher, USA).

- Cell culture material

Roswell Park Memorial Institute (RPMI) 1640 medium (ThermoFisher, Erlangen, Germany) was initially developed for culturing leukemic human cells in suspension and as a monolayer. RPMI 1640 medium has been found suitable for a range of mammalian cells, including human gastric cancer cells.

Dulbecco's Modified Eagle Medium (DMEM) with GlutaMAX™ Supplement (ThermoFisher, Erlangen, Germany) is a widely used essential medium for the growing support of many different mammalian cells, including human ovarian cancer cells. Fetal Bovine Serum (FBS) (ThermoFisher, USA) is derived from the blood drawn from a bovine fetus. FBS is the most commonly used serum in cell culture, providing the most robust culture system for the broadest range of cell types. Monolayered gastric and ovarian cancer cells were cultured in 175 cm^2 flasks (Falcon, Corning, New York, USA) supplemented with 10% FBS and penicillin G 100 U/ml, streptomycin 100 µg/ml in an incubator. The cell culture environment in the incubator (ThermoFisher Scientific, Langenselbold, Germany) was humidified atmosphere of 5% CO_2 and 95% air at 37°C.

- Cell passage

Adherent MKN45 and OAW42 cells were passaged every five days in the confluence phase during the log phase. The cell culture media was removed from the culture flask. Using PBS wash twice, 5ml Trypsin-EDTA 0.05% (ThermoFisher, Erlangen, Germany) was added to one 175 cm^2 flask. The flask was put back into the incubator for 10 minutes. Then, the cell suspension was observed under the microscope for detachment. When more than 90% of the cells had detached, 10ml cell culture medium

was added to the cell suspension at 37°C. The cell suspension was counted by CASY (Schärfe System, Reutlingen, Germany). CASY is a cell counter that measures the conductivity between two electrodes separated by a defined pore. Electronic current exclusion (ECE) and Pulse field analysis technology are used to determine cell viability. Then, part of the cell suspension was transferred to a new flask to ensure healthy growing conditions.

Preparation of pH-conditioned media

After preparing the complete cell culture medium (RPMI and DMEM with 10% FBS), PBS puffers and drops of 0.1 M phosphoric acid or 0.1 M NaOH were added gradually to the media until the desired pH level was reached (pHe 6.0, pHe 6.5, pHe 7.0, and pHe 7.5). Cell culture medium pH was monitored by a pH meter (SevenCompact™ Duo pH/Conductivity S213, Mettler-Toledo GmbH, Greifensee, Switzerland).

Preparation of malignant ascites for cell culture

Ascites fluids were obtained from gastric or ovarian cancer patients during cytoreductive surgeries. Ascites were centrifuged at 2000 rpm for 30 min at four °C, and supernatants were aliquoted into 1ml Eppendorf tubes and stored at -80℃. Before addition to the cell culture medium, ascites was filtered (Millipore Express, SLGP033RS, France) to exclude bacterial contamination.

Cell proliferation assay

We first used a cell proliferation assay to determine the suitable pH range for follow-up experiments. MKN45 cells were detached from cell culture flasks using Trypsin-EDTA (0.05%), diluted cell suspension to 3 X 10^5 cells/ml, and seeded on a 24-well plate at a density of 3 X 10^5 cells/well in 1ml of the medium culture one night in the incubator. The next day, we buffered the RPMI cell culture medium to different pH (pHe 6.0, pHe 6.5, pHe 7.0, and pHe 7.5) and cultured it for seven days. The cell culture mediums were titrated every two days. On day 0, day 2, day 4, and day7, three well per pH were resuspended by 250µl 0.05% trypsin with 750µl RPMI, counted cell numbers using CASY using cell suspension, monitored the growth of MKN45 cells.

Influence of extracellular pH on MKN45 gastric cancer cell and OAW42 ovarian cancer cell metabolic change

The different parameters change in the cell culture medium can indicate how the extracellular pHs affect gastric and ovarian cancer cells. MKN45 and OAW42 cells were detached from cell culture flasks and seeded on 24-well plates at 1 X 10^6 cells/well density with a 1ml cell culture medium. After incubating cells for one night, daily titrated the pH to different pH (pHe 6.0, pHe 6.5, pHe 7.0, and pHe 7.5) of the cell culture medium to maintain a constant pH value. pH, partial gases (O_2, CO_2), electrolytes (Na^+, K^+, Ca^{2+}, Cl^-), and metabolites (glucose and lactate) of the culture medium were measured daily by an industry-standard blood gas analyzer (GEM PREMIER4000, Werfen, Germany). pH6.8 was the technical lower measurement limit of pH by the blood gas analyzer when pH below 6.8 was measured by a conventional pH meter (SevenCompact™ Duo pH/Conductivity S213, Mettler-Toledo GmbH, Greifensee, Switzerland).

Influence of pHe on MKN45 gastric cancer cell and OAW42 ovarian cancer cell metabolic activity

The metabolic activity of MKN45 cells and OAW42 cells was determined by an MTT Assay (R&D Systems, 4890-050-k, Germany). The cellular metabolic activity was detected by the MTT colorimetric assay, which is based on the principle that viable cancer cells contain NAD(P)H-dependent oxidoreductase enzymes that reduce the yellow tetrazolium salt (3-(4,5-dimethylthiazol-2-yl)-2,5-diphenyltetrazolium bromide (MTT)) to the purple formazan crystals. MKN45 and OAW42 cancer cells were resuspended and diluted to 1 X 10^5/ml, seeding 100µl/well to three 96-well plates overnight. On day 0, one plate was taken out and incubated for four hours at 37 °C with 20µl MTT reagent (R&D Systems Nr. 4890-25-01, Wiesbaden, Germany) each well, and the plate was returned to the incubator for 4 hours until the purple dye was visible. 100µl of Detergent Reagent (R&D Systems, 4890-25-02, Germany) was added, and the plate was kept at room temperature overnight. The following day, the absorbance in each well was measured at 560 nm using the NanoQuant Infinite M200

Pro microplate reader (Tecan Austria GmbH, Grödig, Austria). The extracellular pH of two other plates was titered to reach pre-specified conditions (pHe 6.0, pHe 6.5, pHe 7.0, and pHe 7.5). Half of the plates were supplemented with 10% human malignant ascites. On days two and 3, the MTT assay was repeated on the other two plates, and the optical density value changes on different pHe were recorded.

Influence of intraperitoneal pHe on MKN45 GC cell and OAW42 OC cell apoptotic rate (resistance to anoikis)

The effects on the anti-apoptotic capacity of MKN45 cells and OAW42 cells were evaluated in vitro using flow cytometry (FACS) by increasing or decreasing ascites and extracellular pH. Annexin V FITC and Propidium Iodide (PI) are the most commonly used reagents for FACS apoptosis studies. Annexins are a family of calcium-dependent phospholipid-binding proteins, and the Annexin V-FITC can bind phosphatidylserine (PS) on the outer leaflet of the cell membrane. This machinery is activated during the execution of apoptosis. PI binds to double-stranded DNA but is not taken up by cells with intact plasma membranes, allowing the discrimination of apoptotic cells. Apoptosis was measured with the Annexin V-FITC Apoptosis detection kit (ThermoFisher, BMS500FI, Erlangen, Germany) per the manufacturer`s instructions. Shortly, cancer cells were seeded into a 24-well plate; the cell culture medium was changed to a different pH. Then, cells were kept in the cell culture medium at different pH for 12 hours (MKN45), respectively 24 hours (OAW42). 50% of the wells were supplemented with 10% human ascites. Cells were resuspended in 200 ul Binding Buffer (ThermoFisher, BMS500FI, Erlangen, Germany) and diluted to 5 X 10^5. 5µl Annexin V-FITC was added to 195µl cell suspension, mixed, and incubated at room temperature for 10 minutes. After washing, cells were resuspended in 190µl Binding Buffer and 10µl PI. Cells were counted by flow cytometry (FACS Canto II, Becton Dickinson GmbH, Heidelberg, Germany).

Influence of pHe on MKN45 cell and OAW42 cell adhesion onto ECM proteins

Adhesion occurs during migration, invasion, embryogenesis, wound healing, and

tissue remodeling. Cells are thought to adhere to the extracellular matrix, forming complexes with cytoskeleton components that can affect motility, differentiation, proliferation, and survival. Cell Adhesion Assays provide a fully quantitative method for evaluating cell adhesion. The 48-well plate is precoated with a choice of Extracellular Matrix (ECM) proteins. Each of the first five groups of the 48-well plate is precoated with a different ECM protein (Fibronectin, Collagen I, Collagen IV, Laminin I, Fibrinogen), with the last group (BSA) acting as a negative control.

The influence of pHe on the adhesion of MKN45 cells was determined in vitro by a colorimetric cell adhesion assay (CytoSelect 48-Well Cell Adhesion Assay Kit, CBA-070, Cells Biolabs, San Diego, CA, USA). The absorbance was determined with the NanoQuant Infinite M200 Pro microplate reader (Tecan Austria GmbH, Grödig, Austria).

The pH of the cell culture medium was titrated after seeding cancer cells in a 24-well plate. Half of the 24-well plates were supplemented with 10% human ascites, and MKN45 and OAW42 cells were grown in the incubator for 12, respectively, 24 hours. A cell suspension containing 1.0 X 10^6 cells/ml was prepared in serum-free media, and 200 µl of the suspension was pipetted inside 40 ECM protein-coated wells (Fibronectin, Collagen I, Collagen IV, Laminin I, Fibrinogen) and eight BSA-coated wells, and then incubated in a cell culture incubator for eight hours. Cells were washed four times with PBS, stained with 200µl Cell Stain Solution, and incubated for 10 minutes at room temperature. Then, cells were washed four times with deionized water, and 200 µl of Extraction Solution was added to extract the supernatant. An aliquot of 150 µl was transferred from each sample to a 96-well plate. Optical density was then measured by a microplate reader (Tecan Austria GmbH, Grödig, Austria) at a wavelength of 650 nm.

Influence of pHe on MKN45 GC cell and OAW42 OC cell migration: wound scratch assay

The migratory ability of cancer cells at different extracellular pH was measured using a scratch wound assay. MKN45 cells and OAW42 cells were seeded in a 24-well plate overnight. A standardized wound was created using a 10 ul pipette to scratch each well. Cells were washed twice with PBS to remove detached cells. The cell culture medium was titrated to different pH (pHe 6.0, pHe 6.5, pH 7.0, pHe 7.5), and half of the wells were supplemented with 10% human malignant ascites. The plates were placed into an incubator at 37°C for live-cell imaging during cell migration, and the wound healing was monitored in real-time by micro-cinematography (zen Cell-Owl, Bremen, Germany). Wound healing was defined as the wound width relative to the initial scratch, expressed in %.

3D-model

We first established 3D spheroid-matrigel-based models in which cell aggregates are grown in suspension. MKN45 cell and OAW42 cell suspensions were prepared and diluted to 2 X 10^5 cells/well. 150 µl Matrigel (A1413201, ThermoFisher, Erlangen, Germany) was mixed with 6 ml cell culture medium on ice, and 300 µl cell suspension was added. A 200 µl mixture was seeded into 96 U-Form plates per well and centrifuged at 2000 rpm for 10 min at 4°C.

Microscope

3D spheroids were incubated in a standard cell culture medium for seven days. Then, the cell culture medium was titrated to different pH conditions (pHe 6.0, pHe 6.5, pHe 7.0, pHe 7.5). Then, 3D spheroids were transported from a 96-well U-type plate to a 24-well F-type plate with coverslips, and the cell culture medium was buffered every two days. Morphological changes and the growth of 3D spheroids were observed by light microscopy and photo-documented on days 0, 3, 5, and 7.

Scanning electron microscope

After seven days, taking out coverslips from the 24-well plate, 3D spheroids were fixed with 4.5% formaldehyde/ 2.5% glutaraldehyde rinsed in 0.1M PBS at 4℃ overnight. The following day, spheroids were washed three times for 10 minutes with 0.1M PBS, post-fixed for 45 minutes on ice with 1% osmium tetroxide in PBS, followed by soaking for 10 minutes with PBS three times. 3D spheroids were dehydrated in graded 30%, 50%, 70%, 95%, and 100% ethanol for 10 minutes each at room temperature. Then, samples were placed in a critical point dryer (EM CPD300, Leica Microsystems, Wetzlar, Germany) and dried with CO_2 using a semi-automatic device (Leica CPD 300, Jena, Germany). The lyophilisate was coated with platinum by a coater system (EM ACE200, Leica Microsystems, Wetzlar, Germany). The dried and coated 3D spheroids were observed by scanning electron microscope (SEM, Phenom G2pro and Software Phenom ProSuite, Phenom-World BV, Eindhoven, The Netherlands).

Physical-chemical characterization of ascites and peritoneal lavage in-vivo

The physical and chemical characteristics of the peritoneal cavity environment under control and cancer conditions were measured using an industry-standard blood gas analyzer (GEM PREMIER4000, Werfen, Germany). Measured parameters were pH, partial gas (pO_2, pCO_2), metabolites (glucose, lactate), and electrolytes (Na^+, K^+, Ca^{2+}, Cl^-).Every patient's sample was measured three times. The pH and parameters concentration in the ascites samples were compared in cancer vs. lavage of control patients.

^{1}H-NMR spectroscopy equipment and spectra acquisition

^{1}H-NMR spectroscopy was carried out on a Bruker Avance III HD (Bruker BioSpin, Ettlingen, Germany), operated at 14.1 Tesla, 600MHz with a 3.0 mm triple-resonance room temperature probe at 298K using Carr-Purcell-Meiboom-Gill pulse programs (CPMG). CPMG spectra underwent pre-processing with Bruker TopSpin 3.6.1 and were quantified utilizing Chenomx NMR Suite 9.02 software.

Analytical examination of polar metabolites through 1H-NMR spectrometry

Ovarian cancer ascites samples were thawed, and 2 mL from each sample was transferred to an Eppendorf tube. The tubes were then subjected to centrifugation at 30,000G for 10 minutes. A volume of 500 µL from each supernatant was carefully transferred to a Covaris tube (Covaris, Woburn, USA), and subsequently, the tubes were subjected to a SpeedVac (ThermoFisher, SPD300DDAA-230, Erlangen, Germany) for 3 hours to facilitate the evaporation of undesired solvents. To facilitate total lipid extraction, 300 µL of a mixture comprising methanol and tert-butyl methyl ether (MTBE) was added to the Covaris tube using filter-containing pipette tips. The contents were then vortexed to achieve a homogeneous solution. Each sample underwent a 5-minute ultrasound extraction process using the Covaris Ultrasonicator E220 Evolution instrument (Covaris, Woburn, USA). Following ultrasonication, 250 µL of molecular biology water (ultra-pure grade) was introduced, and the tubes underwent centrifugation at 12,000G for 10 minutes to separate into polar and non-polar (lipid) phases. The lipid and polar phases were separated into glass vials and Polytetrafluorethylene (PTFE) tubes.

Analyzing polar metabolites through 1H-NMR spectrometry for metabolomics research

210 µL of deuterated buffer containing one mM (3-(trimethylsilyl) propionic-2,2,3,3-d4 acid sodium salt (TSP)) (prepared with K2HPO4 in D2O + 10 mM NaN3), adjusted to pH 7.44, was pipetted into each dried pellet of the polar sample in an Eppendorf tube. The Eppendorf tubes were vortexed briefly until complete sample dissolution, followed by a short ultrasonication. Subsequently, the PTFE tube underwent centrifugation at 30,000G for 30 minutes. The supernatants were meticulously transferred to a 3 mm NMR spectrometer-compatible tube (Bruker Biospin, Rheinstetten, Germany) in two batches, each containing 95 µL. The NMR tubes were sealed with cap sealing balls and wiped with fusel-free tissue before being placed inside the autosampler unit of the NMR spectrometer. The spectra of the polar samples were captured through Nuclear

Overhauser Spectroscopy (NOESY 1D) and CPMG experiments, lasting 7 minutes and 2 hours, respectively. The CPMG spectra were selected for analysis due to their superior signal-to-noise ratio (SNR) and lipid signal suppression in comparison to 1D NOESY spectra.

Preparation of lipid metabolite samples for metabolomics analysis

Each lipid aliquot (500 µL) in MTBE solvent was transferred to a glass high-performance liquid chromatography (HPLC) vial and dried using a vacuum dryer until complete evaporation. A 200 µL volume of deuterated chloroform solution containing a 1 mM tetramethylsilane (TMS) internal standard was added to the dried lipid pellet in a glass vial and thoroughly mixed using vortex stirring. A 200 µL aliquot of each sample was pipetted into a 3 mm NMR tube using a round solvent-safe tip, with 100 µL of each lipid sample pipetted twice. Close and secure all NMR tubes with a capping bulb and wipe with a lint-free paper towel before placing in the NMR autosampler. Lipid samples underwent analysis through 1H NMR, employing a 1-hour-long simple proton experiment (zg30) and a 1-hour-long J-coupling resolved spectroscopy (JRES) experiment. Proton experiments were selected for spectral assignments of lipid metabolite.

Quantification of cytokines present in malignant ascites

We used a bead-based immunoassay (LEGENDplex™ Human Inflammation Panel 1 (13-plex) #740809, BioLegend, USA) to quantify the cytokines in malignant ascites. This assay uses sandwich ELISAs to quantify soluble analytes using a flow cytometer. All the ascites samples of ovarian cancer were thawed at room temperature. Ascites samples were diluted 2-fold with assay buffer before cytokine quantification. 25 µL of ovarian cancer ascites was mixed with 25 µL of assay buffer. Then, 25 µL of 13-plex beads were pipetted to a 96-well microplate. This assay quantifies the following 13 cytokines/chemokines (the minimum detectable concentration (MDC) in brackets): IL-1β (1.5+0.6pg/ml), IFN-α2 (2.1+0.2pg/ml), IFN-γ (1.3+1.0pg/ml), TNF-α(0.9+0.8pg/ml), MCP-1 (1.1+1.2pg/ml), IL6 (1.5+0.7pg/ml), IL-8 (2.0+0.5pg/ml), IL-10 (2.0+0.5pg/ml),

IL-12p70 (2.0+0.2pg/ml), IL17A (0.5+0.pg/ml), IL-18 (2.0+0.5pg/ml), IL-23 (1.8+0.1pg/ml), and IL-33 (4.4+1.5pg/ml)). To bind the analytes (cytokine) to the antibody-conjugated capture beads, the microtiter plate was incubated at room temperature and shaken for 2 hours. Following two washes, 25 µL of biotinylated detection antibodies were added and bound to the analytes, then incubated and shaken for 1 hour at room temperature. Streptavidin-phycoerythrin (25 µL) was added to bind antibodies, generating a fluorescent signal with intensities proportional to the amount of bound analyte. The mixture was incubated and shaken for 1 hour at room temperature. Then, beads were washed two times using a vacuum filtration unit, and 150µL wash buffer was added. A flow cytometer was employed to quantify the fluorescent signal, and analyte concentrations were determined by referencing a known standard curve through LEGENDplex™ data analysis software (BioLegend, USA).

Chemical Metrology

The metabolite and cytokine data from ovarian cancer ascites were normalized to a pooled sample using probabilistic quotient normalization (PQN), followed by log transformation. Univariate, multivariate, and correlation analyses were conducted using the MetaboAnalyst 5.0. Given the limited total sample size, the comparison was made by combining clinical stages II-III versus stage IV.

Univariate Analysis

Volcano plot analysis was used to screen for polarity and lipid metabolites and cytokines in differentiated II-IV OCs. Significance was determined by a p-value of < 0.05 and a fold change (FC) cut-off greater than 1.2.

Multivariate Analysis

Principal Component Analysis (PCA) and Orthogonal Projections to Latent Structures Discriminant Analysis (OPLS-DA) score plots were employed to visualize the clustering patterns of ovarian cancer (OC) stage samples and their relationships with each other. PCA and OPLS-DA loading plots, along with a PCA bi-plot, were subjected to

additional analysis to elucidate the specific involvement of metabolites in the progression of OC. Correlation analysis was performed to examine the associations between specific lipid metabolite species, polar metabolites, pCO2, pH, and cytokines. Cytokines and polar metabolites such as IL-8, glutathione, acetate, 3-hydroxybutyrate, glycerol, and lactate were selected to demonstrate correlation.

Statistics

This is an exploratory study without pre-determined sample size calculation. Data were initially visualized using pair plots (Seaborn, Anaconda, Berlin). Descriptive statistics and correlations were calculated with Python, Jupiter, R language, and Pandas software (Anaconda, Berlin, Germany). Statistical comparisons were conducted utilizing One-Way ANOVA for normally distributed data and non-parametric tests for skewed data.

Results

Portions of the results section have been published in the following publication: Yang Q, Bae G, Nadiradze G, Castagna A, Berezhnoy G, Zizmare L, Kulkarni A, Singh Y, Weinreich FJ, Kommoss S, Reymond MA, Trautwein C. Acidic ascites inhibits ovarian cancer cell proliferation and correlates with the metabolomic, lipidomic and inflammatory phenotype of human patients. J Transl Med. 2022 Dec 12;20(1):581. doi: 10.1186/s12967-022-03763-3. PMID: 36503580; PMCID: PMC9743551.

In this experimental and clinical study, we first performed functional tests in-vitro, looking for a possible causal relationship between the extracellular pH and a metastatic tumor phenotype. In a second step, we evaluated the intraperitoneal pH, hypoxia, electrolytes, and metabolic parameters in patients undergoing surgery for malignant vs. benign disease, looking for a correlation between the above parameters and malignity. Finally, we compared pH, physical-chemical parameters, metabolites, and cytokines in malignant ovarian ascites to correlate these parameters with the tumor stage in individual patients.

Human samples: test and controls

Test patients were cancer patients, seven were operated on to remove gastrointestinal or gynecological malignancies via laparotomy or laparoscopy. Controls patients were patients undergoing surgery for benign diseases. Table 1 details the patients' characteristics, including age, gender, cancer type, histology, cancer stage, and peritoneal metastasis. Nineteen patients had malignant disease, and five patients had benign disease. Out of the cancer patients, eleven were women with ovarian cancer. The remaining eight patients had gastrointestinal cancer. The control patients (n=5) were operated on for obesity or hernia.

Patient characteristics

Patient characteristics are detailed in Table 1. (see next page)

Functional assays

Functional assays were used to examine how an acidic peritoneal environment affects

cancer cell phenotype. In tumors, the acidity of the interstitial space and the relatively well-maintained intracellular pH has been reported to influence cancer and stromal cell function (Boedtkjer and Pedersen, 2020). In the first step, we aimed to find the suitable pH range for the subsequent cell function study. For this purpose, we cultured the gastric cancer cell line MKN45 for seven days and counted cell numbers by CASY. After finding the optimal pH range, we cultured two human cancer cell lines (gastric cancer: MKN45, ovarian cancer: OAW42) and examined the influence of extracellular pH on several cancer hallmarks, including cancer cell metabolic activity, apoptotic rate, adhesion, and migration ability.

Table 1. *Patients characteristics*

Patient label	Age	Gender	Cancer origin	histology	stage	PM
1	74	female	ovarian	adenocarcinoma	pTx Nx M1 IV	yes
2	54	female	ovarian	adenocarcinoma	pT3b pN0 pMX III	yes
3	76	female	ovarian	adenocarcinoma	pT3a pN2 pM1a IV	yes
4	73	female	ovarian	adenocarcinoma	pT3c pN1a pM0 III	yes
5	54	female	ovarian	adenocarcinoma	pT3b pN0 pMx IV	yes
6	63	female	ovarian	adenocarcinoma	pT2b pN0 cM0 II	no
7	57	female	ovarian	adenocarcinoma	rpT3c rpN1b Mx III	yes
8	61	female	ovarian	adenocarcinoma	Tx Nx Mx IIIc	yes
9	78	female	ovarian	adenocarcinoma	pT3c pN1a Mx III	yes
10	79	female	ovarian	adenocarcinoma	pT3c pN1a cM0 III	yes
11	57	female	ovarian	adenocarcinoma	pT3c pN0 cM0 III	yes
12	57	female	appendix	adenocarcinoma	pT3c pN1b pM1b IV	Yes
13	76	female	appendix	mucinous neoplasia	pT4a pN0 pM1b IV	yes
14	25	female	appendix	mucinous neoplasia	pT4a cN0 Mx IV	yes
15	43	female	appendix	mucinous neoplasia	pT4a pN0 pM1a IV	yes
16	56	male	gastric	adenocarcinoma	ypT3 ypN3a ypM1 IV	yes
17	35	female	gastric	adenocarcinoma	ypT4a ypN1 M0 III	no
18	57	female	Gastrointestinal stromal tumor	adenocarcinoma	pT4 pNx pM1 IV	yes
19	44	female	colon	adenocarcinoma	pT3 pN2 cM1 IV	yes
20	55	male	N/A	benign disease	N/A	no
21	71	female	N/A	benign disease	N/A	no
22	62	male	N/A	benign disease	N/A	no
23	51	female	N/A	benign disease	N/A	no
24	57	female	N/A	benign disease	N/A	no
Legend: N/A: not available; PM: peritoneal metastasis						

Effect of different pH levels on MKN45 cell growth

We cultured the human gastric cancer cells (MKN45) at different pH (pHe 6.0, 6.5, 7.0, and 7.5) by buffering the culture medium every two days for seven days. Cells were trypsinized on day 0, day 2, day 4, and day seven and counted. Figure 1 shows a pH-dependent growth: the MKN45 cell number decreased at pHe 6.0 after seven days, and the growth rate was minimal at pHe 6.5 and 7.0. In contrast, at pHe 7.5, the cell population after seven days was 20 times larger than that at pHe 6.0, a highly significant difference (p<0.0001).

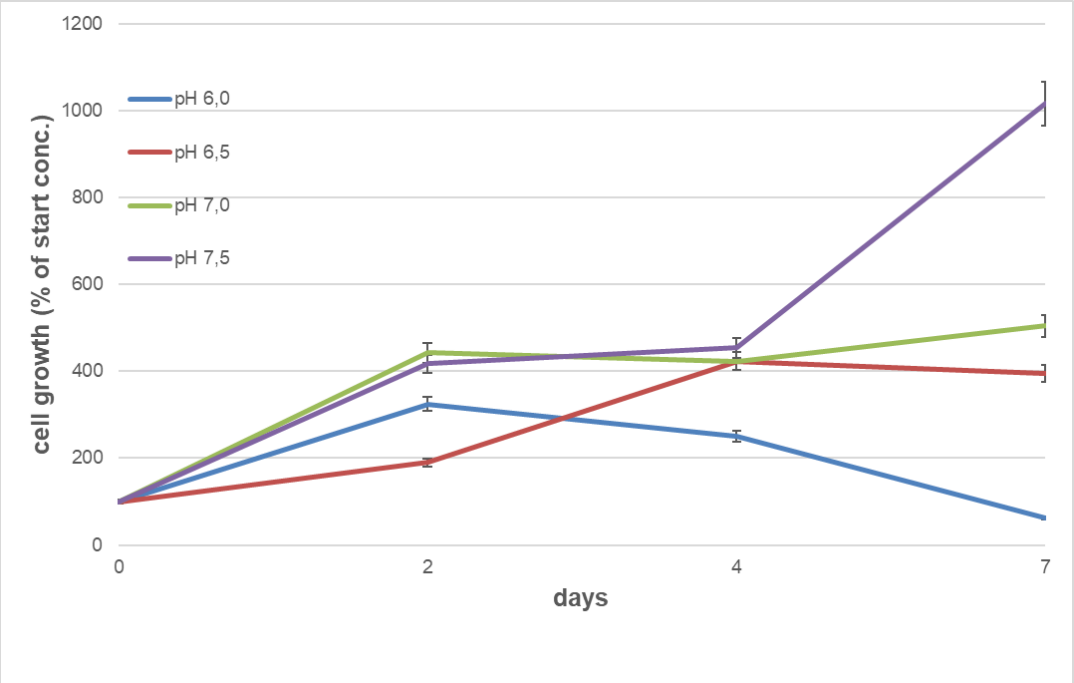

Figure 1. *Gastric cancer cells grow under different pHe conditions*
MKN45 cells were seeded into 24-well plates and incubated at four different pHe (pHe 6.0, 6.5, 7.0, and 7.5). The cell population decreased in the pH 6.0 group; a slow growth rate was observed at pHe 6.5 and 7.0; the cells proliferated rapidly at pHe 7.5.

Metabolic changes in human gastric (MKN45) cells and ovarian (OAW42) cells depending on the environmental pH

We cultured the human cancer cells at different pHs (pHe 6.0, 6.5, 7.0, and 7.5) and measured pHe daily for five days. pH was monitored by a blood gas analyzer and pH meter, and after measurement, the medium was buffered to the initial pHe value. A

distinct behavior of gastric (MKN45) vs. ovarian cells (OAW42) was observed (Figure 2). According to our expectations, MKN45 cells first induced acidification of the pHe when cultured in a slightly alkaline environment (pHe 7.5, equivalent to the normal peritoneal pH = 7.4). A similar trend was observed at pH 7.0. However, when the initial pHe was lower (6.5 and 6.0), the cancer cells turned the extracellular environment somewhat more alkaline.

OAW42 cells induced a similar but more pronounced pHe increase. When cells were cultured in an acidic environment (pHe 6.0 and 6.5), they induced a sharp increase of pHe. At an initial pHe of 7.0, pHe increased marginally to 7.2, then remained stable. At an initial pHe = 7.5, however, the cells acidified their environment slightly. After five days, pHe was stable with daily buffering of the culture medium.

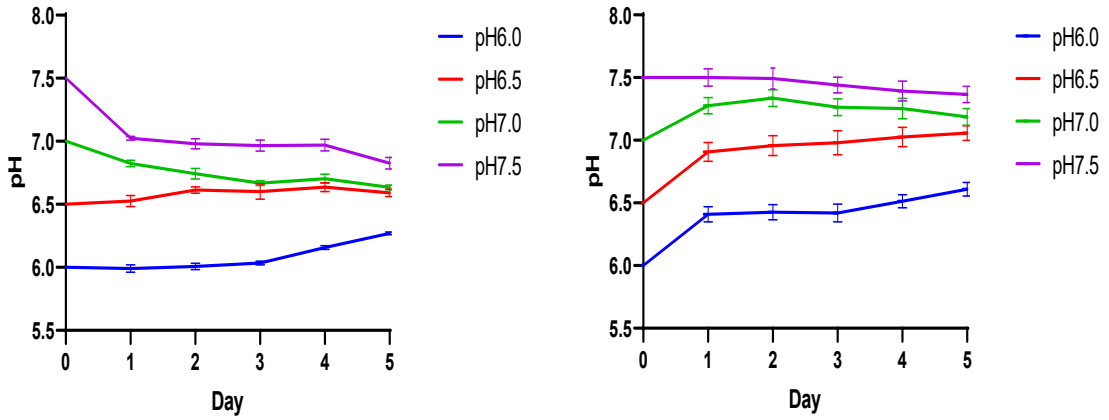

Figure 2. *The changes in pH in the culture medium of MKN45 and OAW42 cells*
Left panel: MKN45: pHe decreased at initial pH 7.5 and pH 7.0 but increased at initial pH = 6.5 and pH 6.0. Right panel: OAW42: The pH of the cell medium decreased at initial pHe = 7.5 but increased at initial pHe values of 7.0, 6.5, and 6.0.

The glucose concentration in the culture medium at different pHe is shown in Figure 3. GC and OC cells showed similar extracellular glucose metabolism during five days. A massive decrease in the extracellular glucose concentration was immediately observed when cells were exposed to an alkaline pH (pHe 7.0 and 7.5). This effect was particularly striking in MKN45 cells, where there was no measurable glucose level in the culture medium at pHe of 7.5 during the whole period under observation,

meaning that all glucose available was metabolized by the cells. In the presence of a slightly basic pHe (pHe 7.0 and 6.5), extracellular glucose levels dropped immediately and stabilized. The cells at pHe 6.0 almost stopped consuming glucose on the last day.

OAW42 cells maintained a steady glucose consumption under alkaline pHe conditions (pHe 7.0 and 7.5). In contrast, their glucose consumption decreased dramatically in acidic environments (pHe 6.0 and 6.5).

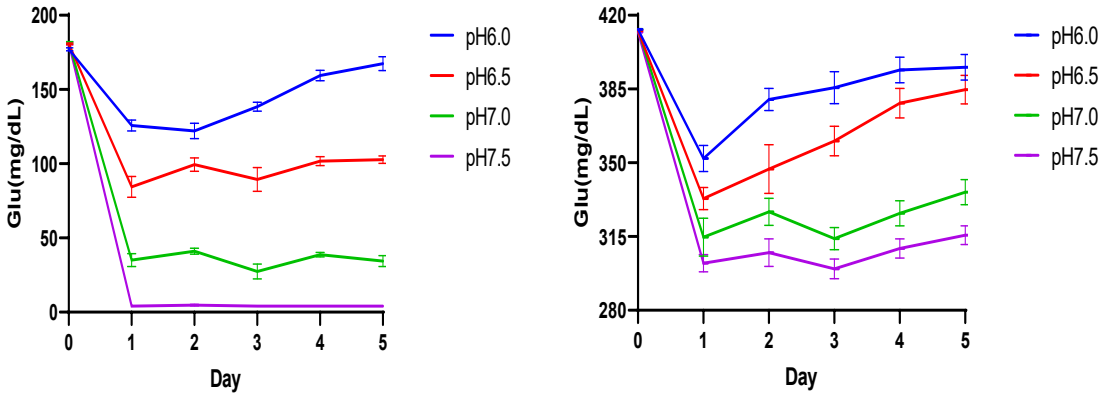

Figure 3. *MKN45 and OAW42 glucose concentration in the culture medium at various pHe*

The glucose concentration in MKN45 (left panel) decreased sharply at pHe 7.5 and remained stable at pHe 7.0 and 7.5, but its consumption decreased at pH 6.0. OAW42 (right panel) cells were kept stable at pHe 7.5 and 7.0, but consumption decreased at pHe 6.5 and 6.0.

This finding suggests that cancer cells consume large amounts of glucose under alkaline pH conditions to meet their proliferation requirements. In parallel, we examined the lactate concentra,tion in the culture medium at different pHe. The concentration of glucose and lactate exhibited opposite trends. As shown in Figure 4, at pHe 7.5, MKN45 cancer cells produced large amounts of lactate that were even above 20 mmol/L, our technology's technical upper measurement limit. The lactate concentration kept stable at pHe 6.5 and pHe 7.0 but decreased sharply under extremely acidic extracellular conditions (pHe 6.0). Similarly, OAW42 cells secreted the most lactate at an extracellular pH of 7.5 and maintained a high concentration level.

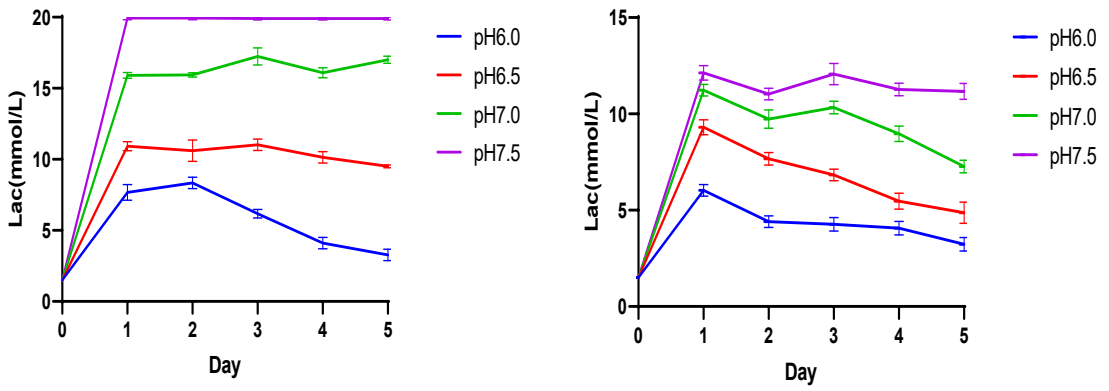

Figure 4. *MKN45 and OAW42 lactate concentration in the culture medium at various pHe*

The lactate concentration in MKN45 (left panel) increased sharply at pHe 7.5 and 7.0 and decreased at pHe 6.5 and 6.0 over time. OAW42 (right panel) cells were kept stable at pHe 7.5 but dropped at pHe 7.0, 6.5, and 6.0.

A strong positive correlation was seen between lactate concentration and pHe in the culture medium (Figure 5). In the gastric cancer cell medium, the correlation was R=0.92, p<0.0001; in the ovarian cancer cell medium, R=0.87, p<0.0001 (Spearman test).

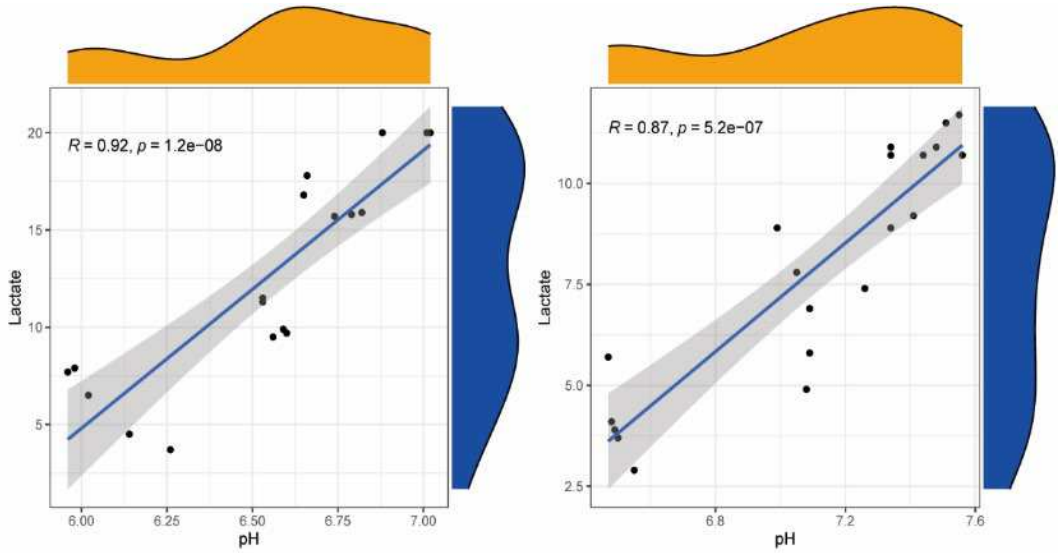

Figure 5. *Lactate concentration in the culture medium strongly correlated with pHe in MKN45 and OAW42.*

Spearman analysis indicates a positive correlation between pH and lactate concentration in MKN45 (left panel) and OAW42 (right panel) cancer cell cultures for five days.

Metabolic activity of human gastric (MKN45) cells and ovarian (OAW42) cells depending on the environmental pH

Glucose is the primary nutrient of cancer cells, so a concentration decreases in the medium probably reflects a higher metabolic activity under alkaline extracellular conditions. Inversely, we hypothesized that intentionally reducing pHe would reduce the metabolic activity of cancer cells. We used an MTT assay to determine MKN45 and OAW42 cancer cell metabolic activity levels in an extracellular pH range between 6.0 and 7.5. Figure 6 shows that cellular metabolism was directly proportional to the pHe during the observation period in MKN45 cells (p<0.0001). An acidic extracellular pH considerably inhibited the cell metabolic activity.

We then examined whether malignant ascites preserve cancer cell metabolism against changes in pHe. We added 10% of malignant ascites from patients with gastric cancer to the human MKN45 cells at various pHe. The MTT assay showed some protective effect of ascites on MKN45 cancer cells; the metabolic activity of MKN45 increased at the same pHe conditions. However, even with the help of malignant ascites support, an acidic extracellular pH considerably inhibited cell metabolic activity (p<0.0001).

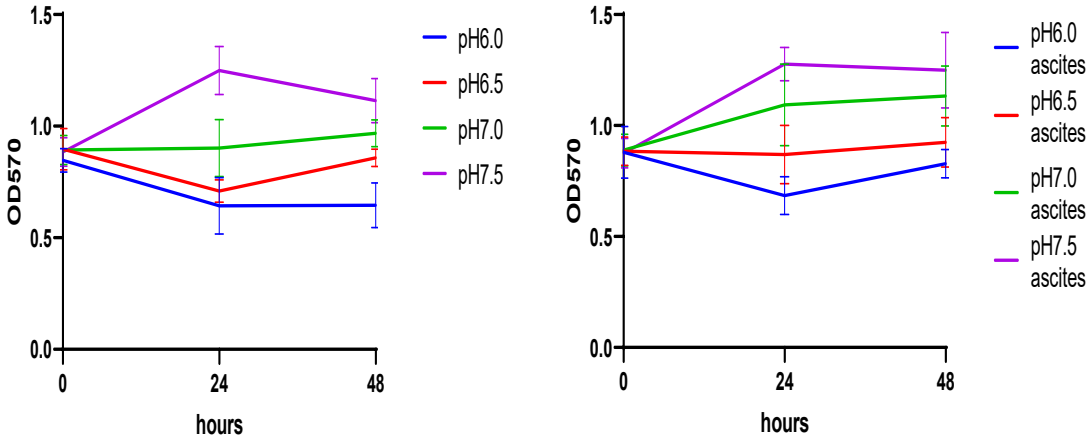

Figure 6. *pHe and malignant ascites influence the metabolic activity of MKN45 cells.* An acidic environment effectively inhibits the metabolic activity of MNK45 cells *(left panel).* Malignant ascites could resist the inhibitory effect of the acidic environment (right panel).

Acidic pHe also influenced OAW42 ovarian cancer cells' metabolic activity. As shown in Figure 7, the metabolic rate of cells was directly proportional to the pHe during the observation period (p<0.0001). An MTT assay also revealed ascites increased metabolic activity of OAW42 cancer cells but did not differ significantly between the pHe conditions. In the acidic extracellular environment, the human OAW42 cells were still significantly reduced despite malignant ascites (p<0.0001).

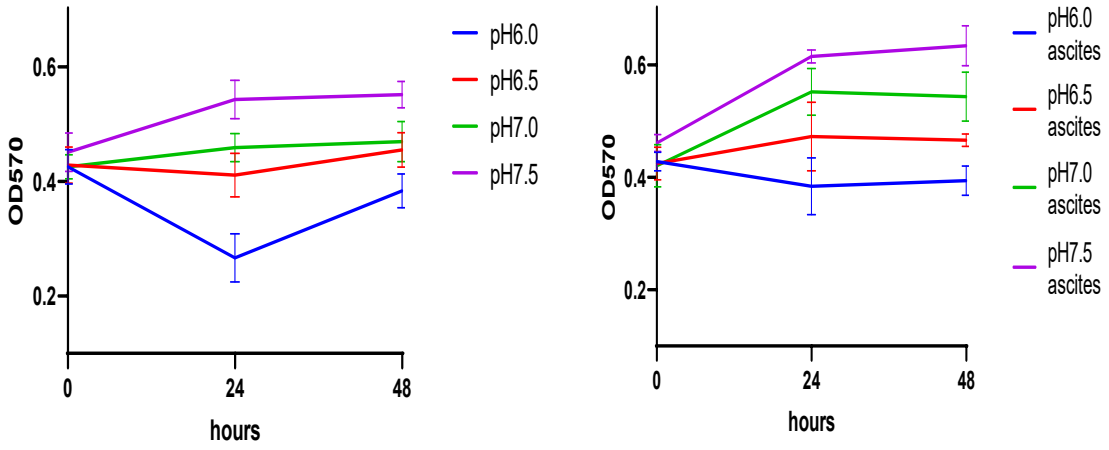

Figure 7. *Extracellular pH and malignant ascites influence the metabolic activity of OAW42 cells.*
An acidic environment effectively inhibits the metabolic activity of OAW42 cells (left panel). Malignant ascites could resist the inhibitory effect of the acidic environment (right panel).

Influence of pHe on apoptosis rate (resistance to anoikis) of detached MKN45 cells and OAW42 cells

Assays using Annexin V FITC/Propidium Iodide (PI) are widely used to study cancer cell apoptosis. Cell populations are sorted depending on their fluorescence, so it is possible to differentiate between apoptotic vs. viable cells. Annexin V positive/PI negative cells can be considered to die by apoptosis at early time points shown in Q4, the late apoptosis cell in Q2, the necrotic cell in Q1, and the viable cell in Q3.

We modified MKN45 gastric cancer cells' pHe to different values for 12 hours, double-stained Annexin V and PI in these cells, and measured their fluorescence by flow cytometry. As Table 2 shows, the viable cell population increased together with pHe. Conversely, necrotic cells were reduced.

Table 2. *The proportion of viable (Q3) and necrotic (Q1) cells of gastric cancer cells at different pHe.*

The viable cell population is shown in Q3 and the necrotic cell population in Q1.

	pHe 6.0	pHe 6.5	pHe 7.0	pHe 7.5
Q3	69.23%	73.10%	76.13%	80.08%
Q1	30.40%	25.73%	22.13%	18.10%

Figure 8 below shows a significant difference in the apoptotic rate between pHe 6.0 and 7.5 ($P<0.001$). More cells were apoptotic and necrotic at an acidic vs. an alkaline pHe. Extreme acidic pHe induced gastric cancer cell death via necrosis and apoptosis.

A

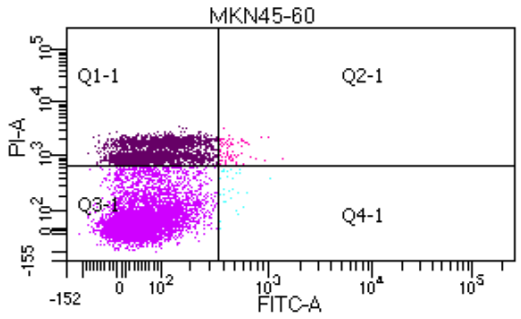

B

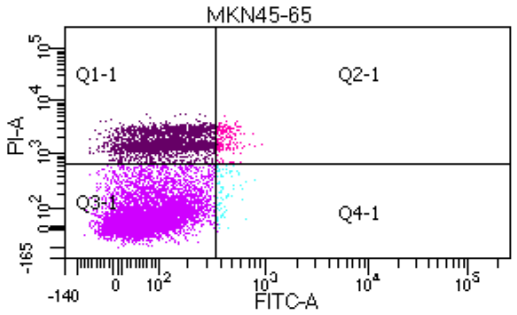

C

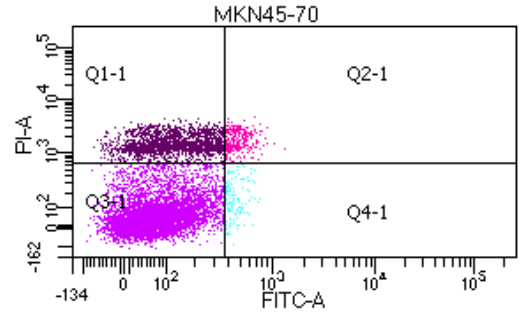

D

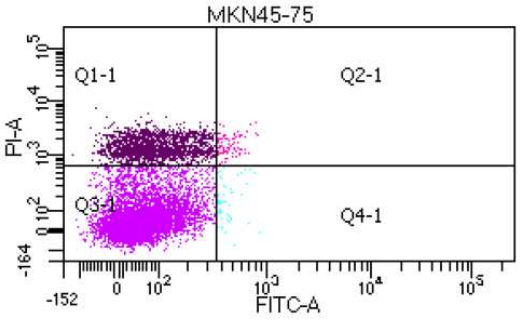

E

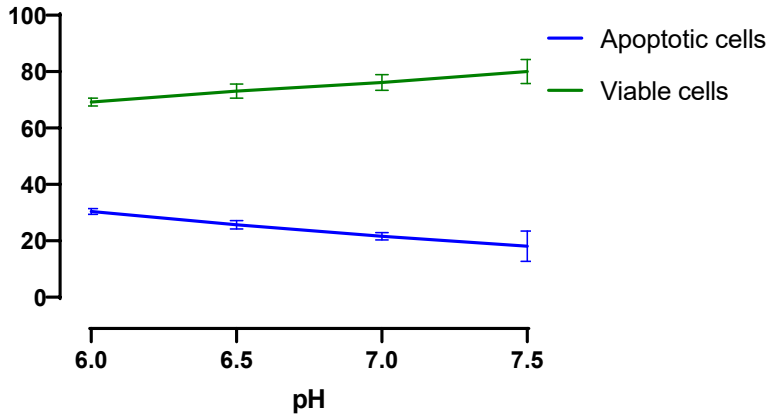

Figure 8. *The influence of pH on the apoptosis rate of MKN45 cells*
FACS analysis confirmed that an alkaline environment protects MKN45 cells from apoptosis. The apoptosis of MKN45 cells: A) pHe 6.0; B) pHe 6.5; C) pHe 7.0; and D) pHe 7.5.
E) the apoptotic cell ratio decreases with increasing pH.

As Table 3 shows, ascites (10%) had an antiapoptotic effect in GC cells, and the viable cell population increased with pHe. At the same time, the number of necrotic cells decreased. Significantly, in gastric cancer cells in the slightly acidic group (pH 7.0), the ability of resistant apoptosis somehow increased with treatment with 10% gastric malignant ascites.

Table 3: *The percentage of viable (Q3) and necrotic (Q1) cells of gastric cancer cells with 10% ascites in different pHs.*

10% ascites	pHe 6.0	pHe 6.5	pHe 7.0	pHe 7.5
Q3	71.90%	74.68%	81.55%	80.08%
Q1	27.33%	23.63%	19.4%	18.15%

A similar experiment was performed in ovarian OAW42 cancer cells (Table 4). Results are consistent with those obtained with gastric cancer cell lines (see above). Resistance to apoptosis increased with pH, and the viable cell population at a pHe of 7.0 and 7.5 increased sharply vs. pHe 6.0 and 6.5.

Table 4:*The percentage of viable (Q3) and necrotic (Q1) cells of ovarian cancer*

cells in different pHs.

	pHe 6.0	pHe 6.5	pHe 7.0	pHe 7.5
Q3	61.63%	64.73%	86.63%	91.77%
Q1	35.10%	32.13%	10.77%	6.33%

Figure 9 shows a significant difference in the apoptotic rate of GC cells between pH 6.0 and 7.5 ($P<0.001$), despite ascites in the medium.

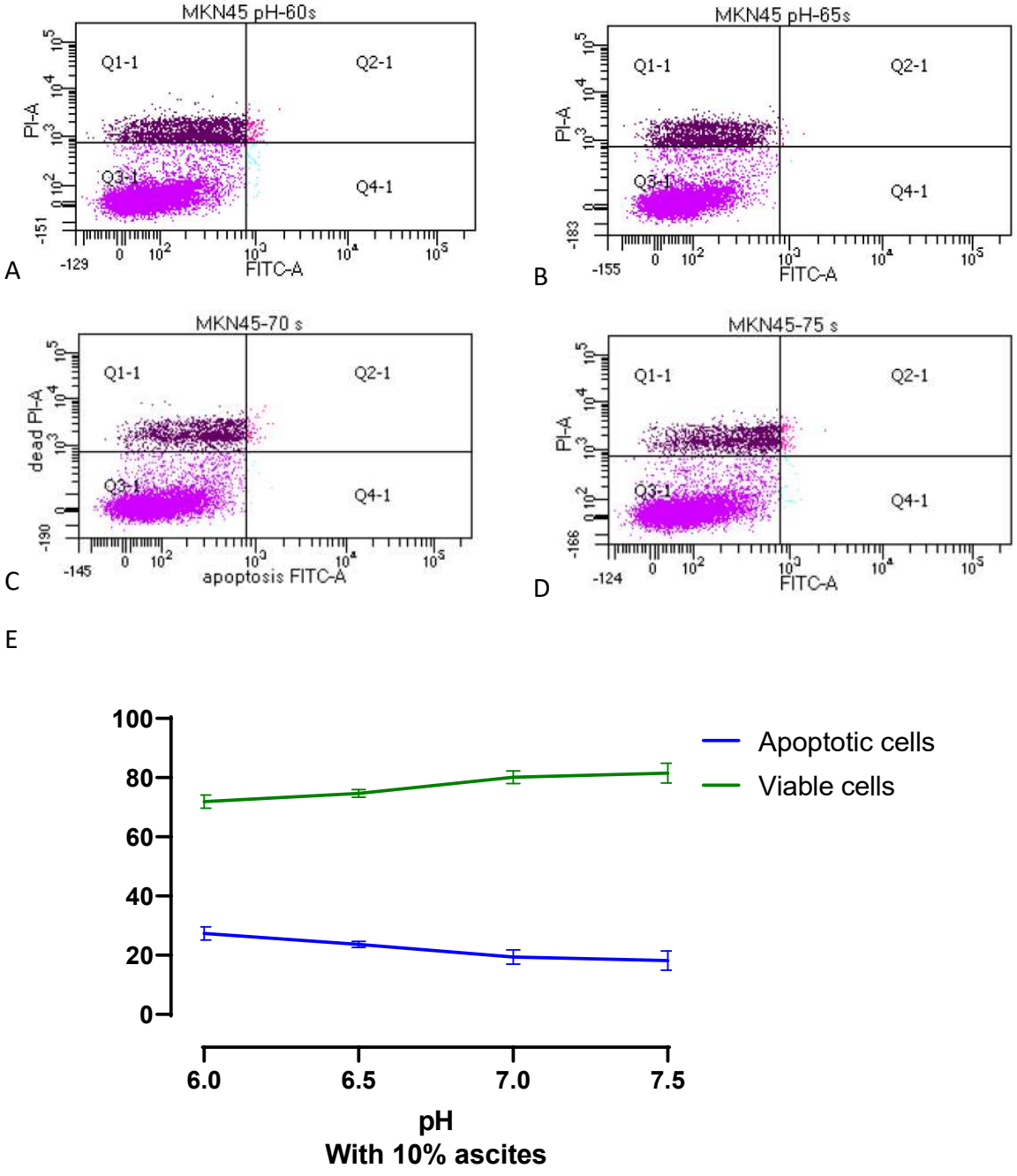

Figure 9. *The influences of pH on the apoptosis of MKN45 cells with 10% ascites.*
FACS analysis confirmed that with 10% ascites, an alkaline environment could still protect MKN45 cells from resistant apoptosis. The apoptosis of MKN45 cells with 10% ascites: A)

pH 6.0; B) pH 6.5; C) pH 7.0; and D) pH 7.5.
E) the apoptotic cell ratio decreases with increasing pH with 10% ascites.

A partial protective effect of ascites against apoptosis of MKN45 gastric cancer cells can be observed. However, an acidic pHe still affects cell apoptotic and necrotic vs. an alkaline pHe.

In Figure 10, significant differences in the apoptotic rate can be seen between pHe 6.0 and 7.5 (p<0.001). Apoptosis increased in acidic extracellular environments.

A

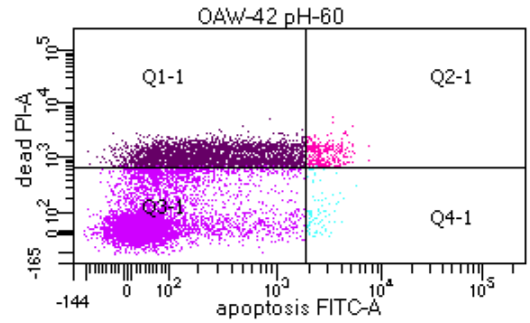

B

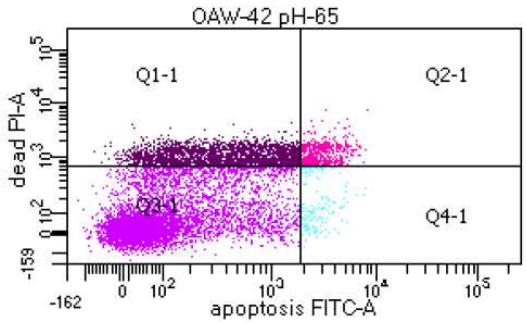

C

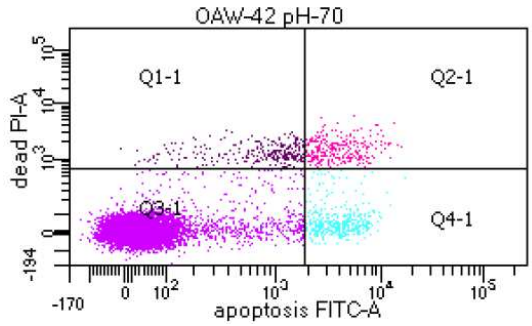

D

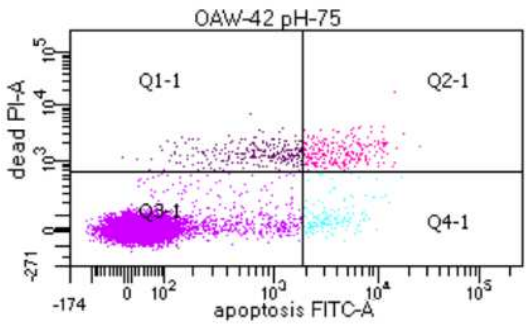

E

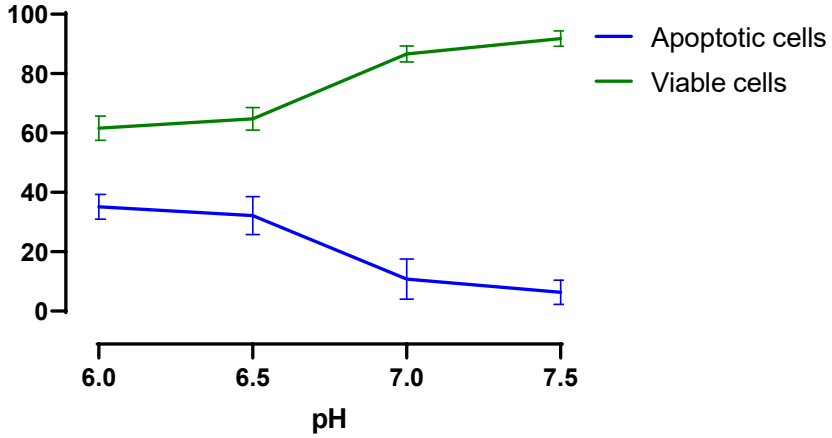

Figure 10. *The effect of pHe on the apoptosis of OAW42 cells*
FACS analysis confirms that an alkaline environment protects OAW42 cells from apoptosis. The apoptosis of OAW42 cells: A) pHe 6.0; B) pHe 6.5; C) pHe 7.0; and D) pHe 7.5. E) the apoptotic cell ratio decreases with increasing pHe.

Table 5 shows that the ovarian cancer cells supplemented with 10% of malignant ovarian ascites have a similar apoptotic rate vs. those without ascites. However, the pHe 6.5 group treated with ascites has a significantly higher viable cell population than those without ascites (p<0.05).

Table 5: *The percentage of viable (Q3) and necrotic (Q1) cells of OAW42 ovarian cancer cells supplemented with 10% ascites at different pHe.*

10% ascites	pHe 6.0	pHe 6.5	pHe 7.0	pHe 7.5
Q3	67.90%	79.17%	90.83%	94.40%
Q1	21.67%	15.40%	7.50%	4.20%

(The remaining page is left empty for better reading of the following figure)

Similarly, Figure 11 shows that an acidic extracellular environment could still inhibit OAW42 cancer cell growth in the presence of malignant ascites. An extremely acidic pH caused ovarian cancer cell death via necrosis.

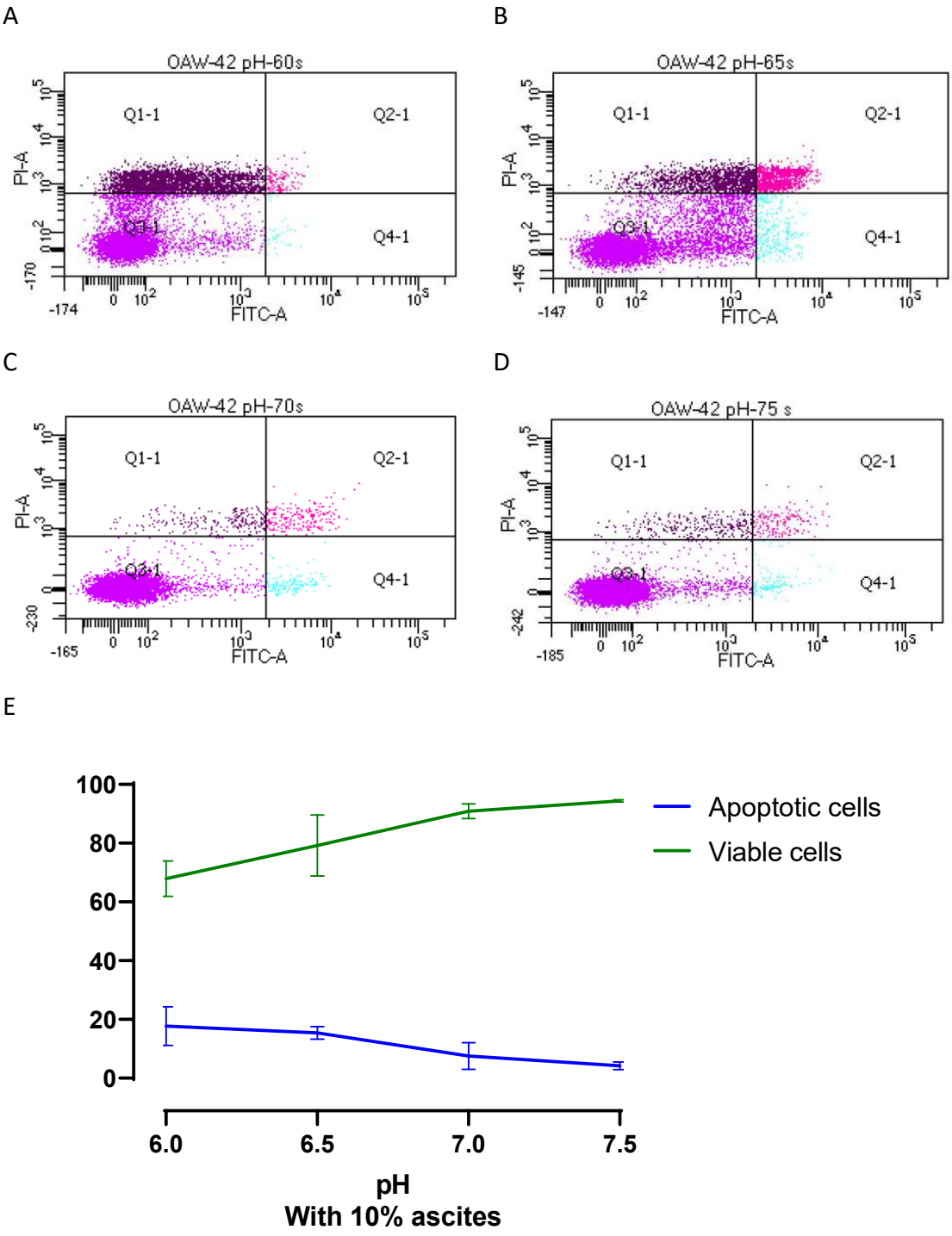

Figure 11. *The influences of pHe on the apoptosis of OAW42 cells in the presence of ascites.*

FACS analysis confirmed that when the medium was supplemented with 10% ascites, an alkaline environment could still reduce the apoptotic death of OAW42

cells. Inversely, there were fewer viable cells in an acidic extracellular environment.

Influence of pH on MKN45 cells and OAW42 cells' adhesion onto ECM protein components

Figure 12 summarizes the effect of four different pHe on MKN45 human gastric cancer cell adhesion ability, with and without malignant ascites. The influence of different pHe conditions on the adhesion of MNK45 cells was determined quantitatively by Colorimetric Cell Adhesion Assay (ECM Array). Adhesion to the ECM components Fibronectin, Collagen I, Collagen IV, Laminin I, and Fibrinogen, and BSA (control) was determined by colorimetry (OD650) after the culture of MKN45 cells at various pHe for 12 hours. The cell adhesion to ECM protein components was the lowest under acidic conditions (pHe 6.0). The proportion of MNK45 cells adhering to ECM components increased in the slightly alkaline extracellular medium (pHe 7.5) compared to more acidic groups (pHe 6.0 and 6.5). An acidic extracellular environment still reduced the ability of MKN45 cells to adhere even in the presence of ascites.

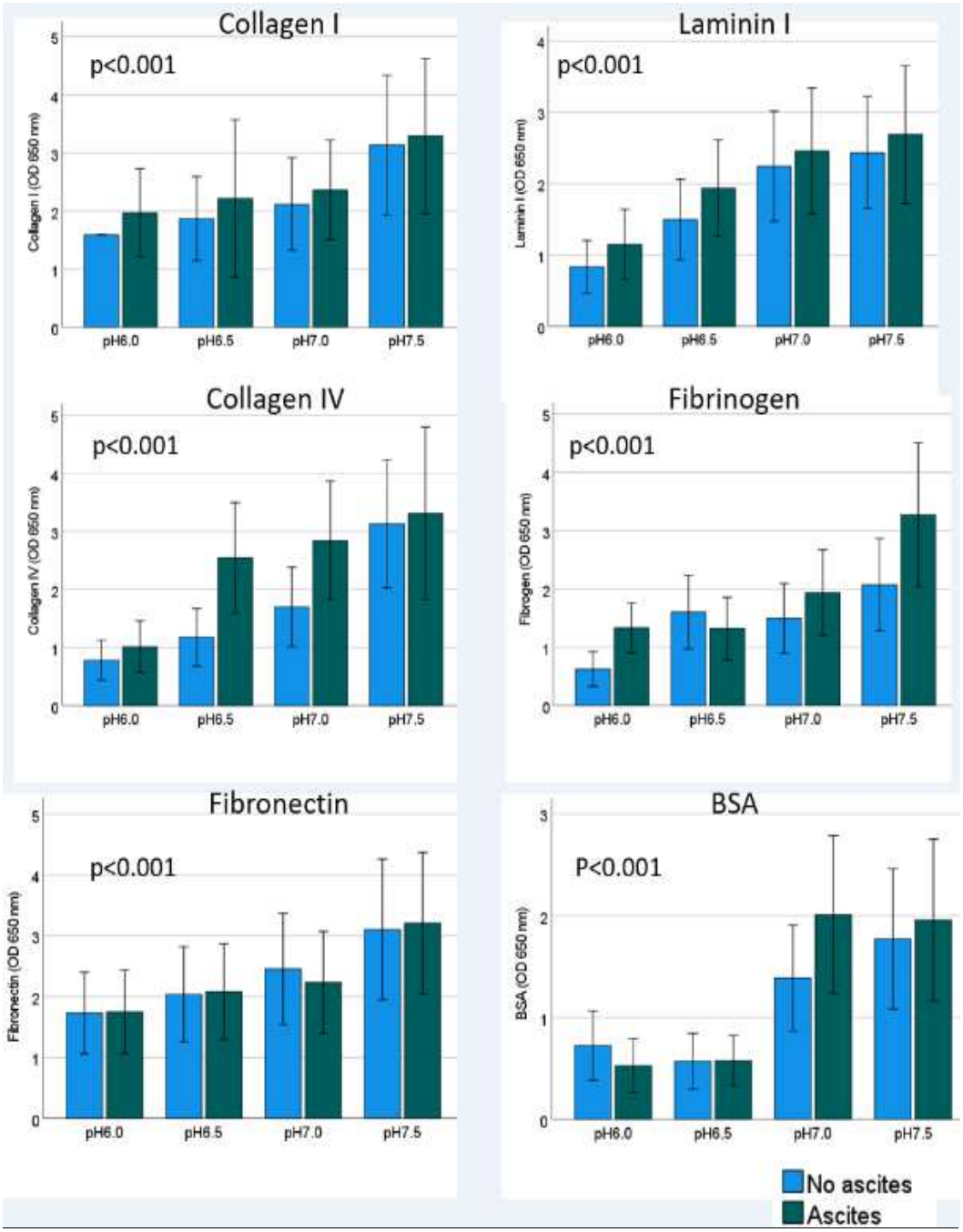

Figure 12. *Influence of pHe on MKN45 gastric cancer cells adhesion with or without ascites*

The adhesion assay shows the influence of pHe on MKN45 cells at different pHe with or without 10% malignant human ascites of gastric origin: the adhesion ability to Collagen I; Laminin I; Collagen IV; Fibrinogen; Fibronectin; BSA increased with pHe. Adhesion to various substrates increased with 10% ascites. The highest adhesion was observed at alkaline pHe in the presence of ascites, in particular for fibrinogen.

Similarly, the influence of different pHe conditions on the adhesion of OAW42 ovarian cancer cells was determined after 24 hours at various pHe. Figure 13 illustrates quantitatively the adhesion of these cells to ECM protein at various pHe. The OD650,

an indirect measure of the number of adherent cells, was the lowest at pHe 6.0. As expected, the OD650 was the highest in a slightly alkaline extracellular environment (pHe 7.5). Malignant ascites increased the adhesion ability of cancer cells, especially at pHe 6.5, where a significant difference (p<0.05) was noted. The presence of ascites did not eliminate this difference; an acidic extracellular environment still reduced the adhesion ability of ovarian cancer cells.

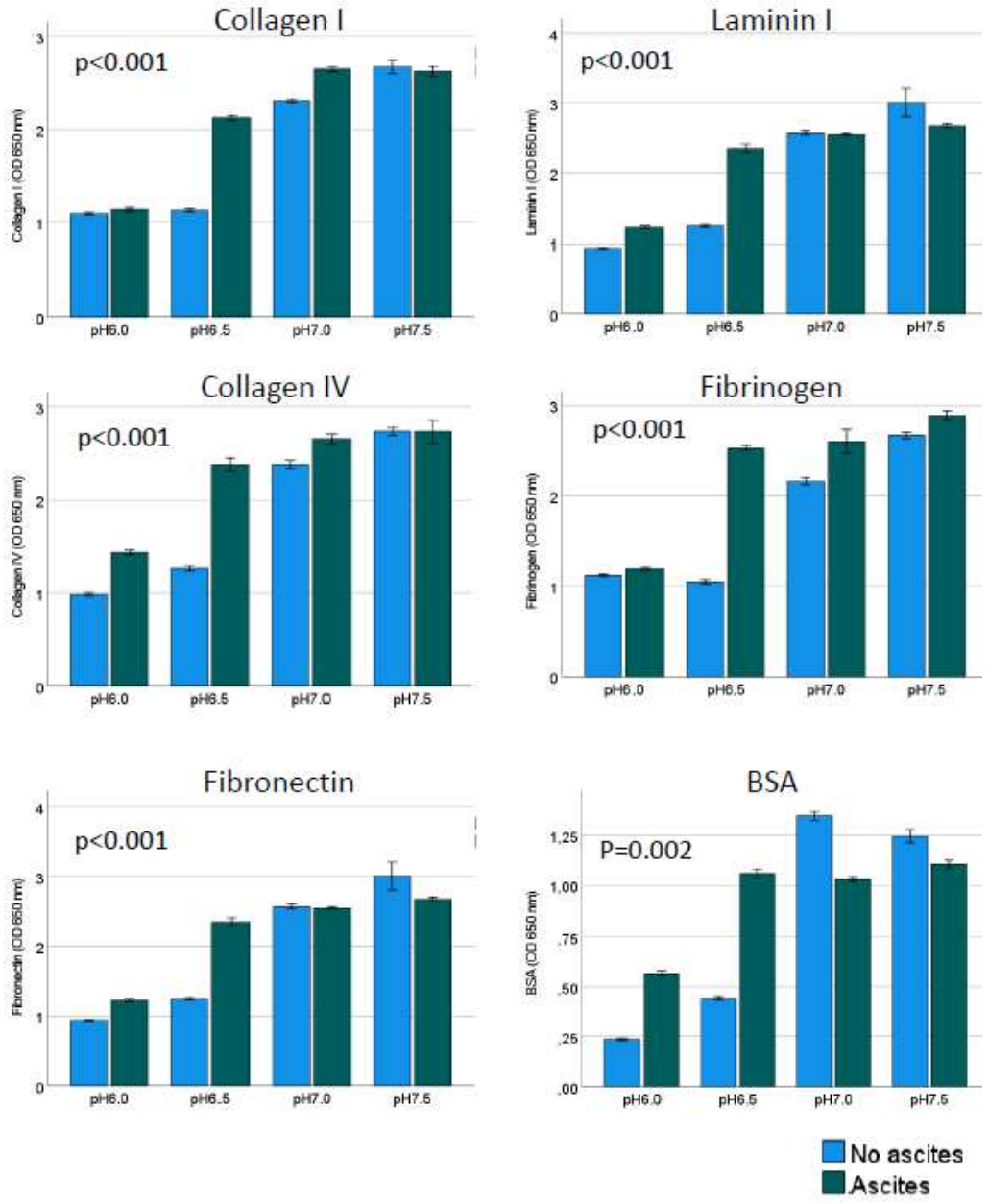

Figure 13. *Influence of pHe on OAW42 ovarian cancer cell adhesion with or without ascites*

Thus assay shows the influence of pHe on the adhesion of OAW42 cells onto various substrates with or without malignant ovarian ascites: the adhesion ability to Collagen I;

Laminin I; Collagen IV; Fibrinogen; Fibronectin, and BSA increased with pHe. The presence of 10% ascites further enhances the adhesion ability, at various pHe. (modified from Yang et al., 2022)

The migration of MKN45 cells depends on the environmental pH.

Scratch-wound assays measure cell migration parameters ammeters parameters such as speed, persistence, and cellular polarity. Figure 14 shows MKN45 cells' migration ability at four different pHe in the presence or not of malignant gastric ascites, as monitored by in-situ micro-cinematography (Cell-Owl) over 72h. The percentage of wound closure rate in MKN45 gastric cancer cells was higher in a slightly alkaline extracellular environment (pHe 7.5) compared with an acidic extracellular environment (pHe 6.0) (p<0.001). Gastric cancer cell mobility declined together with pHe. Malignant ascites did not affect MKN45 migration ability in gastric cancer cells: pHe had the same effect on MKN45 with or without 10% of malignant gastric ascites, and there was still a significant difference between pHe 7.5 and pHe 6.0 (p<0.001) in the presence of ascites.

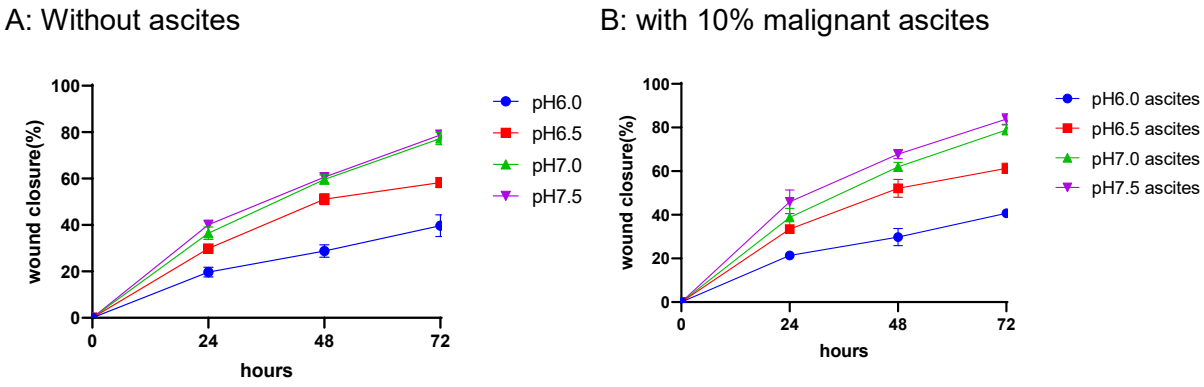

Figure 14. *Influence of pHe on the migration of MKN45 human gastric cancer cells with or without medium enrichment with ascites*

Panel A: The scratch assay shows the migration ability of MKN45 human gastric cancer cells at different pHe without ascites (Panel A) and with 10% ascites (Panel B) from human patients with gastric cancer. Panel B: The acidic environment inhibits the migration ability of gastric cancer cells, the effect of malignant ascites is marginal.

OAW42 cells migrated faster than MKN45 cells. The wound closure rate was 100% already after 36 hours. OAW42 cells' migration ability decreased in an acidic

extracellular environment (Figure 15), the difference between pHe 6.0 and 7.5 was highly significant (p<0.001). In the presence of ascites, OAW42 ovarian cancer cells showed higher migration ability at an acidic pHe vs. MKN45 cells. Significant differences in the migration ability were observed at 24 and 36 hours between pHe 6.0 and 6.5 without ascites and between pHe 6.0 and 6.5 in the presence of 10% ascites (p<0.005).

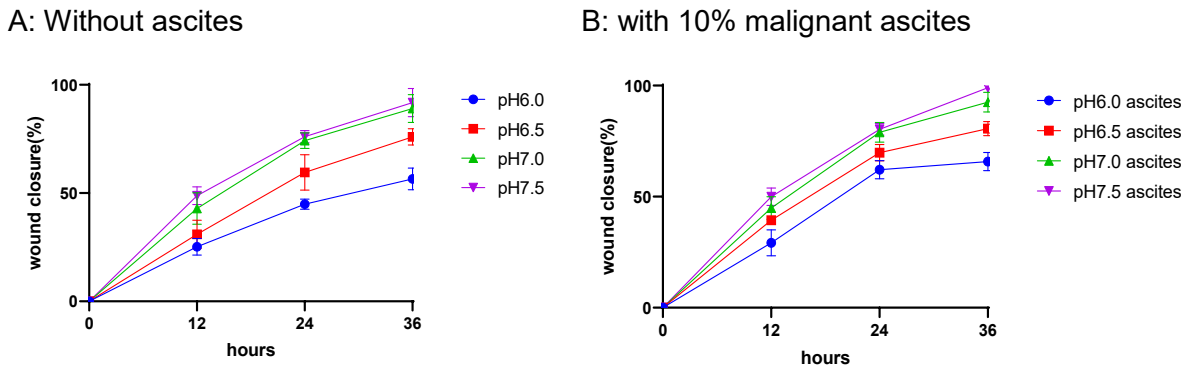

Figure 15. *Influence of pHe on the migration of OAW42 with or without 10% malignant ascites*

Scratch assay showing the migration ability of OAW42 cells at different pHe (Panel A) and with 10% ascites (Panel B). The acidic environment inhibited the migration ability of ovarian cancer cells, and the presence of ascites stimulated cancer cell migration. Migration was monitored by multichannel micro-cinematography in situ.

3D cancer spheroid model culture in different pH conditions

Microscopy

We created 3D gastric cancer spheroids in RPMI cell culture medium. After seven days, the cell culture medium was titered to different pHs (pHe 6.0, pHe 6.5, pHe 7.0, and pHe 7.5), and cell morphology was monitored by light microscopy. Evolution was photo documented at a 10x magnification on days 0, 3, 5, and 7.

On the next page, Figure 16 shows that all 3D spheroids had the same size at day 0, independently of pHe. Later on, an alkaline extracellular environment encouraged tumor growth: the diameter increased by six to seven times at pHe 7.0 and 7.5 groups,

vs. three times at pHe 6.5. However, highly acidic extracellular (pHe 6.0) inhibited 3D gastric cancer spheroid growth.

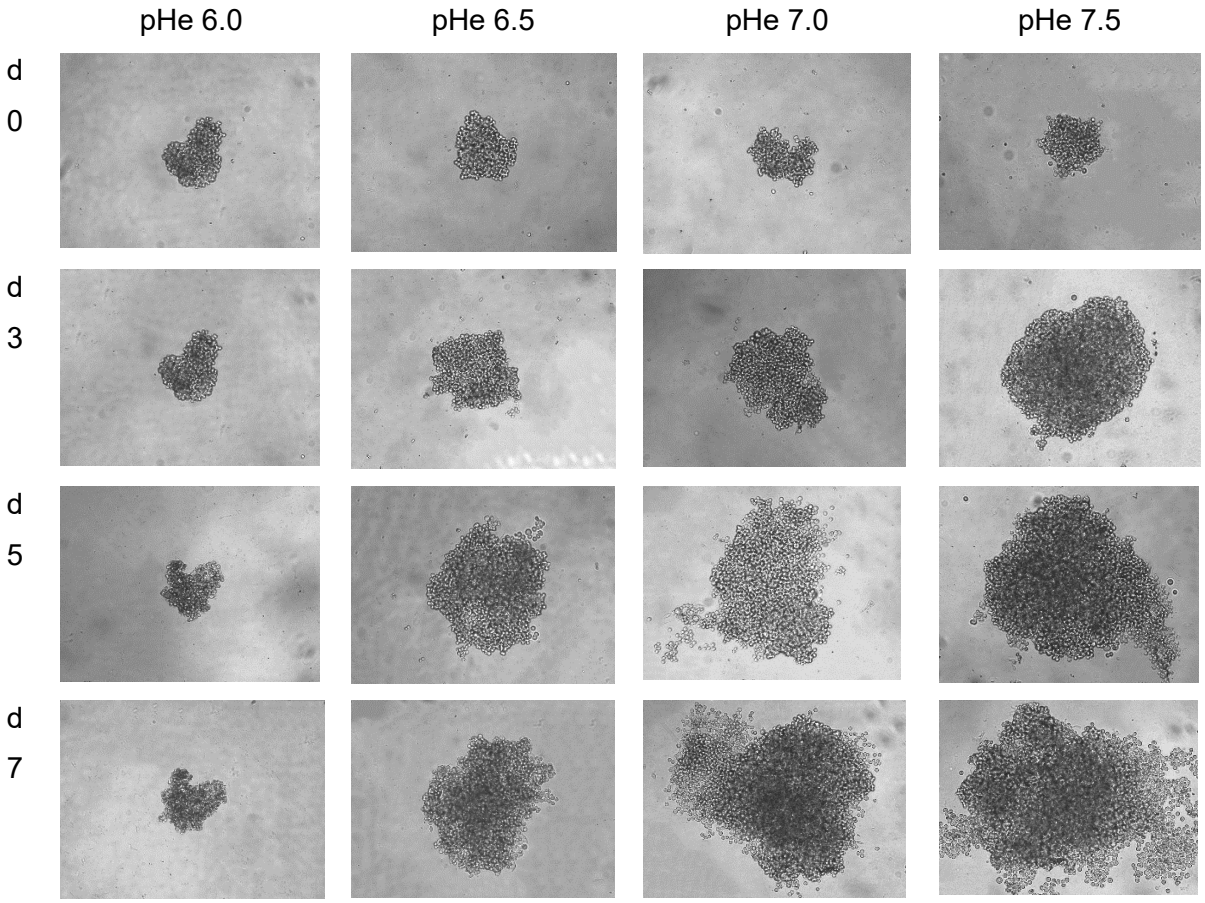

Figure 16. *Extracellular pH influence on 3D gastric cancer spheroid growth*
Light microscopy (magnification 10X) shows ovarian cancer spheroids with barely any change in the lower pHe = 6.0, vs. rapid growth in the slightly alkaline environment (pHe range: 7.0 – 7.5)

The corresponding surface area was then calculated from the radius of the 3D spheroids. Figure 17 shows that 3D spheroids surface area after seven days differed significantly within the pHe range examined (p<0.0001). Whereas there was no measurable growth at pH 6.0, the 3D spheroids grew exponentially at pHe 7.5.

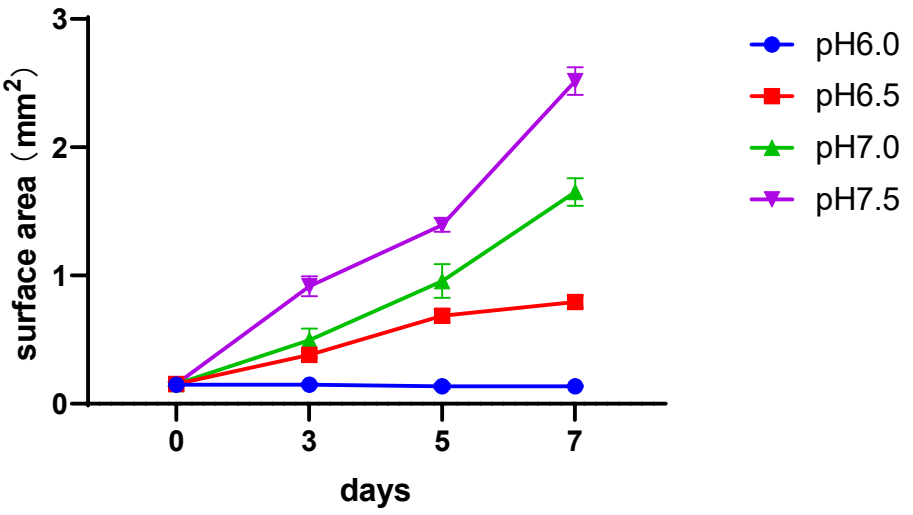

Figure 17. *Effect of extracellular pH on the surface area of 3D gastric cancer spheroids*

The surface area reflected the growth of the 3D gastric cancer spheroids, and the surface area of spheroids increased with pH.

We then reproduced the experiment with a 3D ovarian cancer spheroid model in a DMEM culture medium. The cell culture medium was titered to different pHs (pHe 6.0, pHe 6.5, pHe 7.0, and pHe 7.5) over seven days, and cell growth was monitored by light microscopy (magnification 10X). As Figure 18 shows, on day 0, all 3D spheroids had the same size, independently of pHe. Similarly, to gastric spheroids, 3D ovarian cancer spheroids grew faster in an alkaline extracellular environment: the growth rate was twelve to fifteen times higher at pHe 7.0 and 7.5. In contrast, ovarian cancer spheroids showed little to no growth at pHe 6.0 to 6.5. Therefore, an acidic extracellular environment can inhibit the growth of ovarian cancer spheroids.

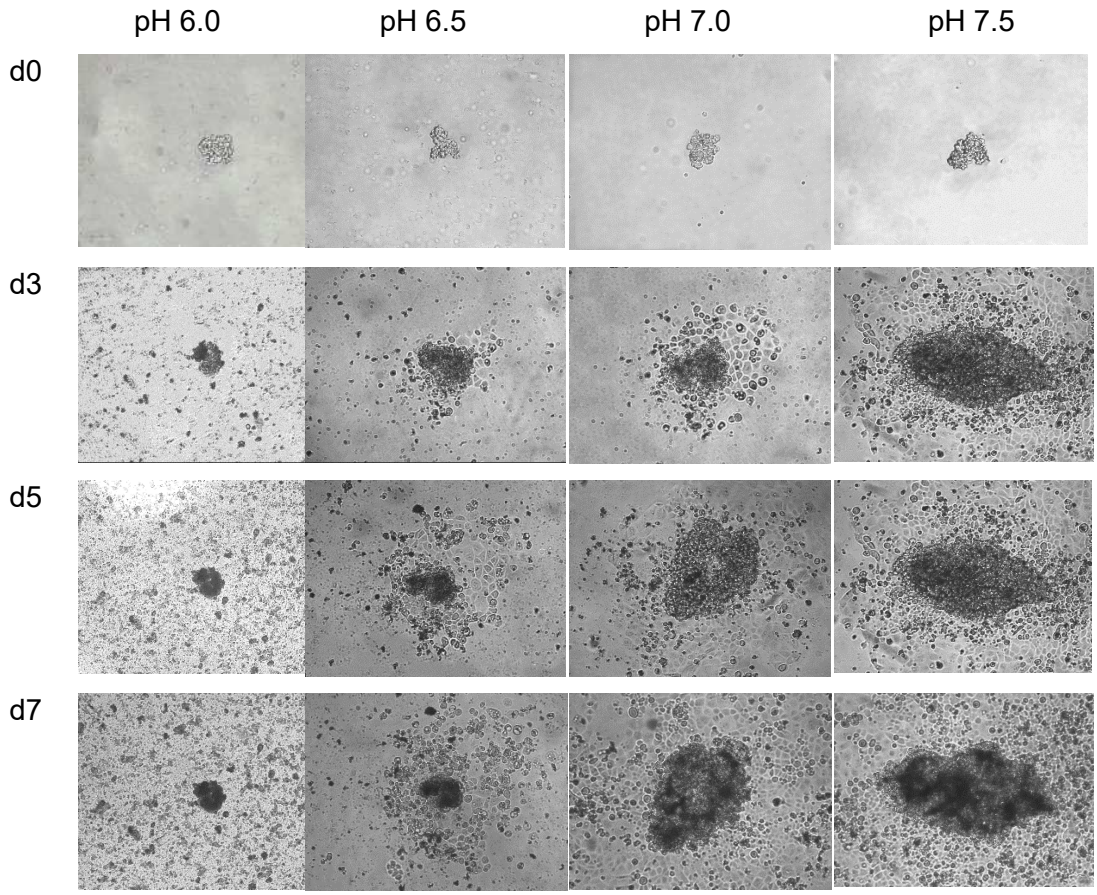

Figure 18. *Extracellular pH influence on 3D ovarian cancer spheroid growth*
Light microscopy (magnification 10X) shows ovarian cancer spheroids inhibited growth in the lower pH group and rapid growth in the slightly alkaline environment (pHe range: 6.0, 6.5, 7.0, 7.5; period of observation = 7 days).

The surface area of the 3D spheroids was calculated, and a highly significant difference between different pHe was documented after seven days (p<0.0001). (Figure 19).

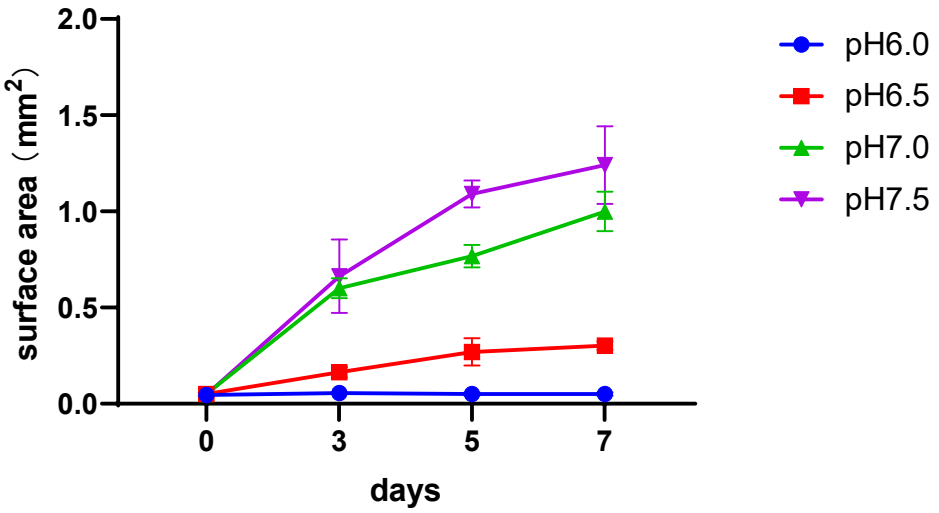

Figure 19. *Effect of extracellular pH on the surface area of 3D ovarian cancer spheroids*

The surface area reflected the growth of the 3D ovarian cancer spheroids, and the surface area of spheroids increased with pHe.

- Scanning electron microscopy (SEM)

After breeding 3D gastric cancer spheroids at different pHe in culture mediums for seven days, we fixed them with 4.5% formaldehyde/ 2.5% glutaraldehyde and examined their surface by scanning electron microscopy at magnification 570X.

(The remaining page is left empty for better reading of the following figure)

As Figure 20 shows, the cell surface of MKN45 3D spheroids cultured at pHe 6.0 was irregular. In contrast, at pHe 6.5, 7.0, and 7.5, the surface of the spheroids was smoother and more flattened.

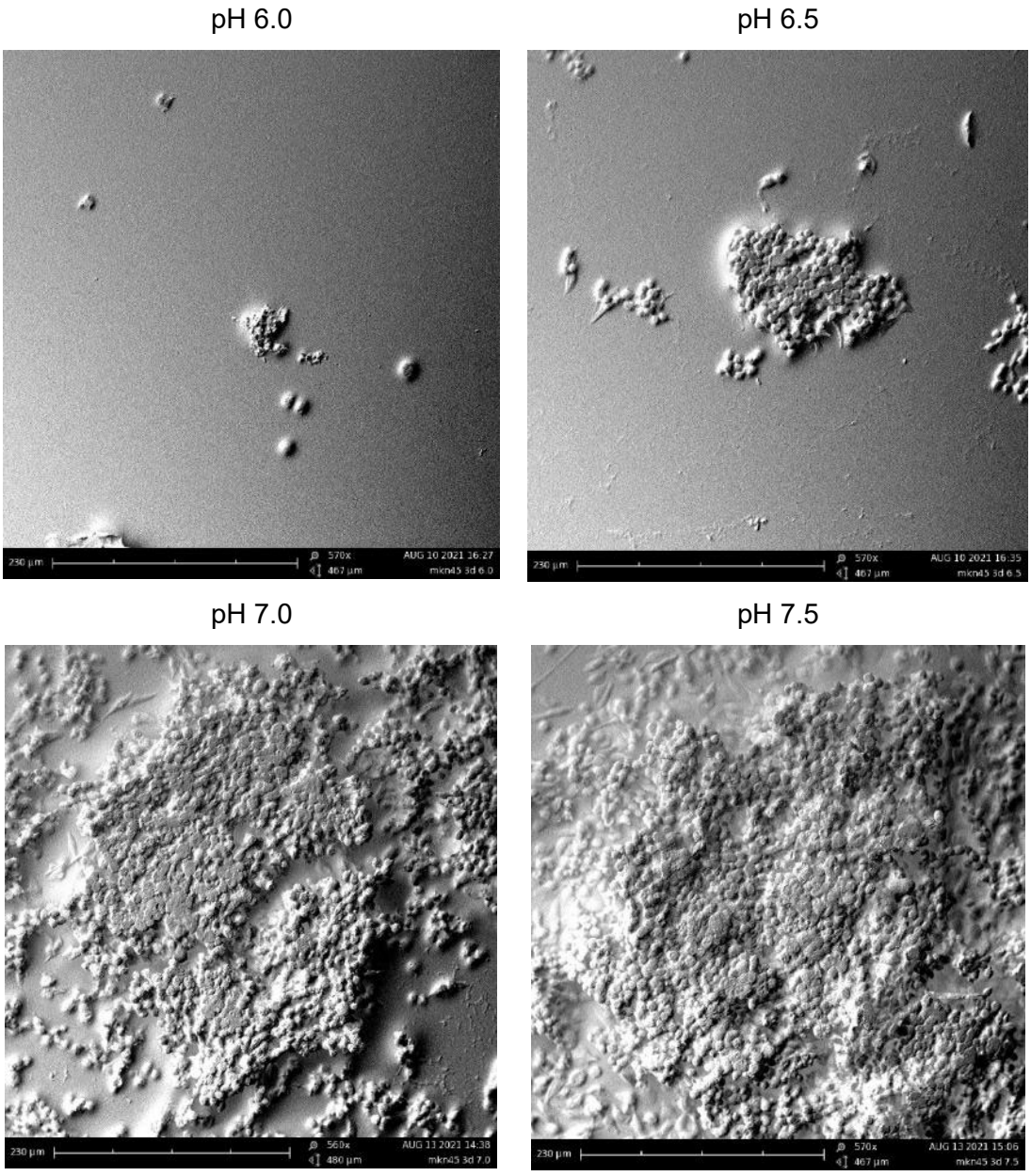

Figure 20. *3D MKN45 gastric cancer spheroid surface at different pHe*
Scanning electron microscopy shows that in an acidic environment (pHe 6.0), the surface of 3D spheroid cells was uneven, and tumor cell rupture and shrinkage can be seen.

As Figure 21 shows that the surface of OAW42 3D spheroids cultured at pHe 6.0 and 6.5 was irregular. Some structures with no characteristic cell form can be seen, corresponding probably to cell fragments. In contrast and in analogy with gastric cancer cells, the organoid surface was flattened at pHe 7.0 and 7.5.

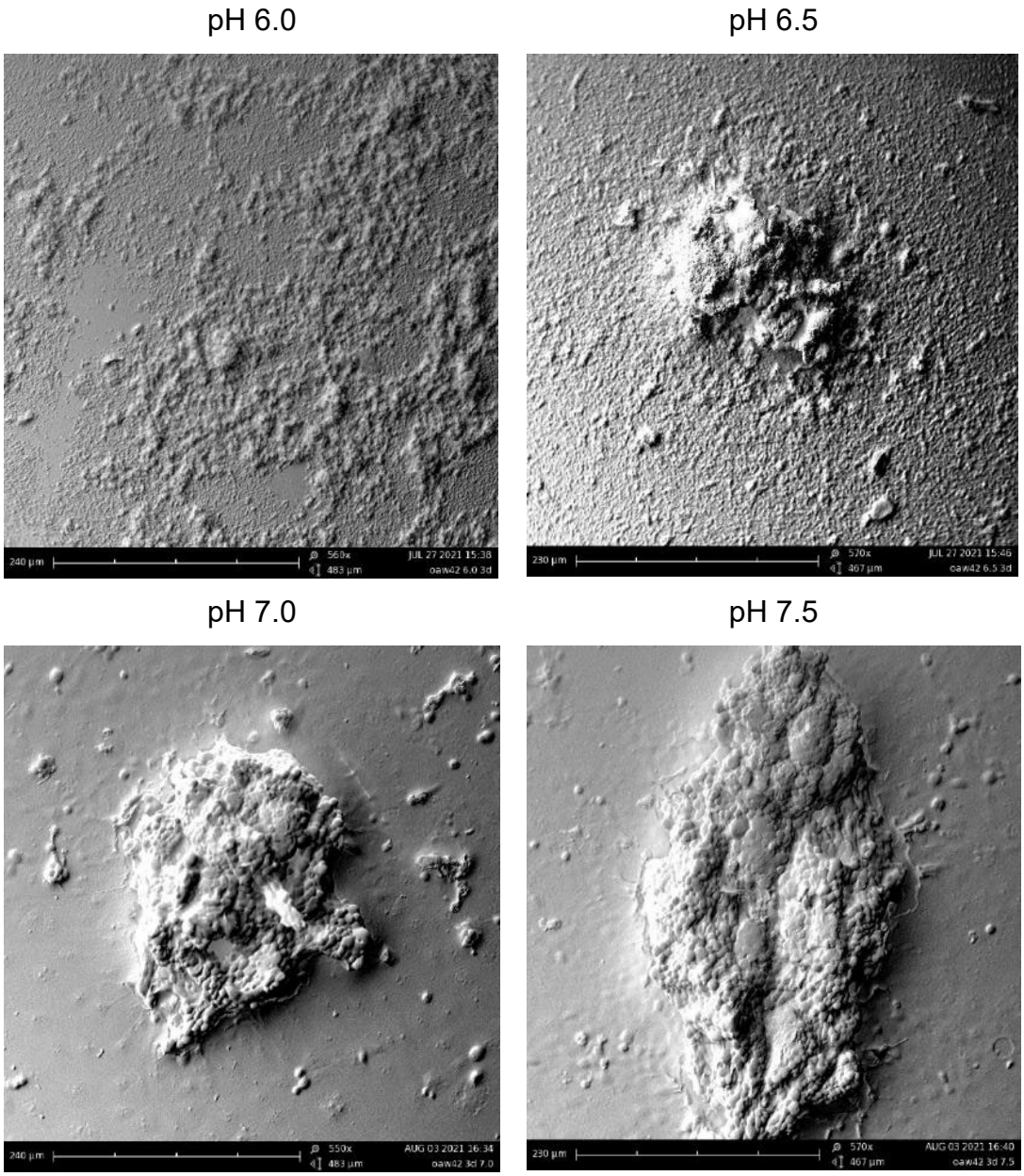

Figure 21. *3D ovarian cancer spheroid surfaces of OAW42 in different pHe*
Scanning electron microscopy shows that in an acidic environment (pHe 6.0 and 6.5), the surface of 3D spheroid cells was uneven, and tumor cell rupture and shrinkage can be seen. (modified from Yang et al., 2022)

Physical-chemical characterization of ascites

Metabolic parameters in malignant ascites

Figure 22 shows the correlation of different metabolic parameters in malignant ascites. pHe was positively correlated with K^+, glucose, lactate, and cancer stage and negatively correlated with pCO_2, Cl^-, and Ca^{2+}. The correlation coefficients in the heatmap below indicate that tumor stages were positively correlated with pH, pCO^2, pO^2, K^+, Ca^{2+}, glucose, and lactate concentration in malignant ascites. There was a positive correlation between the presence of malignant ascites and K^+, lactate, and glucose. Inversely, the absence of ascites correlated with pCO_2, Ca^{2+}, and Cl^-.

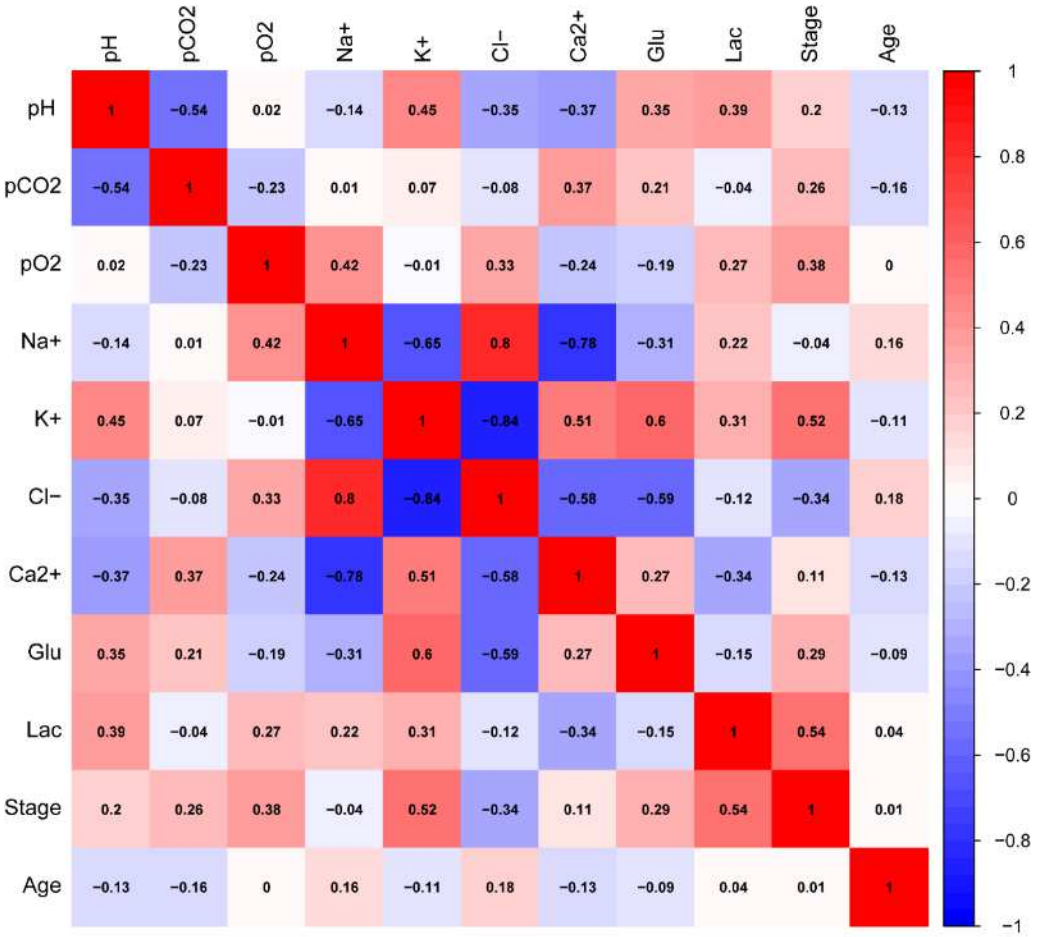

Figure 22. *Correlations of different physical-chemical parameters in malignant ascites*

Correlation of physical-chemical parameters of ascites, pH was positively correlated with K^+, glucose, lactate, and cancer stage, and negatively correlated with pCO_2, Cl^-, and Ca^{2+}.

Intraperitoneal pH in cancer vs. control patient

The mean and standard deviation of intraperitoneal pH in cancer patients is 7.60±0.38, and the control group is 6.99±0.19. It is highly significant between cancer and control groups (p<0.0001). Figure 23 shows that malignant ascites were significantly and consistently more alkaline than the control.

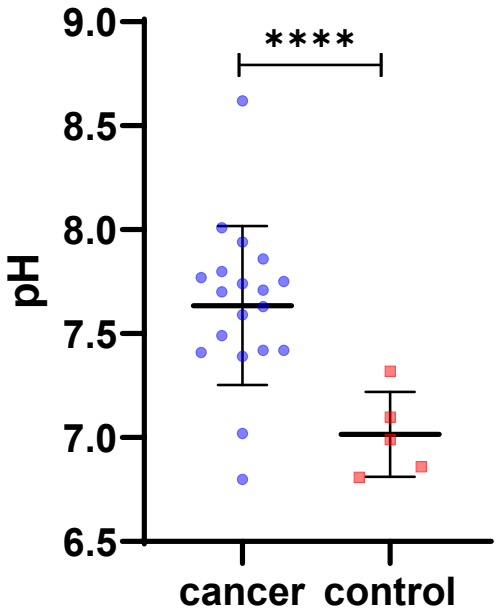

Figure 23. *Intraperitoneal pH in cancer vs. control patients*
The pH was measured by a blood-gas analyzer from 19 patients with malignant and 5 with benign disease patients, p<0.0001.

The mean and standard deviation of intraperitoneal pH in stage II-III ovarian cancer patients is 7.50±0.27, and pH in stage IV is 7.81±0.20 (p<0.05), as shown in Figure 24.

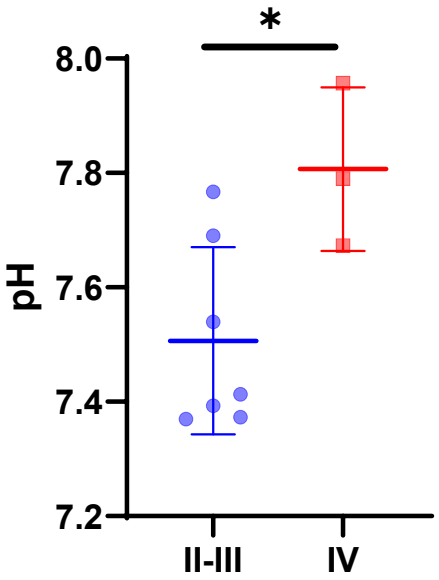

Figure 24. *Intraperitoneal pH in ovarian cancer Stages III vs. IV patients*
The pH in stage IV was significantly higher than in stage II-III, p<0.05. (modified from Yang et al., 2022)

Electrolytes

As Table 6 shown, the mean and standard deviation of malignant ascites electrolytes (Na^+, K^+, Cl^-, Ca^{2+}) were lower than control groups. Primarily there is significant hypocalcemia and hypochloremia in ascites (p< 0.0001).

Table 6. *Electrolytes concentration in malignant ascites and benign lavage*

Parameter	Units	Malignant ascites	Control	P-Value
Na^+	mmol/L	140.23±9.34	143.47±2.00	0.006
K^+	mmol/L	3.78±1.16	4.62±1.37	0.431
Cl^-	mmol/L	118.56±14.01	147.53±4.03	<0.0001
Ca^{2+}	mmol/L	1.02±0.41	2.18±0.18	<0.0001

Figure 25 illustrates the positive correlation between pH and K^+ concentration in malignant ascites (R=0.54, p<0.0001), and negative correlation between pH with Ca^{2+}(R=-0.35, p=0.007), Cl^- (R=-0.33, p<0.05), and Na^+ (R=-0.31, p<0.05).

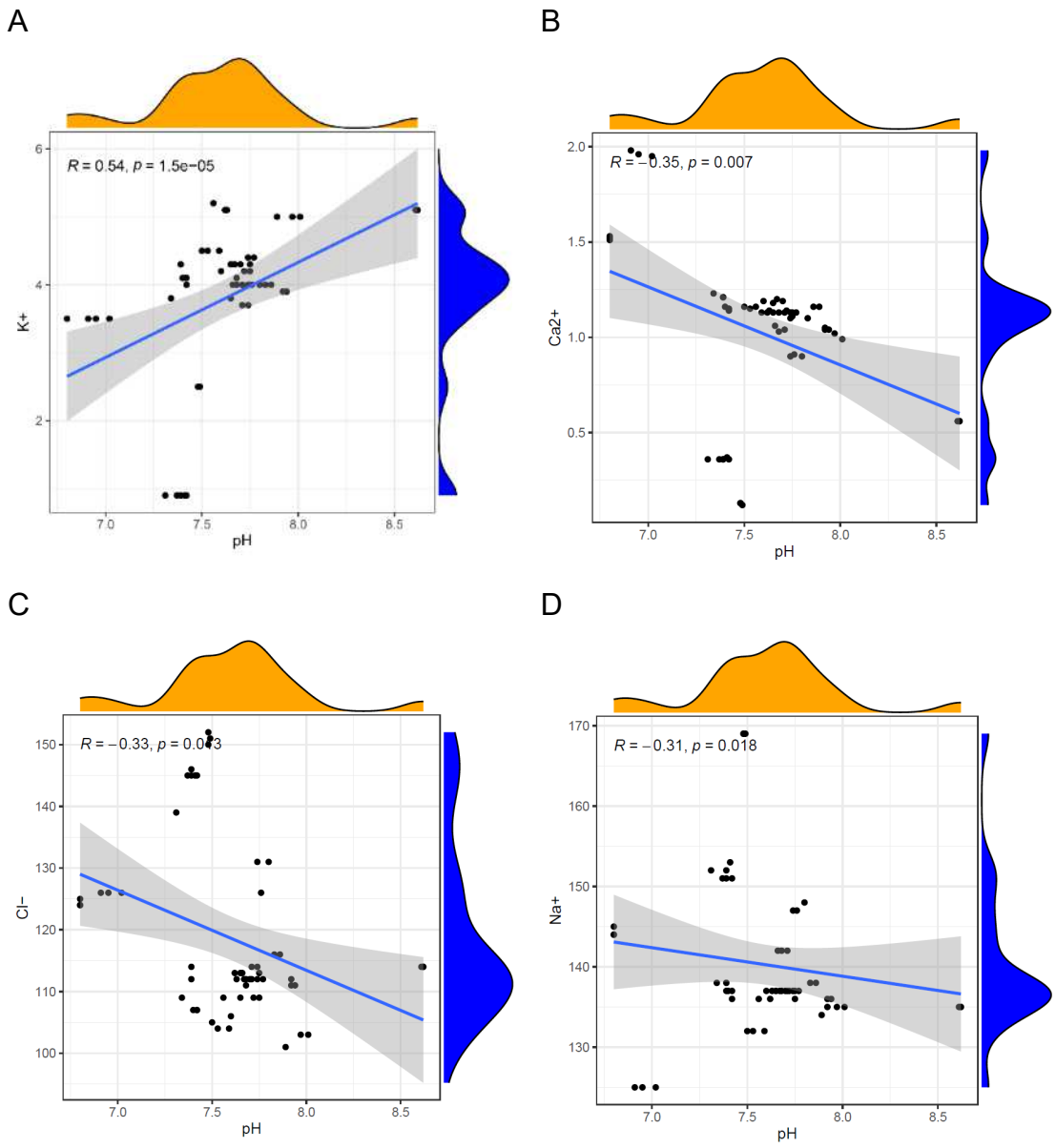

Figure 25. *Correlation between pH and K^+(A), Ca^{2+}(B), Cl^-(C), Na^+(D) in cancer patients (n=19)*

Spearman analysis between pH and electrolytes concentrations in malignant ascites. Correlation between pH and electrolytes: panel A) K^+; B) Ca^{2+}; C) Cl^-, and D) Na^+, p<0.05.

Partial gases distribution (pCO_2, pO_2)

Table 7 shows that pO_2 and pCO_2 were significantly higher in malignant ascites than in the control group. In malignant ascites, pCO_2 increased four-fold (p< 0.0001), indicating an increased hypercarbia level. Interestingly, malignant ascites were not hypoxic compared to the control.

Table 7. *The mean and standard deviation of malignant ascites and lavage gas distribution*

Parameter	Units	Cancer ascites	Control (lavage NaCl 0.9%)	P-Value
pCO_2	mmHg	24.49±31.25	6.92±1.16	<0.0001
pO_2	mmHg	183.42±16.74	173.75±9.49	0.033

Metabolites (Glucose, Lactate)

Malignant ascites are more nutrient-rich than the control. Table 8 shows that lactate and glucose concentration in malignant ascites was higher than in the control (p<0.001). Ascites contain about eight times more glucose than lavage fluid and nearly six times more lactate than the control group.

Table 8. *The mean and standard deviation of malignant ascites and lavage metabolism*

Parameter	Units	Cancer ascites	Control (lavage NaCl 0.9%)	P-Value
Glu	mg/dL	71.23±34.06	9.00±9.06	<0.0001
Lac	mmol/L	2.15±1.50	0.32±0.04	<0.0001

As shown in Figure 26, the mean and standard deviation of lactate in stage III cancer patients is 1.34±0.87, and in the stage IV group is 2.70±1.59. These two stages have a significant difference (p<0.05).

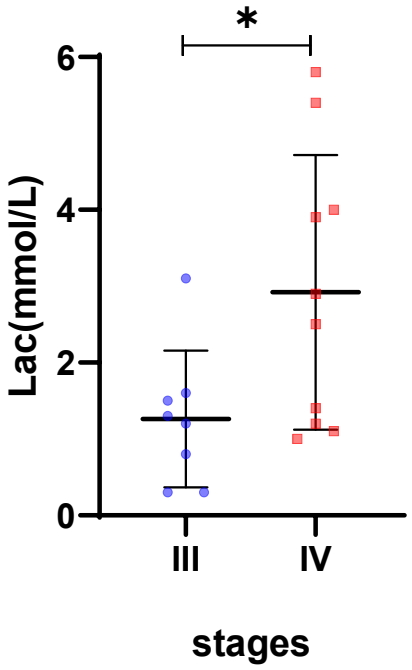

Figure 26. *Lactate concentration of malignant ascites at stage III versus stage IV*
The lactate concentration in stage IV was significantly higher than in stage III, $p<0.05$.

According to Figure 27, the pH value was positively correlated with lactate concentration (R=0.26, $p<0.05$) and glucose (R=0.48, $p=0.00014$) in malignant ascites.

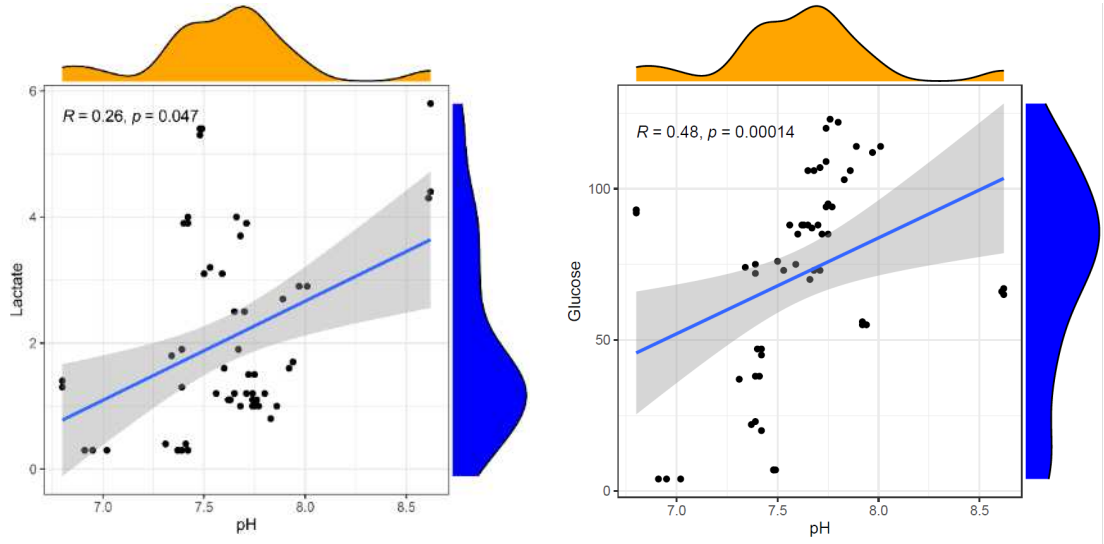

Figure 27. *Correlation between pH and lactate(left panel) and glucose(right panel) in cancer patients*
Spearman analysis between pH and lactate and glucose concentrations in malignant ascites. Positive correlation between pH and lactate(left panel) and glucose(right panel), $p<0.05$.

Deep-phenotype analysis of ovarian cancer

Clinical information on ovarian cancer patients

Ascites samples were obtained from ovarian cancer patients undergoing open surgery for the removal of gynecologic malignancies. Table 9 illustrates the clinicopathological characteristics of the patients. Prior to ascites collection, none of the patients underwent any treatment. Additionally, the patient diagnosed with clear cell carcinoma did not have endometriosis.

Table 9. *Clinic opathological characteristics*

Number of patients	10
Age (mean±SD)	65.30 ± 9.67
Gender	Female
Cancer Type	Ovarian cancer
BMI (Kg/m^2) (mean±SD)	25.16 ± 8.86
ECOG	
0	6 (60%)
1	2 (20%)
2	1 (10%)
3	1 (10%)
Histology	
High-grade serous carcinoma	8 (80%)
Low-grade serous carcinoma	1 (10%)
Clear cell carcinoma	1 (10%)

Federation of Gynecology and Obstetrics Stage (FIGO)	
Stage II	1 (10%)
Stage III	6 (60%)
Stage IV	3 (30%)
T Stage	
T2	1 (10%)
T3	7 (70%)
Tx	2 (20%)
N Stage	
N0	3 (30%)
N1	5 (50%)
Nx	2 (20%)
M Stage	
M0	4 (40%)
M1	2 (20%)
Mx	4 (40%)

Primary surgery	
Stage II	1 (100%)
Stage III	5 (83%)
Stage IV	2 (66%)

Residual disease	
Stage II	R0: 1 (100%)
Stage III	R0: 2 (33%), R1: 3 (60%), R2: 1 (17%)
Stage IV	R2: 3 (100%)

Legend: Residual disease after surgery was reported as R0, R1, and R2. R0 was defined as no macroscopic residual disease. R1 and R2 were defined as macroscopic residual disease with maximal diameter of <1 cm and >1 cm, respectively. (modified from Yang et al., 2022)

The analysis of differential genes between cancer cells in ascites versus primary and metastatic cancer cells primarily emphasizes metabolic and immune pathways.

In cellular experiments, we observed an augmentation in the biological properties of

cancer cells induced by malignant ascites. Subsequently, we delved into the genetic impact of malignant ascites on cancer cells. We conducted an analysis of the GSE73065 database (Gao et al., 2019b) to identify differential gene expression between ascites and primary cells, employing criteria of $\log_2|FC| > 1$ and $p < 0.05$. In comparison to primary cancer cells, ascites cells exhibited the expression of 517 upregulated genes and 222 downregulated genes. As illustrated in Figure 28, GSEA demonstrated that genes in ascites cells were significantly enriched in metabolic pathways, such as glycolysis and oxidative phosphorylation, as well as immune responses, including complement and inflammatory response, in comparison to primary cells ($p < 0.05$). The top five ascites cells Gene Ontology (GO) also enriched in immune responses.

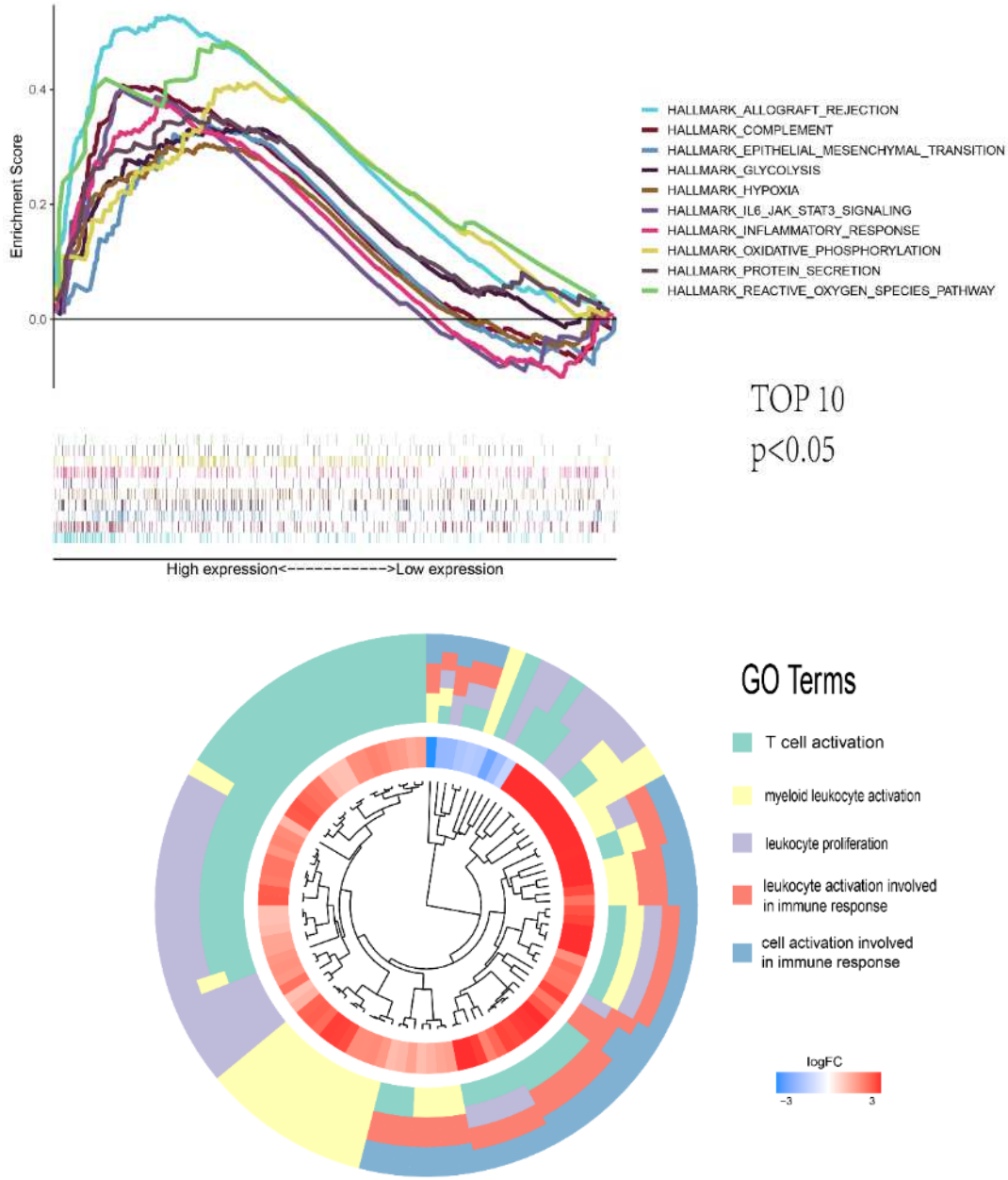

Figure 28. *Bioinformatics analysis was performed on ascites ovarian cancer cells in comparison to primary or metastatic cancer cells.*
Gene Set Enrichment Analysis (GSEA): The upper panel displays the first ten hallmark gene sets of ascites cells versus primary cells ($p < 0.05$). The lower panel depicts circle plots illustrating Gene Ontology (GO) pathway enrichment data for differentially expressed genes in ascites cells ($p < 0.05$). (modified from Yang et al., 2022)

Univariate analysis of malignant ovarian ascites polar, lipid metabolomics, and cytokines

Table 10 presented the physical-chemical parameters, polar metabolites, lipid

metabolites, and cytokines in stages II-III and I of malignant ovarian ascites.

Table 10. *Full matrix of all obtained molecular and physical-chemical ascites parameters from ovarian cancers FIGO stages II-II vs. stage IV*

Parameters	Stage II-III	Stage IV
Metabolites		
2-Hydroxybutyrate	2.13±1.42	2.22±0.96
3-Hydroxybutyrate	25.64±15.04	11.31±17.39
3-Hydroxyisobutyrate	0.32±0.17	0.68±0.45
3-Hydroxyisovaleric acid	1.91±1.01	1.81±0.66
Acetate	3.29±0.15	3.29±0.21
Acetone	2.69±4.96	0.57±0.72
Alanine	3.87±1.92	9.73±3.35
Asparagine	1.45±0.62	1.37±0.81
Carnitine	0.74±0.41	1.15±0.87
Choline	0.22±0.19	0.32±0.11
Citric acid	0.74±0.34	0.98±0.19
Creatine	1.34±0.83	1.21±1.21
Creatine phosphate	1.06±0.56	1.44±0.26
Formate	0.86±0.57	0.96±0.22
Glucose	75.72±33.67	138.16±47.17
Glutamate	4.60±3.54	3.75±3.09
Glutamine	7.95±3.73	14.15±1.68
Glutathione	0.45±0.24	0.41±0.07
Glycerol	6.23±2.95	7.27±1.72
Glycine	5.69±3.02	8.58±1.96
Histidine	1.41±0.72	1.79±0.28
Hypotaurine	1.13±0.61	1.92±1.86
Isoleucine	1.49±0.55	2.21±0.31
Lactate	38.13±30.99	69.74±35.05
Leucine	3.25±1.59	3.66±0.60
Lysine	3.36±1.43	4.86±0.82
O-Phosphocholine	0.43±0.19	0.482±0.08
Ornithine	1.47±0.44	1.921±0.68
Phenylalanine	1.08±0.43	3.378±2.75
Proline	2.83±1.73	3.358±1.11
Threonine	4.09±3.09	5.09±0.89
Tyrosine	1.10±0.51	1.69±0.18
Valine	5.09±2.11	7.97±0.93
sn-Glycerol-3-phosphocholine	1.34±0.54	1.26±0.65
CE (Cholesterol Ester)	0.39±0.32	0.32±0.07
FA (Fatty Acids)	0.01±0.01	0.006±0.00
FC (Free Cholesterol)	0.29±0.19	0.26±0.13
LA (Linoleic Acid)	0.03±0.02	0.02±0.01
MUFA (Monounsaturated Fatty Acids)	0.01±0.01	0.008±0.00
PL (Phospholipids)	0.32±0.06	0.20±0.02
PUFA (Polyunsaturated Fatty Acids)	0.03±0.02	0.02±0.00
SFA (Saturated Fatty Acids)	0.10±0.07	0.07±0.01
TC (Total Cholesterol)	0.362±0.29	0.29±0.06
TG (Triglycerides)	0.008±0.01	0.004±0.00
UFA (Unsaturated Fatty Acids)	0.04±0.03	0.03±0.01
w-3 FA (Omega-3 Fatty Acids)	0.08±0.06	0.06±0.01

Table 10 (continued)

Parameters	Stage II-III	Stage IV
Cytokines and chemokines		
MCP-1 (A8)	840.45±1359.80	1998.66±3120.40
IL-6 (A10)	4510.35±3502.17	15267.12±14619.95
IL-8 (B2)	650.87±1138.10	281.04±297.60
IL-10 (B3)	115.67±76.64	166.62±228.32
IL-18 (B6)	179.14±162.49	322.41±283.25
Electrolytes		
pH	7.51±0.16	7.78±0.16
pCO2 (mmHg)	22.05±14.56	17.33±2.08
Na^+ (mmol/L)	142.00±8.04	136.22±1.35
K^+ (mmol/L)	3.24±1.61	4.34±0.63
Ca^{2+} (mmol/L)	0.89±0.38	1.12±0.06
Cl^- (mmol/L)	121.24±17.67	108.77±5.59
Glu (mg/dL)	65.81±33.54	102.78±13.42
Lac (mmol/L)	1.73±1.36	2.10±0.85

As shown in Figure 29, fold change > 1.2, nineteen metabolites and cytokines exhibited upregulation in stage IV compared to stage II and stage III, while twenty-one showed downregulation.

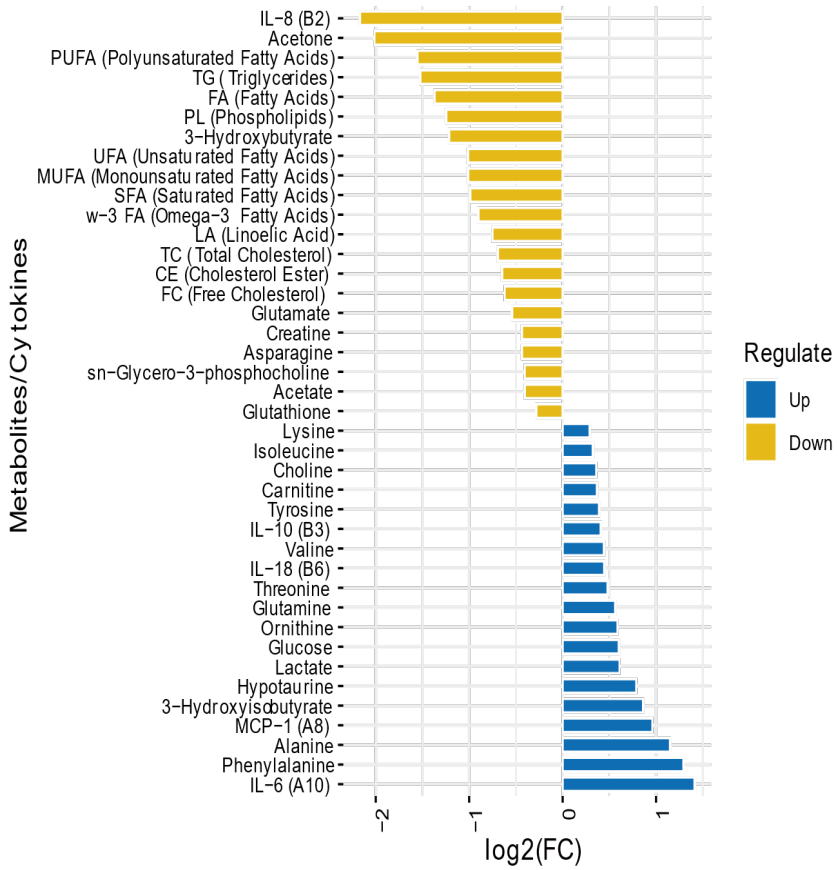

Figure 29. *Differential metabolites and cytokines of malignant ovarian ascites.* Differential metabolites and cytokines, with a fold change of more than 1.2, demonstrated 19 upregulated and 21 downregulated entities in ovarian cancer stage IV compared to stage II-III. (modified from Yang et al., 2022)

With a cutoff at a fold change FC >1.2, corresponding to a probability <0.05, we identified upregulation of alanine, isoleucine, phenylalanine, and glutamine, while 3-hydroxybutyrate was downregulated in OC FIGO stage IV compared to II-III (Table 11).

Table 11. *The fold changes of polar metabolites in ovarian cancers between stages II-III and IV.*

	FC	log2(FC)	raw.pval	-log10(p)
Alanine	0.44628	-1.164	0.002351	2.6288
Isoleucine	0.79325	-0.33415	0.0040014	2.3978
Phenylalanine	0.39805	-1.329	0.014645	1.8343
3-Hydroxybutyrate	2.3475	1.2311	0.02715	1.5662
Glutamine	0.66784	-0.58243	0.049762	1.3031

Figure 30, the volcano plot, illustrates significant differential metabolites upregulated in FIGO stage IV ovarian cancer, including alanine, isoleucine, phenylalanine, and glutamine. 3-hydroxybutyrate was upregulated in FIGO stages II-III.

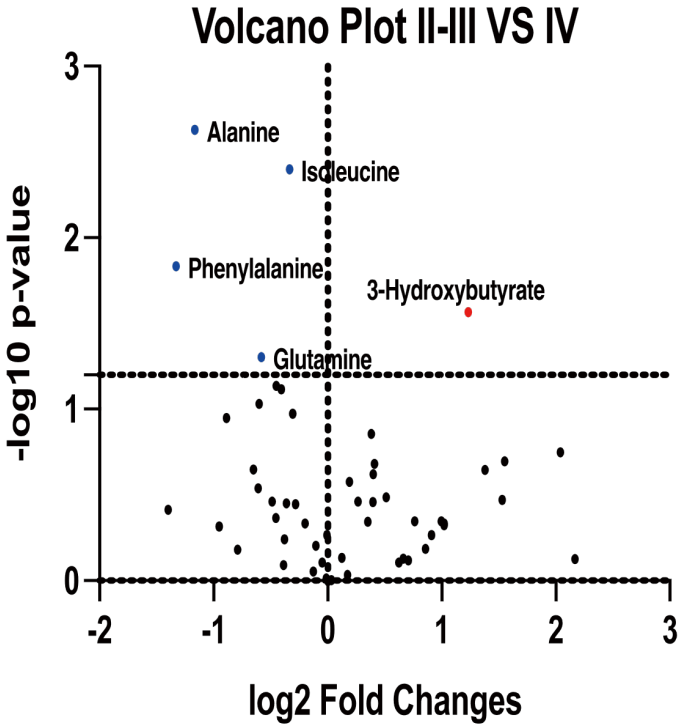

Figure 30. *Volcano plot of significant differential parameters.*
Volcano plot of significant differential metabolites, blue points were upregulated in FIGO stage IV, red points upregulated in stage II-III. (modified from Yang et al., 2022)

In Figure 31, t-test analysis was conducted based on the ovarian cancer patients' stage. Box plots showed that the concentration of alanine, glutamine, isoleucine, and phenylalanine significant upregulated, while 3-hydroxybutyrate was significantly downregulated in ovarian cancer stage IV compared to stage II-III.

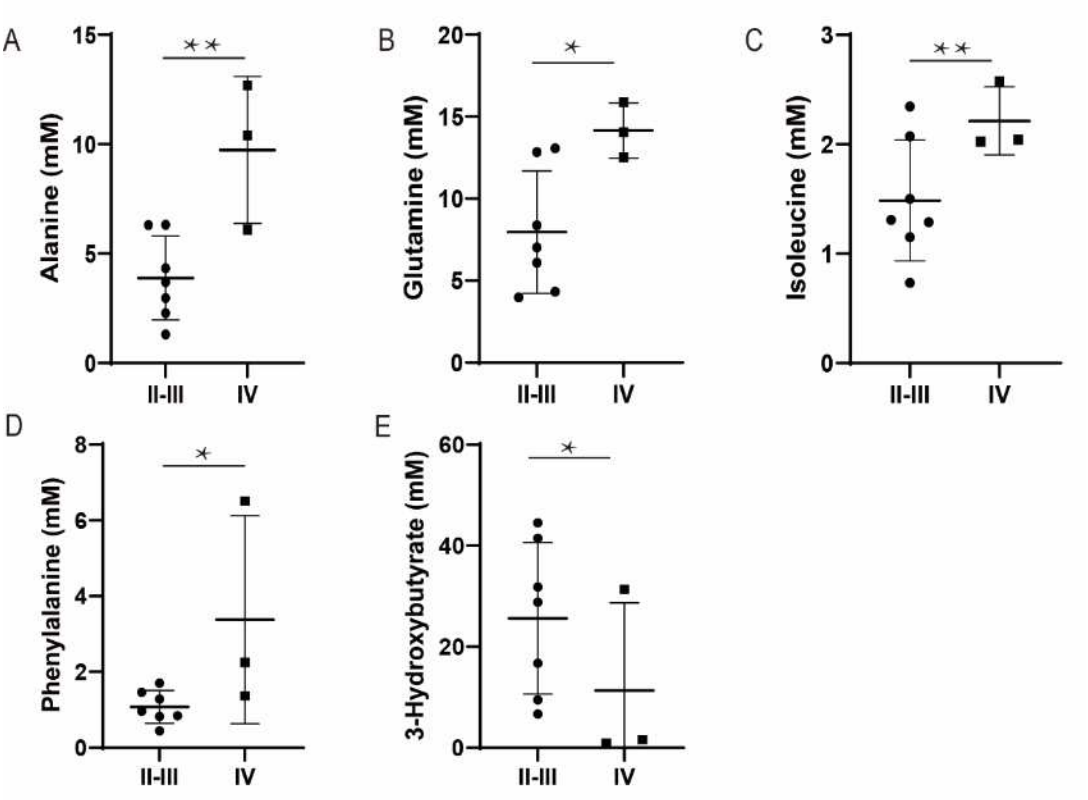

Figure 29. *Significant differential parameters of malignant ovarian ascites.*
Alanine (A), glutamine (B), isoleucine (C), and phenylalanine (D) were significantly upregulated in stage IV. 3-hydroxybutyrate (E) was significantly downregulated in stage IV (*<0.05, **<0.01). (modified from Yang et al., 2022)

As shown in Figure 32, among these metabolites, alanine (R=0.65, p=0.04), glutamine (R=0.65, p=0.041), and phenylalanine (R=0.70, p=0.024) were positively associated with the stage of the disease.

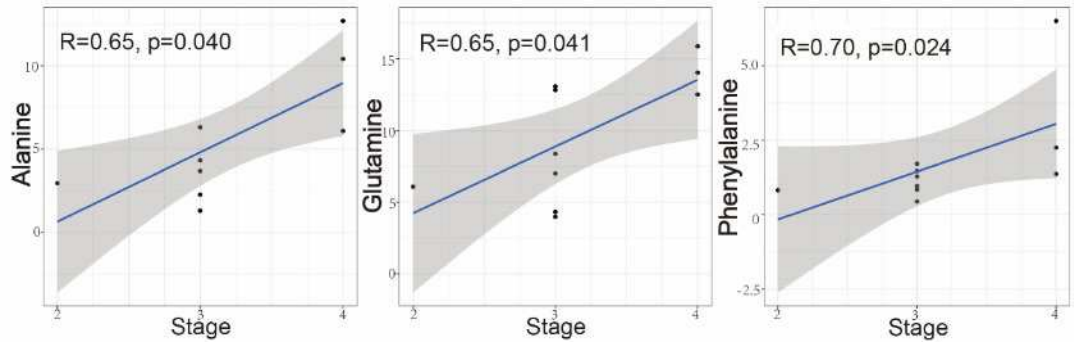

Figure 30. *Amino acid correlations with disease stages*

Alanine, glutamine, and phenylalanine were significantly positively correlated with disease stages.

Multivariate analysis of malignant ovarian ascites polar, lipid metabolomics, and cytokines

PCA and OPLS analyses were subsequently conducted to illustrate the clustering of ovarian cancer ascites based on their metabolic phenotypes.

In Figure 33, the PCA-score plot indicates that ovarian cancer ascites share similar metabolic phenotypes in different stages, with ASC-OC-T-7 in stage IV clustering with ascites in stages II-III. However, the OPLS score plot reveals that the metabolic phenotype of OC ascites varies across each clinical stage.

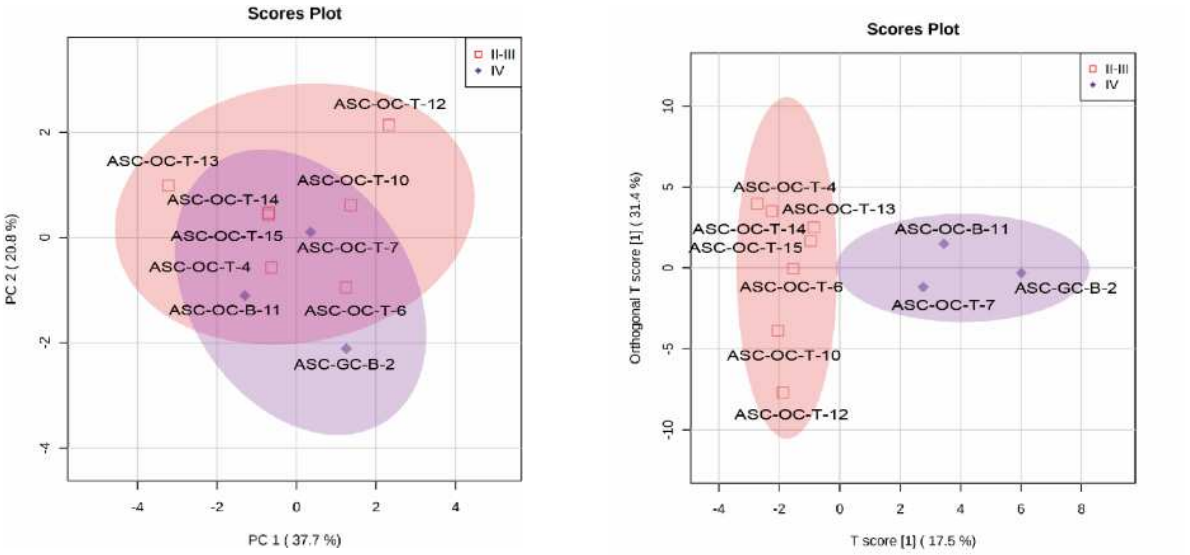

Figure 31. *Ovarian cancer clusters based on different stage metabolic phenotypes*
Principal component analysis (PCA) scores plot of OCs shows a similar metabolic phenotype (left panel). However, the OPLS-scores plot of OCs illustrates clearcut metabolic clustering between patients with OC FIGO II-III vs. FIGO IV (right panel). (modified from Yang et al., 2022)

As shown in Figure 34, the metabolic phenotype of the OC with FIGO stages II-IV varied due to various metabolite involvements. The heatmap further confirms that the clusters of samples are mixed in different FIGO stages.

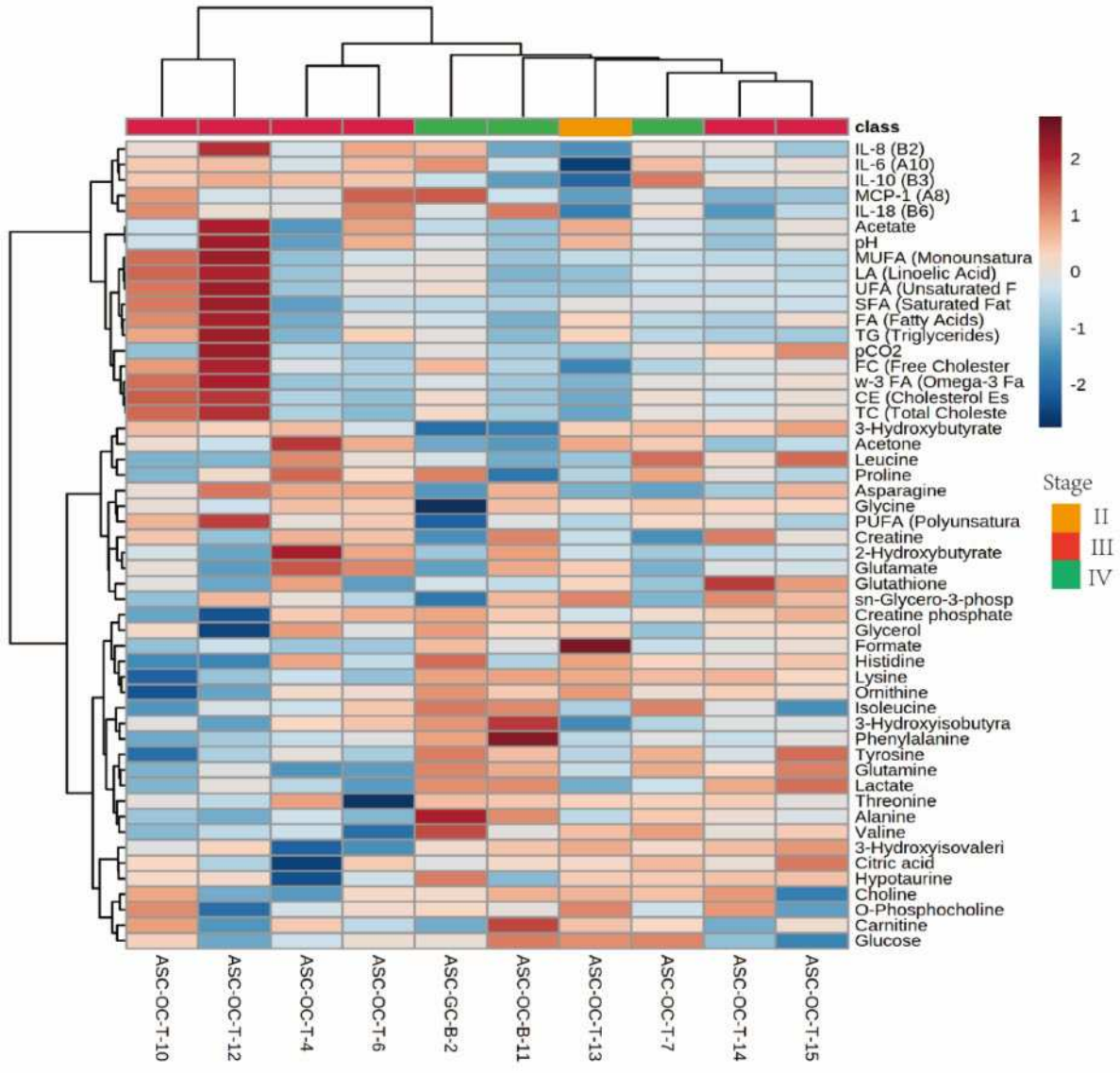

Figure 32. *Heatmap with all the physicochemical, metabolic parameters, and cytokines stratified by tumor stage (ovarian cancer, FIGO stages II-III versus IV).*
Heatmap of all parameters based on FIGO stages II-III versus IV, ascites samples were clustered according to metabolic phenotypes. Samples are clustered by metabolic characteristics of ascites. (modified from Yang et al., 2022)

In the PCA-loading plot depicted in Figure 35, cytokines including Interleukin 6 (IL-6), Interleukin 8 (IL-8), and Monocyte chemoattractant protein-1 (MCP-1) strongly influence PC1, while metabolites like polyunsaturated fatty acid (PUFA), 3-hydroxybutyrate, and phospholipids have more influence on PC2.

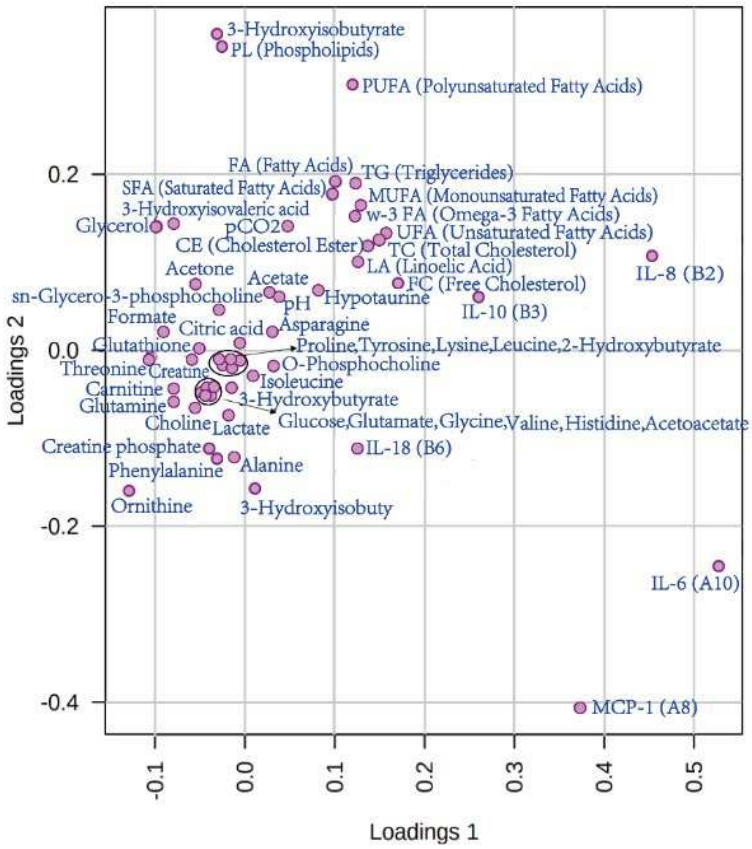

Figure 33. *The PCA-loading plot of all parameters.*
Interleukin 6 (IL-6), Interleukin 8 (IL-8), and Monocyte chemoattractant protein-1 (MCP-1) strongly influence PC1, while polyunsaturated fatty acid (PUFA), 3-hydroxybutyrate, and phospholipids influence PC2. (modified from Yang et al., 2022)

The PCA biplot was employed to combines both the scores and loadings plots into a single visualization to discern the distinct metabolic phenotype in each patient. In Figure 36, as illustrated by the PCA biplot, patients ASC-OC-B-11 and ASC-GC-B-2 within the green box exhibited a distinct metabolic phenotype, providing evidence of metastases to other organs in the progression of their tumors. As shown in the purple box, ASC-OC-T-13 stood out as the sole ascites sample without peritoneal metastasis, exhibiting the highest concentration of formate. Orthogonal Partial Least Squares

Discriminant Analysis (OPLS-DA), an enhanced PLS-DA approach for discriminating different stage ascites using multivariate data, reveals that the orange box signifies metabolite involvement in the metastasis to the omentum, while the red box indicates involvement in metastasis to other organs.

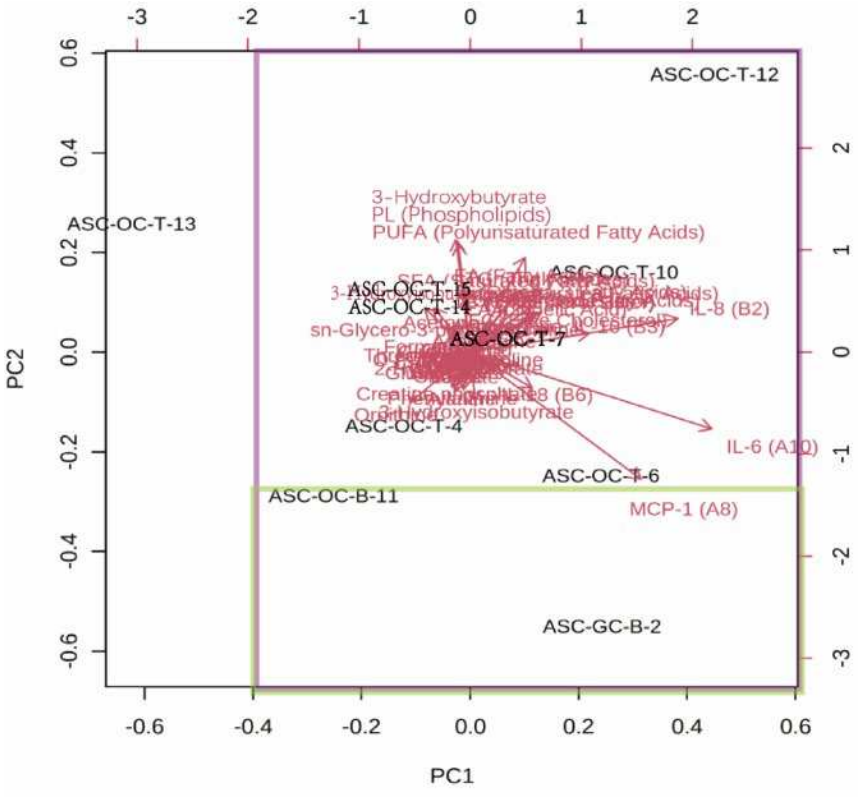

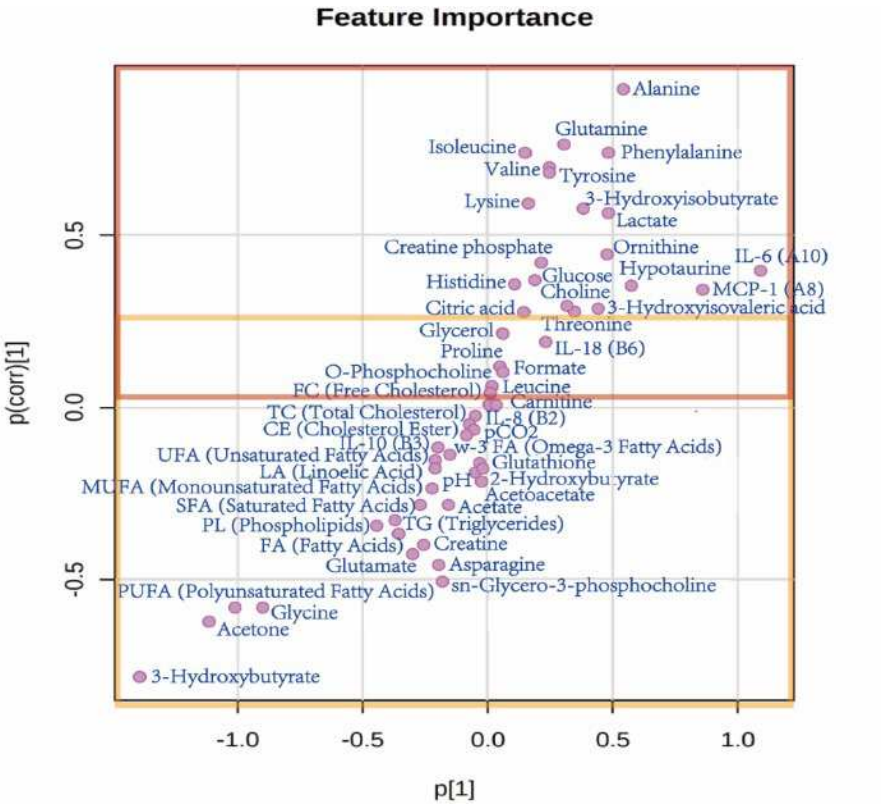

Figure 34. *The PCA biplot and OPLS-DA-loadings plot of OCs.*
In the PCA plot, the green box indicates metabolites involved in metastasis to other organs, while the purple box indicates metabolites involved in metastasis to the omentum (upper panel). Orthogonal partial least-squares discrimination analysis (OPLS-DA) - loadings plot, the orange box indicates metabolite involvement in the omentum, while the red box indicates involvement in other organs (lower panel). (modified from Yang et al., 2022)

As Table 12 shows, clinicopathological information of ovarian cancer patients demonstrated that only the patients ASC-OC-T-13 did not have peritoneal metastasis, ASC-GC-B-2 and ASC-OC-B-11 had distant organ metastasis, and ASC-OC-T-10 and ASC-OC-T-12 had extensive omental metastases.

Table 12. *Detailed clinicopathological information on the metastatic status*

ID	peritoneal metastasis
ASC-GC-B-2	Extensive peritoneal metastasis, M1b: Gastric metastasis
ASC-OC-T-4	Greater omentum: 0.9cm, colonic mesentery:0.2cm, splenic hilum:0.5cm, hepatoduodenal ligament:0.3cm
ASC-OC-T-6	extensive peritoneal metastasis
ASC-OC-T-7	Greater omentum: 0.7cm, diaphragm: 3.5cm, hepatoduodenal ligament: 1.5cm, gallbladder peritoneum: 0.3cm, pancreas: 2.5cm, omentum minus:0.2cm, M1b:

	pleura
ASC-OC-T-10	Greater omentum: multiple (3.5cm max), small intestinal plasma membrane: 0.3cm, hepatoduodenal ligament: 0.5cm, hepatic hilar: 1.2cm, small intestinal plasma membrane: 2.5cm
ASC-OC-B-11	extensive peritoneal metastasis, M1b: pleura
ASC-OC-T-12	Greater omentum: 5.5cm, omentum minus: 1.0cm, gallbladder peritoneum: 0.5cm, ileocecal: 3.5cm, bladder peritoneum: 3.5cm, left septum adipose tissue: 9cm, spleen peritoneum: 9.5cm
ASC-OC-T-13	no
ASC-OC-T-14	omental capsule: 0.5cm, colonic mesentery: 0.3cm, splenic peritoneum: 6.5cm, pancreas: 0.3cm
ASC-OC-T-15	Greater omentum: 3.2cm, multiple rectal walls: 1.9cm, colonic plasma membrane: 0.5cm, small intestinal plasma membrane: 1cm, colonic plasma membrane: 1.5cm, peripancreatic tissue: 2.8cm, splenic peritoneum: 2.5cm, renal peritoneum: 0.9cm

Survival in ovarian cancer patients is associated with dysregulated polar and lipid metabolism and inflammation.

Ovarian cancer patients with stage IV tumors exhibited a shorter overall survival time, as depicted by the Kaplan-Meier calculation method (Figure 37). However, due to the small cohort size, the observed difference did not reach statistical significance (p=0.54).

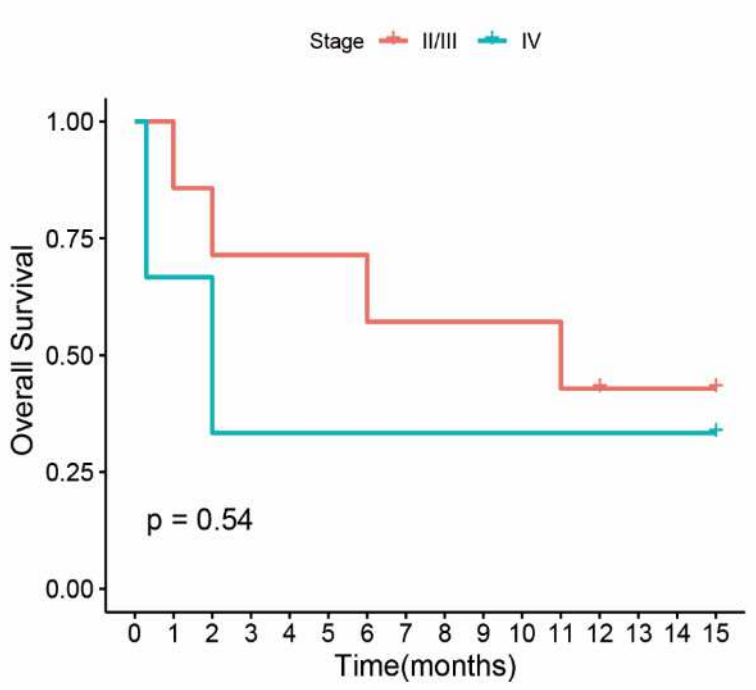

Figure 35. *Stage-dependent overall survival curve of OCs.*
Ovarian cancer patients with FIGO stage IV had a shorter overall survival time than FIGO stage II-III patients (Kaplan-Meier). (modified from Yang et al., 2022)

As indicated by the correlation heat map (Figure 38, next page), The extracellular pH (ascites) increased with the concentration of acetate, branched-chain amino acids (BCAAs), asparagine, and sn-glycerol-3-phosphocholine, and decreased with creatine phosphate.

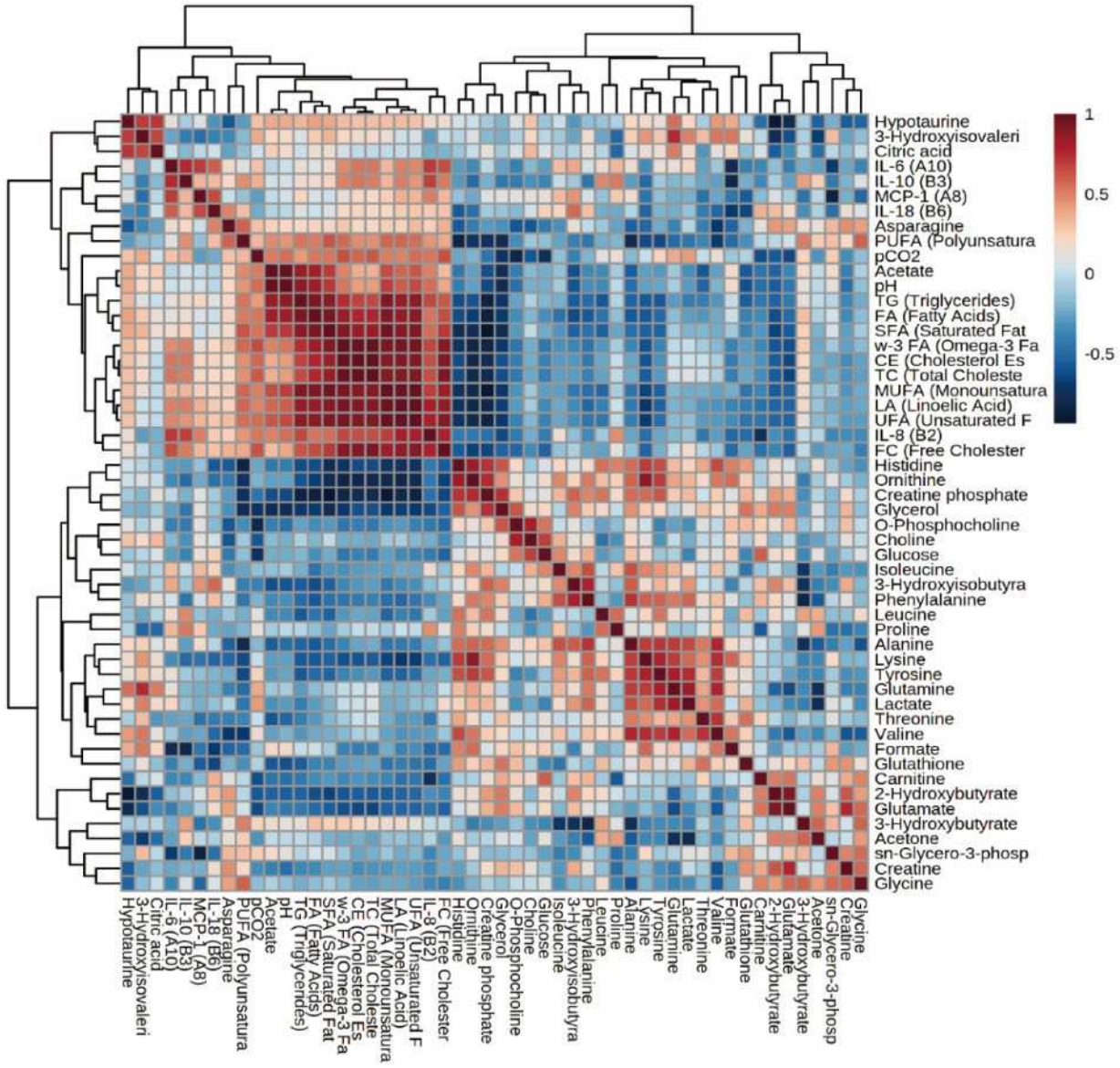

Figure 36. *Correlation heatmap of metabolites, cytokines, pH, and physical parameters*
Correlation heatmap of all the parameters, red indicates positive correlation, and blue indicates negative correlation. (modified from Yang et al., 2022)

Pattern hunter correlation analysis showed that pHe positively correlated with acetate, lipid metabolites, IL-8, and pCO_2. Acetate positively correlated with lipid compounds. pH negatively correlated with glycerol and creatine phosphate (Figure 39, next page).

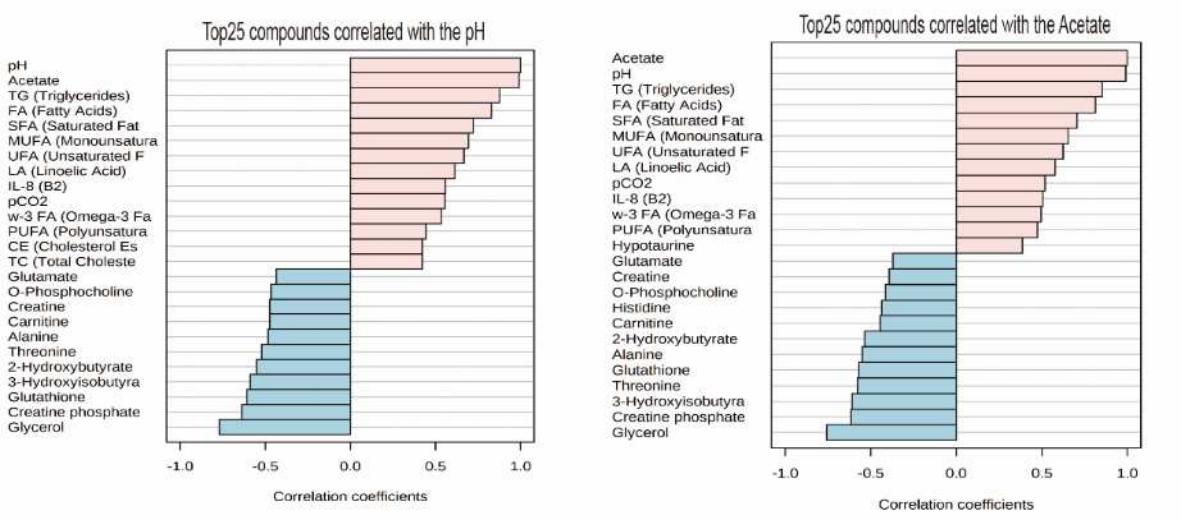

Figure 37. *Pattern hunter correlation analysis of pH and acetate*
Pattern hunter correlation analysis of the top 25 compounds correlated with pH (left panel) and acetate (right panel). The pH levels increased with the concentration of acetate, and acetate concentrations correspondingly increased with lipid compounds in ascites. (modified from Yang et al., 2022)

Tumor cells in ascites demonstrated a genetic predisposition towards lipid metabolism, as revealed by Figure 40, GSEA indicated enrichment in the reactive oxygen pathway (NES=1.765, P=0.003), fatty acid metabolism (NES=1.259, P=0.069), and adipogenesis (NES=1.249, P=0.064) in ascites cancer cells.

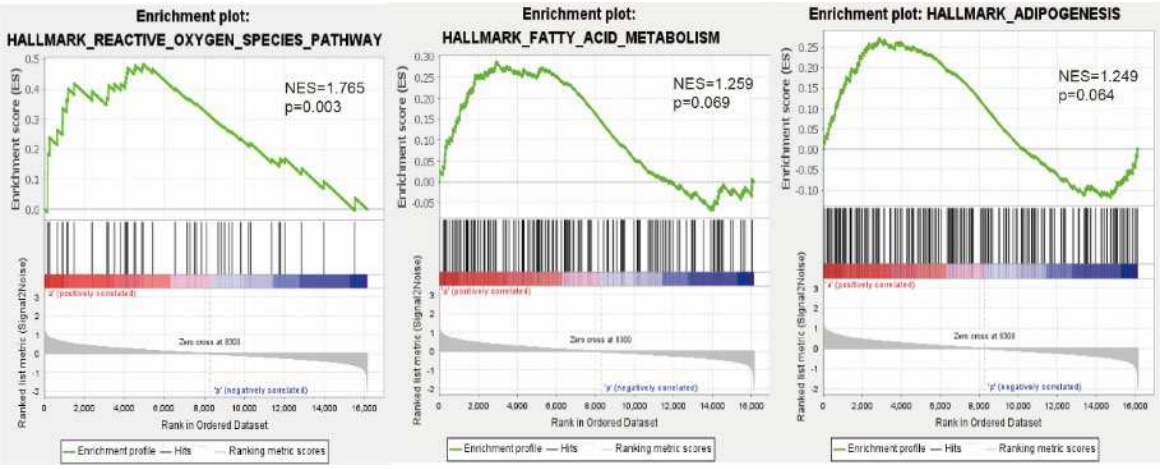

Figure 40. *GSEA plots of ovarian cancer ascites cells*
Ovarian cancer ascites cells gene enrichment in reactive oxygen species pathway (left panel), fatty acid metabolism (middle panel), and adipogenesis (right panel). (modified from Yang et al., 2022)

According to Pearson's r-test correlation analysis, IL-8 exhibited a positive correlation with LA, UFA, and FC, and a negative correlation with carnitine and glycerol in ascites (Figure 41A). Glutathione, a substance synthesized from amino acids, exhibited a positive correlation with threonine and glycerol and a negative correlation with IL-8 and pH (Figure 41B). Glycerol demonstrated a negative correlation with pH, SFA, PUFA and acetate, and a positive correlation with creatine phosphate (Figure 41C). The partial pressure of carbon dioxide was negatively correlated with o-phosphocholine, glucose, and glycerol in ascites (Figure 41D). Furthermore, 3-Hydroxybutyrate was mostly negatively correlated with phenylalanine and alanine in ovarian cancer ascites (Figure 41E, next page).

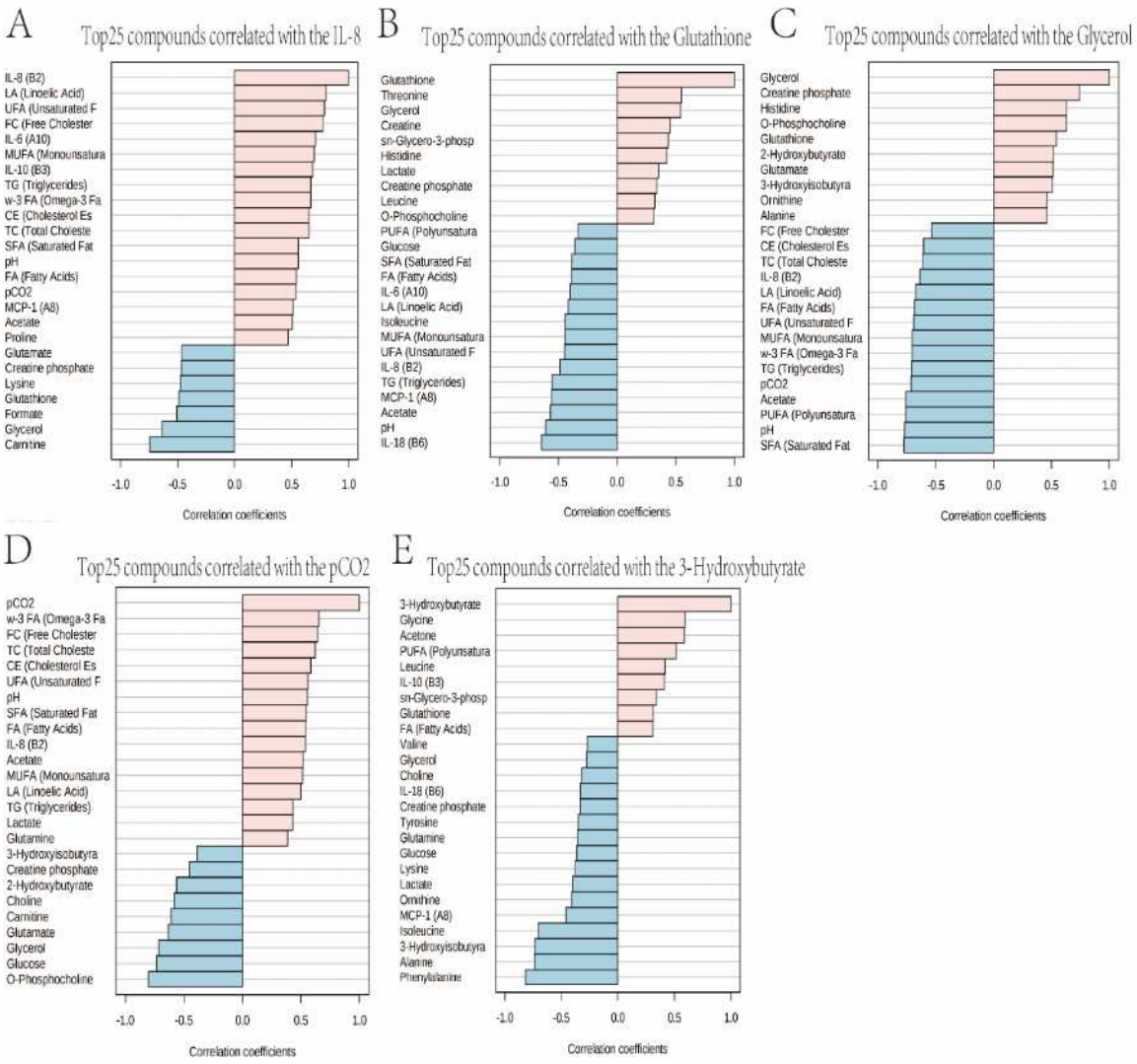

Figure 38. *Pattern hunter correlation analysis of IL-8, glutathione, glycerol, pCO_2 and 3-hydroxybutyrate* (modified from Yang et al., 2022)

As Figure 42 shows, genes of ascites cancer cells were enriched in epithelial-mesenchymal-transition (NES=1.541, p<0.001) and inflammatory response (NES=1.757, p<0.001).

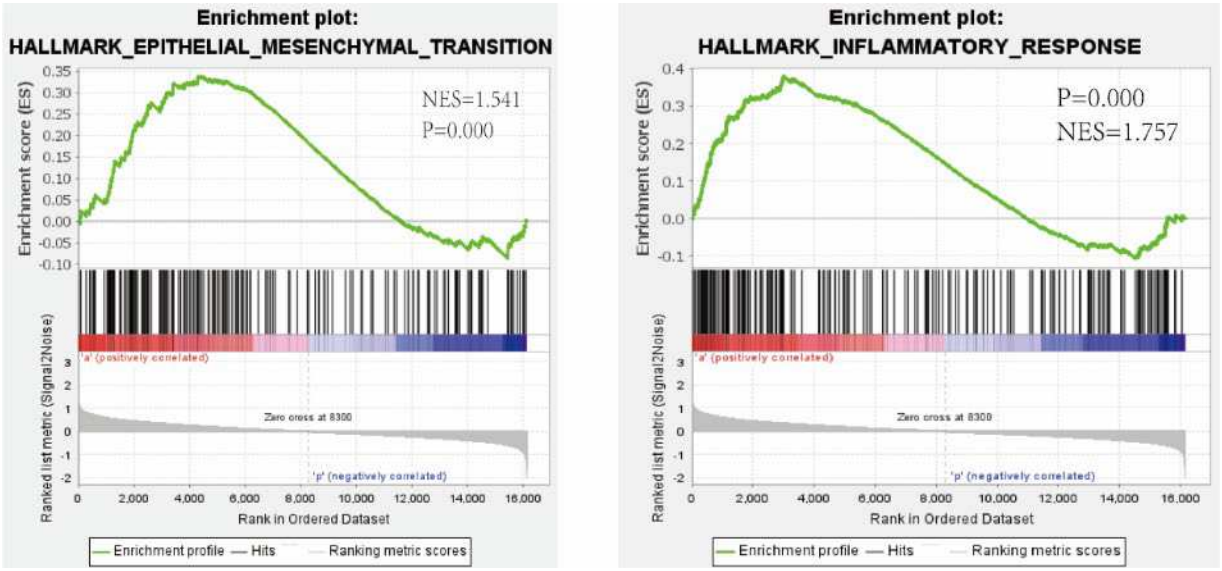

Figure 39. *Gene enrichment plots of ascites cancer cells*
Gene enrichment plots of ascites cancer cells on epithelial-mesenchymal-transition (left panel) and inflammatory response (right panel). (modified from Yang et al., 2022)

In summary of all the findings, a graphical abstract (Figure 43, next page) was generated to depict the interactions among pH, cytokines, and polar and lipid metabolites in ascites. The graphical abstract aims to showcase their association with ovarian cancer cell proliferation and organ metastasis in abdominal cavity. When ovarian cancer occurs, especially if the patient has peritoneal metastases, ascites developed. The metabolic activity of ascites increases as the stage of OC progresses, and the concentration of metabolites in ascites including ketone bodies, NEAAs, BCAAs, and AAAs progressively increases, as well as the pH. Increased ascites pH may be associated with the use of adipocytes by tumor cells for lipid metabolism, which in turn promotes further tumor cell proliferation. However, as OC patients progressed

to stage IV, lipid metabolism in the peritoneal cavity decreased steadily, but amino acid metabolism increased further.

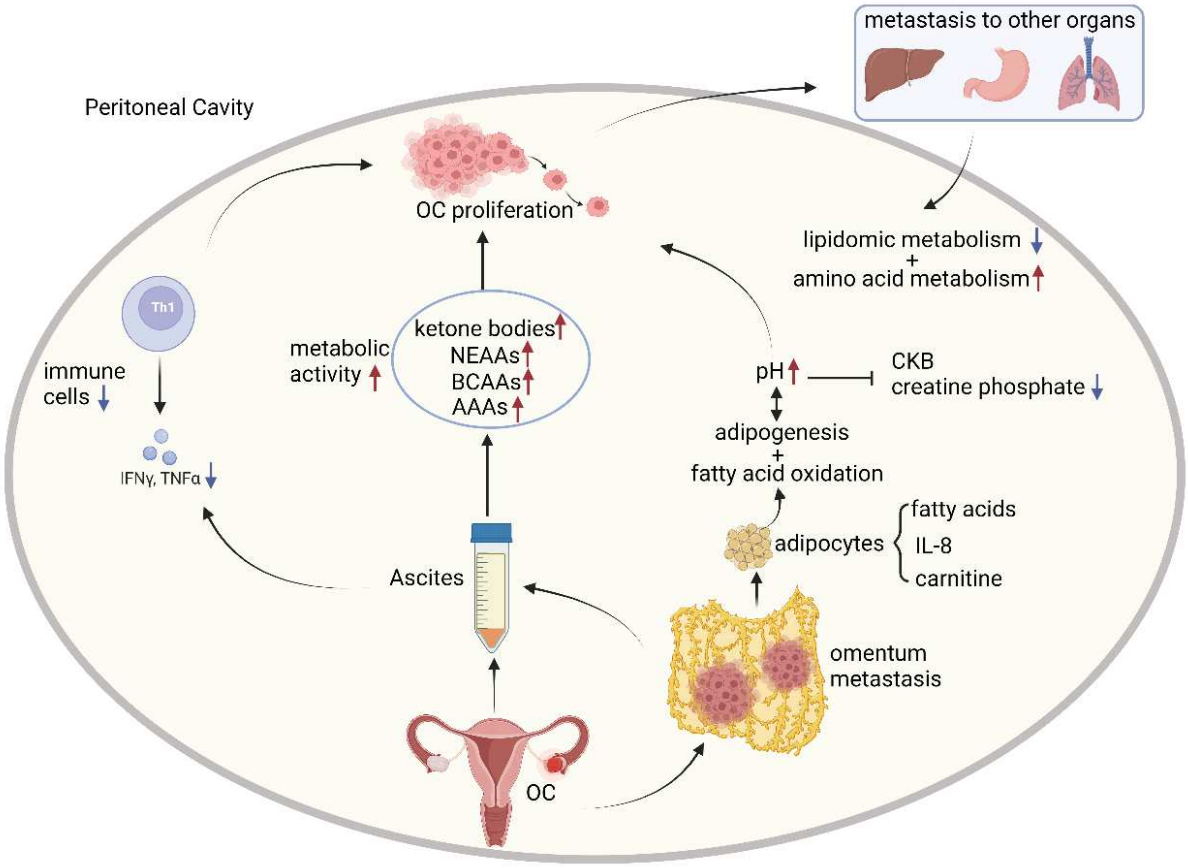

Figure 40. *Graphical abstract of ovarian ascites*

The graphical abstract depicts the interactions among pH, cytokines, and polar and lipid metabolites in ascites and their association with cellular proliferation and organ metastasis in ovarian cancer. NEAA: non-essential amino acid; BCAA: branched-chain amino acid; AAA: aromatic amino acid; CKB: creatine kinase B; IL-8: Interleukin-8; IFNγ: Interferon-γ, TNFα: tumor-necrosis factor α. (modified from Yang et al., 2022)

Discussion

Portions of the discussion section have been published in the following publication: Yang Q, Bae G, Nadiradze G, Castagna A, Berezhnoy G, Zizmare L, Kulkarni A, Singh Y, Weinreich FJ, Kommoss S, Reymond MA, Trautwein C. Acidic ascites inhibits ovarian cancer cell proliferation and correlates with the metabolomic, lipidomic and inflammatory phenotype of human patients. J Transl Med. 2022 Dec 12;20(1):581. doi: 10.1186/s12967-022-03763-3. PMID: 36503580; PMCID: PMC9743551.

Peritoneal metastasis is a primary spreading route of many intra-abdominal cancers (Yonemura et al., 2010, Cho and Shih, 2009) and is associated with aggressive histology, poor prognosis, and short survival. Diagnosing malignant ascites worsens the patient's prognosis and negatively impacts the quality of life (QoL). For example, in gastric cancer, survival after diagnosing malignant ascites is typically limited to six months (Maeda et al., 2015, Sangisetty and Miner, 2012). In ovarian cancer, despite the longer life expectancy compared to other types of cancer, survival after diagnosis of ascites does not exceed 10 to 24 months (Garrison et al., 1986).

Malignant ascites significantly contributes to the intraperitoneal dissemination and progression of ovarian cancer.

Our findings offer compelling evidence supporting the significant role of malignant ascites in the peritoneal progression of OC. Clinically, ovarian cancer cells often disseminate within the peritoneal cavity, where ascites accumulates. Biologically, ascites creates a microenvironment conducive to the dissemination and progression of ovarian cancer cells. Previous research has shown that OC cells within ascites can interact with other cells in the ascitic fluid, such as the host's fibroblasts and peritoneal mesothelial cells (MCs). These interactions lead to the formation of multicellular aggregates and clusters of cancer cells, co-called metastatic units (MU), which create metabolic synergies with a competitive survival advantage compared to isolated cells (Gao et al., 2019b).

Furthermore, malignant ascites not only establishes an immunosuppressive

environment (Yigit et al., 2010) but also fosters tissue vascularization by releasing proangiogenic proteins (Thibault et al., 2014). It induces epithelial-mesenchymal transition (EMT), promotes the trans-mesothelial invasion of cancer cells (Uruski et al., 2021), and triggers premature senescence in normal peritoneal mesothelial cells (PMCs), compelling them to adopt a cancer-promoting phenotype (Pakuła et al., 2019, Yang et al., 2022).

Investigating the role of ascites in OC progression

The relationship between ascites and intraperitoneal cell dissemination in OC is complex and poorly understood. An extensive experimental and preclinical dataset shows that an acidic pH promotes tumor growth in-vitro. However, it remains unclear whether the intra-peritoneal environment pH (ascites pH) affects abdominal OC proliferation in the human patient. How ascites production changes tumor immunity, metabolism, and recurrence in the human peritoneal cavity remain an open question.

This study provides an essential contribution to the research field of metabolomics of malignant ascites. We utilized a multi-omics approach to characterize ascites and investigate the impact of ascites on ovarian cancer progression. The ascites samples were deeply phenotyped in three ways:

1) peritoneal pH and different physical-chemical parameters of malignant ascites vs. benign lavages were measured by blood-gas analyzer;
2) cytokines of malignant ascites were measured by flow cytometry based on a 13-plex cytokine panel;
3) nuclear magnetic resonance (NMR) measured metabolites in malignant ascites.

Then, functional assays were used to verify the effect of pHe on several cancer hallmarks of human gastric and ovarian cancer cell lines.

Our observations in women with OC and our functional studies in human cancer cell lines revealed an alkaline pH of ascites, and typical metabolic patterns correlating with

OC progression. They unraveled the metabolic changes empowering the greater omentum as a cell-homing organ in OC.

The pH of malignant ascites is alkaline and correlates with tumor progression.

The pH of normal human blood is around 7.35 to 7.45, which is slightly alkaline. Several proton pumps on tumor cell membranes maintain the balance between the extracellular and the intracellular pHe/pHi (Hao et al., 2018). Dysregulation of cellular pH is a common occurrence in solid tumors, and an acidic extracellular pH is recognized as a hallmark of cancer (Hanahan, 2022). In cancer cells, a high pHe/pHi ratio is caused by the high rate of anaerobic glycolysis, producing numerous acidic metabolites (such as CO_2 and H_2CO_3). These factors lead to a reversed pHe in the tumor, which is further cursed by hypoxia due to poor blood delivery and fluid clearance.

Based on previous art, we expected malignant ascites to be more acidic than normal physiological conditions. Surprisingly, our results show unequivocally that the extracellular environment in abdominal cavities of OC patients is characterized by hypercarbia (pCO_2: 24.49 ± 31.25 mmHg), an alkaline pH (7.60 ± 0.38) and the absence of hypoxia (pO_2: 183.42 ± 16.74 mmHg), as compared with control patients. Thus, our experimental results diverge from the established dogma that extracellular fluid is acidic in cancer. However, our measurements in the human patient are confirmed by functional studies. Moreover, the pH becomes increasingly alkaline with tumor progression in the abdominal cavity of OC patients. Thus, our results provide compelling evidence for a tumor-facilitating effect of an alkaline pH in the peritoneal cavity.

Decreasing the pH of the culture medium suppresses the aggressive phenotype of gastric and ovarian cancer cells in vitro

To investigate a possible causal relationship between the intraperitoneal pH and an aggressive tumor phenotype, we performed functional metabolic experiments in-vitro by modifying the pH in the growth medium of human gastric and ovarian cancer cell lines. We observed that decreasing the pH of the culture medium suppressed the

aggressive phenotype of gastric and ovarian cancer cells. Specifically, the cancer cells' metabolic activity and adhesive properties were reduced by a lower pH, their apoptotic rate increased, and their migratory ability was reduced.

According to our expectations, gastric cancer cells first induced acidification of the pHe when cultured in a slightly alkaline environment. However, when the initial pHe was lower than 6.5, the cancer cells turned the extracellular environment somewhat alkaline. Ovarian cancer cells induced a similar but more pronounced pHe increase. A massive decrease in the extracellular glucose concentration was immediately observed after exposition to alkaline pHe, suggesting that cancer cells consume large amounts of glucose under alkaline pH conditions to meet their proliferation requirements. In parallel, the concentration of glucose and lactate exhibited opposite trends.

.

- Cancer cell growth

The gastric cancer cell population decreased in the pH 6.0 group; a slow growth rate was observed at pHe 6.5 and 7.0; the cells proliferated rapidly at pHe 7.5. An acidic extracellular environment inhibited OAW42 cancer cell growth even in the presence of malignant ascites. An extremely acidic pH caused ovarian cancer cell death via necrosis.

- Metabolic activity

The cellular metabolism in cultured cancer cells was directly proportional to the pHe. An acidic extracellular pH considerably inhibited the activity of both MKN45 and OW42 cancer cells. The MTT assay showed some protective effect of ascites on MKN45 cancer cells; the metabolic activity of MKN45 increased at the same pH conditions. However, even with the help of malignant ascites support, an acidic pHe considerably inhibited cell metabolic activity.

- Apoptotic rate

A significant difference in the apoptotic rate was observed between pHe 6.0 and pHe 7.5 in gastric cancer cells: more cells were apoptotic and necrotic at an acidic vs. an alkaline pHe. Extreme acidic pHe induced gastric cancer cell death via necrosis and

apoptosis. A (10%) had an antiapoptotic effect in G ascites (10%) had an antiapoptotic effect in GC cells, and the viable cell population increased with pHe. At the same time, the number of necrotic cells decreased. C cells and the viable cell population increased with pHe. At the same time, the number of necrotic cells decreased. Results obtained in OAW42 cancer cells were consistent with those obtained with gastric cancer cell lines.

- Adhesion

Adhesion of gastric cancer cells to the ECM components Fibronectin, Collagen I, Collagen IV, Laminin I, and Fibrinogen, and BSA (control) was the lowest under acidic conditions (pH 6.0), even in the presence of ascites. Similar results were obtained in ovarian cancer cell lines.

- Migration ability

The percentage of wound closure rate in MKN45 gastric cancer cells was higher in a slightly alkaline extracellular environment (pHe 7.5) compared with an acidic extracellular environment (pHe 6.0). Gastric cancer cell mobility declined together with pHe. Malignant ascites did not affect MKN45 migration ability in gastric cancer cells. These results were, again, confirmed in ovarian cancer cells.

Metabolic and immune pathways are enriched in ascites cells

Our analysis showed that cancer cells in ascites were enriched for differential genes in metabolic and immune pathways of the Hallmark pathway, including reactive oxygen species, fatty acid metabolism, adipogenesis, and inflammatory responses, compared to primary ovarian cancer cells. Thus, ascites' pH may influence tumor cell proliferation by affecting their metabolism or immunity.

Metabolic changes in malignant ascites in ovarian cancer patients

We first determined the metabolic changes in malignant ascites sampled from ovarian cancer patients.

- High acetate concentration

Ascites from patients with stage IV ovarian cancer had a high pH and were alkaline, and further analysis based on pattern hunter showed that this could be due to high levels of acetate, which is a conjugate base of acetic acid, a weak acid. Based on our results further a positive correlation was found between acetate and fatty acids, which suggests that the increased concentration of acetate in ascites with staging may be associated with increased fatty acid synthesis in highly aggressive tumor cells. Accumulation of acetate is often observed when cancer cells face nutritional challenges, making it a significant energy source.

It remains unclear if acetate production is carried out only in ovarian cancer cells since glycolysis and the TCA cycle also occur in adipocyte lipid metabolism (Morigny et al., 2021). Thus, adipocytes in the omentum would also complete acetate production, where fatty acids would be subsequently synthesized and transferred to the ovarian cancer cells via FABP4 fatty acid oxidation. Hence, the positive correlation of pHe with acetate may explain why the malignant ascites were basic and how the greater omentum can be involved in ovarian cancer progression.

- High lipid metabolic activity

It has been reported that ovarian cancer cells exhibit heightened aggressiveness in the ascites microenvironment, a phenomenon attributed to the reprogramming of lipid metabolism (Chen et al., 2019). The observation of elevated lipid metabolic activity in ovarian cancer cells cultured in the ascites microenvironment suggests that adipocytes may function as an energy source for cancer cells (Chen et al., 2019).

Ovarian cancer cells possess the ability to induce lipolysis in adipocytes, enabling them to adapt to lipid metabolism during periods of nutrient deprivation and thrive on lipids accumulated in adipocytes (Nieman et al., 2011). The greater omentum is the primary fatty organ in the abdomen. Hence, the observed positive correlation between pH, acetate, and lipids in our results may suggest a potential connection between malignant ovarian cancer cells causing ascites and their interaction with the greater omentum. In the omentum, processes such as fatty acid synthesis, fatty acid oxidation,

and subsequent ketogenesis play a role in the formation of ascites. Therefore, our hypothesis posits that metastatic ovarian cancer cells alter normal metabolism to a more oncogenic phenotype through interactions with the omentum.

- Changes in the hexokinase metabolism

Our results show a negative correlation between lactate and acetate. This fits nicely into the research map. Due to hypermetabolism in tumor cells, the incomplete metabolism of absorbed glucose leads to the conversion of pyruvate to acetate, which is then released into the extracellular space (Liu et al., 2018). The spillover of acetate from pyruvate involves two mechanisms: first, ROS-mediated oxidative decarboxylation, and second, incomplete oxidation mediated by thiamine- and glutathione-induced ketoacid dehydrogenase (kDH) (Bose et al., 2019).

A hallmark of cancer cells is the production of large amounts of hydrogen peroxide production, which leads to tumor progression and immune evasion (Arfin et al., 2021). Acetate levels are increased through radical enzyme scavengers (ROS) catalyzing the decarboxylation of pyruvate dehydrogenase (PDH) (Liu et al., 2018). Furthermore, alpha-ketoglutarate dehydrogenase (aKGDH) that functions as PDH would also convert pyruvate to acetaldehyde and acetate, yet all of the plausible reactions depend on the activity of KGDH or PDH and the availability of CoA and NAD+ (Liu et al., 2018).

Amino acid metabolism in ascites is associated with tumor stage in ovarian cancer.

Our metabolomics results revealed a significant increase in the levels of alanine, glutamine, isoleucine, and phenylalanine with advancing ovarian cancer stages, while 3-hydroxybutyric acid exhibited a metabolization pattern in the opposite direction.

- Alanine

Alanine, glutamine, and isoleucine (branch chain amino acids (BBCAs)), were significantly higher in OC ascites with stage IV vs. earlier stages. The substantial

increase in the concentration of alanine in the ascites of stage IV ovarian cancer, along with the incremental rise with advancing stages, supports the theory that tumor malignancy is linked to an elevated glycolytic flux and an augmented demand for protein synthesis within the tumor (Caneba et al., 2014).

- Glutamine

In our results, ascites ovarian cancer cells gene expression wad highly enriched in ROS pathway. Reactive oxygen species are generated by cancer cells as a result of an elevated metabolic rate, genetic mutations, and relative hypoxia (Perillo et al., 2020). The oxidation of glutamate is thought to be a significant source of respiratory energy for cancer cells (Moreadith and Lehninger, 1984). Indeed, studies have demonstrated that depriving cancer cells of glutamine can be an effective strategy in tumor therapy (Wise and Thompson, 2010). Glutamine is also essential for the production of glutathione, which plays a crucial role in removing ROS and rescuing cancer cells from apoptosis induced by oxidative stress.

Numerous studies have reported that cancer cells upscale high-affinity glutamine transporters (Freidman et al., 2020). For instance, the alanine-serine-cysteine transporter 2 (ASCT2), responsible for transporting neutral amino acids such as alanine, serine, cysteine, glutamine, and asparagine, has been demonstrated to play a central role in maintaining glutamine homeostasis in Myc-driven cancer cells (Gao et al., 2009, Wise et al., 2008). The ASCT2 inhibitor (L-g-glutamyl-p-nitroanilide or GPNA) has been shown to inhibit glutamine uptake and mTOR activation in cell culture which regulates processes such as protein translation, cell growth, and autophagy (Nicklin et al., 2009). High expression of ASCT2 gene and protein are observed in cancer cells, supporting their glutamine addiction as glutamine plays a central role in non-essential amino acid (NEAA) metabolism (Choi and Coloff, 2019, Ren et al., 2015).

Branched-chain amino acids (BCAAs) are utilized for the synthesis of glutamate and glutathione, contributing to therapeutic resistance. This resistance is often associated with the overexpression of SLC7A5, a BCAA transporter observed in pancreatic,

colorectal, gastric, and ovarian cancer cells (Saito and Soga, 2021, Tang et al., 2021, Yoo and Han, 2022). Hence, ovarian cancer patients in stage IV may exhibit heightened Myc-driven characteristics, leading to the overexpression of both ASCT2 and SLC7A5 to facilitate glutamine homeostasis. Additional research demonstrates a significant positive correlation between Myc mRNA expression and clinical stages (Ning et al., 2017). Mass spectrometry-based metabolomics on the serum of ovarian cancers ranging from stage I to IV confirms a significantly higher concentration of alanine in OCs compared to healthy controls (Zhou et al., 2010). Moreover, SLC7A5 overexpression is significantly associated with Myc expression and is elevated in high-grade serous ovarian cancer compared to normal tissues (Gong et al., 2021).

- Phenylalanine levels and their role in immune response

Elevated serum phenylalanine concentrations have previously been reported in patients with OC (Neurauter et al., 2008). Phenylalanine is converted into tyrosine by phenylalanine hydroxylase (PAH) in the liver and then degraded into precursors for gluconeogenesis and ketogenesis, indicating alternative energy supply for OC cells (Calvo et al., 2008). L-type amino acid transporters 1 (LAT1) are highly expressed for aromatic AA tyrosine and phenylalanine and hereby contribute to proliferation and migration of OC cells (Fotiadis et al., 2013). In our study, phenylalanine levels were significantly higher in malignant ascites from women with FIGO stage IV OC vs. earlier stages, thus correlating with tumor progression.

Phenylalanine levels play a significant role in immune response in OC. Previous studies have demonstrated significant correlations between phenylalanine, the phenylalanine/tyrosine ratio, and immune activation markers in cancer (Neurauter et al., 2008). Similar to cancer, patients with chronic conditions have shown moderately elevated phenylalanine levels and phenylalanine-to-tyrosine ratios (Phe/Tyr). These observations are associated with immune activation and inflammation (Neurauter et al., 2008). Increased phenylalanine levels in individuals with moderate hyperphenylalaninemia may be attributed to an oxidative environment generated by

chronic immune responses (Strasser et al., 2016). Additionally, studies have reported that phenylalanine metabolism plays a role in suppressing T-cell immune responses. Phenylalanine and its metabolism have been shown to exert regulatory effects on T-cell proliferation, activation, and subsequent immune responses (Sikalidis and Research, 2015).

- 3-hydroxybutyrate

Our results indicate that 3-hydroxybutyrate was significantly higher in earlier stages of ovarian cancer compared to late stages. This metabolite has also been found to be elevated in the serum of epithelial ovarian cancer patients in stages I and II, suggesting a positive correlation between 3-hydroxybutyrate and the clinical stage of OCs (Garcia et al., 2011). Additionally, 3-hydroxybutyrate serves as an energy source for cancer cells in the absence of sufficient blood glucose (Maurer et al., 2011). It is also recognized as a biomarker for fatty acid oxidation and ketone metabolism (Mierziak et al., 2021) , providing further evidence of the reverse Warburg effect and the involvement of the greater omentum.

Metabolic changes, cytokines/chemokines signalling and physico-chemical parameters in malignant ascites play a critical role in OC progression

We investigated correlations between polar and lipid metabolites, cytokines, chemokines, and physicochemical parameters present in the malignant ascites of ovarian cancer (OC) patients. Our goal was to elucidate patterns and their implications in the context of immune response and tumor progression.

In our study, we observed a negative correlation between glutathione levels in ascites and cytokines/chemokines such as IL-6, IL-18, IL-8, and MCP-1. The negative correlation observed may indicate higher glutathione consumption and suppressed immunosurveillance in ovarian cancer cells. This aligns with current knowledge, as glucose is utilized to regenerate NADPH in the pentose phosphate pathway (PPP), enhancing glutathione regeneration (Jin and Zhou, 2019). Previous reports have

demonstrated a significant negative correlation between IL-18, MCP-1, and glutathione. This suggests a direct anti-tumor immunity role of Interferon-γ (IFN-γ) producing T helper type 1 (Th1) cells. In response to reactive oxygen species produced by cancers, the innate immune system is activated. Macrophages and dendritic cells then produce proinflammatory cytokines such as tumor necrosis factor (TNF-α) and Interleukin-1β (IL-1β) to enhance adaptive immunity (Jin and Zhou, 2019, MacPherson et al., 2016, Pape et al., 1997).

In simpler terms, the adaptive anti-tumor immune response generates reactive oxygen species, which necessitates the presence of glutathione to prevent oxidative stress-induced cellular damage (Mak et al., 2017, Wheeler and DeFranco, 2012). Furthermore, endogenous glutathione is shown to enhance the innate immune system (Diotallevi et al., 2017). However, anti-tumor immune cells may experience dysfunction and apoptosis due to lower antioxidant capacity in the tumor microenvironment compared to cancer cells (C Sheng et al., 2011, Cordani et al., 2019, Yarosz and Chang, 2018). This explains the negative correlation observed between proinflammatory cytokines and chemokines, the role of MCP-1 as an indicator of a proinflammatory state (Lim et al., 2015), and might also provide an explanation for the almost undetectable levels of interferons (IFNs) and TNF-α in our ovarian cancer cases.

Lipid metabolism patterns in OC cancer patients

Fatty acid oxidation serves as an alternative pathway for ATP production in both normal and cancer cells. In our metabolomics study, we observed an inverse correlation between carnitine levels and all the cytokines/chemokines except IL-18. This negative correlation may indicate omentum involvement, especially considering that all ovarian cancers (OCs) exhibited peritoneal metastasis except for ASC-OC-T-13. Carnitine plays a critical role in this process, as fatty acids are transported as acyl-carnitine into the mitochondria, where they undergo oxidation (Fielding et al., 2018). Studies have shown that carnitine palmitoyl transferase (CPT1) is overexpressed in OC cell lines and primary ovarian serous carcinoma, and its overexpression is correlated with poor

survival in OCs (Shao et al., 2016). Additionally, other research has uncovered that ovarian cancer (OC) cells obtain exogenous fatty acids from the omentum, contributing to tumorigenesis and metastasis (Cheon et al., 2014, Nieman et al., 2011).

- Carnitine

In our study, IL-8 was only significantly negatively correlated with carnitine and glycerol, IL-8 significantly positively correlated with acetate. Adipocytes play a role in promoting the metastasis of ovarian cancer cells by secreting adipokines such as IL-6, IL-8, and MCP-1. Specifically, IL-8, in conjunction with fatty acid-binding protein 4 (FABP4), activates adipocytes to provide fatty acids in the OC microenvironment (Nieman et al., 2011, von Strandmann et al., 2017). The negative correlation between glycerol and IL-8 may indicate lipolysis, where triglycerides are broken down into fatty acids and glycerol in ovarian cancers. This is further supported by the negative correlation observed between glycerol and lipid metabolite species. A recent study demonstrated that overexpression of glycerol-3-phosphate acyltransferase 1 (GPAT) enhances adhesion and migration, and is associated with poor survival in ovarian cancers (Marchan et al., 2017).

The positive correlation observed between acetate and fatty acids in our study may indicate metabolic stress with lipid depletion in ovarian cancers. This accumulation of acetate has been observed to benefit various cancers, including breast, ovarian, and lung cancers, where acetyl-CoA synthetases (ACS) are highly expressed to utilize acetate for the formation of acetyl CoA (Schug et al., 2015). Visceral adipose tissue (VAT)-associated $CD4^+$ Tregs are located in the omentum, where they produce elevated levels of IL-10. This contributes to the formation of a Treg subpopulation, which subsequently suppresses the anti-tumor immune system (Cipolletta et al., 2015, Liu et al., 2022). A positive correlation was observed between 3-hydroxybutyrate and branched-chain amino acids (BCAAs), aromatic amino acids (AAs), and glutathione was found in ovarian cancer ascites. This suggests a high rate of fatty acid oxidation followed by ketogenesis for ATP production, leading to elevated levels of reactive

oxygen species intracellularly in ovarian cancers.

- 3-hydroxybutyrate

Furthermore, in our study, 3-hydroxybutyric acid exhibited a higher positive correlation with polyunsaturated fatty acids than with other lipid metabolites. This observation may align with previous findings indicating that PUFA can mediate the suppression of T cell immune responses by altering lipid rafts associated with T cell immunoreactivity, as previously described (Geyeregger et al., 2005). PUFA-mediated tumor progression was also reported in colorectal cancer and in recurrent endometrial cancer (Li et al., 2020, Mika et al., 2020). These findings elucidate the negative correlation between ketone bodies and MCP-1 and IL-18, as well as the positive correlation with IL-10.

The negative correlation suggests potential omentum involvement in glutamine synthesis, supporting tumor progression, with contributions from alanine and BCAAs in maintaining glutamine homeostasis and promoting glutathione production. In pancreatic cancers, adipocytes downregulate glutaminase to secrete and transfer glutamine under glutamine-deprived conditions. The observed glutamines may reflect the catabolism of lipid stores (Meyer et al., 2016). Finally, the negative correlation with phosphocreatine may also imply that the ATP of ovarian cancer cells, once they are transferred into the peritoneal omentum, is obtained mainly by fatty acid oxidation. The overexpression of creatine kinase B (CKB) has been observed in breast, colorectal, and ovarian cancers in response to acute hypoxia exposure (Krutilina et al., 2021, Li et al., 2013, Mooney et al., 2011) , indicating an increased demand for ATP production to support proliferation (Fenouille et al., 2017, Kurmi et al., 2018, MacPherson et al., 2016). This suggests that hypoxic ovarian cancer cells may increase glucose consumption and lactate production while decreasing reactive oxygen species production through the overexpression of creatine kinase B (Papalazarou et al., 2020). The decrease or low negative correlation between lactate production and pH suggests reduced glycolysis activity. This could indicate inactivated CKB in the omentum, causing ovarian cancer cells to rely on fatty acid oxidation for ATP and depend on

adipocytes. As a result, the acetate produced by ovarian cancer cells and adipocytes may contribute to an alkaline microenvironment. In this basic pH environment, CKB is likely inactivated, explaining why CKB may not be considered a prognostic marker for advanced-stage ovarian cancers or those with ascites.

The integration of metabolites, lipids, cytokines, chemokines, and physical-chemical parameters enables a more precise stratification of ovarian cancer patients

The PCA and OPLS-DA loading plots, along with PCA biplots, revealed distinctive carcinogenic phenotypes for each stage of ovarian cancer. A comprehensive heatmap was generated to assess the contribution of various parameters to OC progression, encompassing clinical stage and TNM classification. Notably, OCs with omental metastasis exhibited a shorter survival time compared to those without omental involvement. Studies have shown that the 5-year overall survival rates in ovarian cancer with omental metastasis were 43.4% (Iwagoi et al., 2021) However, the median survival following the diagnosis of ascites is considerably shorter, with a reported duration of only 5.7 months. (Ayantunde and Parsons, 2007). Hence, by analyzing the metabolomics, cytokine, and physicochemical parameters of ascites in a finely stratified manner, potential future treatment modalities can be developed and tailored to target individual patient differences more effectively.

Metabolic phenotype of OC patients with massive omental infiltration (“omental cake”)

Special attention must be paid to ASC-OC-T-10 and ASC-OC-T-12 patients. Both patients were FIGO -stage IV patients with distant metastasis to the pleura. Moreover, they showed large omental metastases (so-called called "omental cakes"), as a result of massive tumor dissemination from the ovary to the omentum.

These two OC patients had the highest concentrations of multiple lipid metabolites among all patients. This observation suggests that the endogenous production of fatty

acids may act as an oncogenic stimulant, contributing to the malignant progression of tumors (Menendez and Lipids, 2010). The shift between anabolic and catabolic processes in cancer cells, often referred to as the anabolic/catabolic switch, enables these cells to proliferate and progress aggressively. Elevated lipolytic enzyme activity, increased levels of fatty acids, and glycerol are responses to metabolic stress. The presence of a fatty acid cycling network supports malignancy, involving heightened processes of both lipolysis and lipogenesis in cancer cells (Luo et al., 2017). The observed metabolic profile, characterized by anabolic/catabolic switch and heightened lipolysis and lipogenesis, in ASC-OC-T-10 and ASC-OC-T-12 may provide insights into the poorer prognosis of these patients, reflected in their OS durations of only six and eleven months, respectively.

The presence of omental metastases was common among all OC patients except for ASC-OC-T-13, but variations in metabolic phenotypes were observed, particularly in fat metabolism and organ metastases. Patients ASC-OC-B-11 and ASC-GC-B-2 exhibited higher concentrations of cytokines including IL-6, IL-8, and MCP-1 compared to others. The PCA-loading plot reveals interesting insights. Despite being diagnosed as stage III, ASC-OC-T-6 exhibited a metabolic phenotype closer to stage IV, resembling ASC-GC-B-2 and ASC-OC-B-11. Conversely, ASC-OC-T-7, classified as stage IV, demonstrated a metabolic phenotype closer to stage III, resembling ASC-OC-T-4 and ASC-OC-T-14. This metabolic characterization may shed light on the progression of each OC and its relevance to survival rates. Notably, the prognosis aligns with the metabolic phenotypes, as ASC-GC-B-2, ASC-OC-B-11, and ASC-OC-T-6 patients had shorter overall survival (0.3, 2, and 2 months, respectively). In contrast, ASC-OC-T-7, ASC-OC-T-4, and ASC-OC-T-14 patients, with a similar metabolic phenotype, survived longer (15, 15, and 12 months, respectively). Interestingly, ASC-OC-T-15, despite sharing a closer metabolic phenotype with ASC-OC-T-4 and ASC-OC-T-14, had a shorter survival. This might be attributed to the patient's initial ovarian cancer diagnosis in 2017, with the current hospitalization being a recurrence,

potentially impacting overall survival.

ASC-OC-T-13, despite being classified as stage II, displayed a distinct metabolic and cytokine profile. Notably, it exhibited the highest formate levels and the lowest cytokine levels. This unique metabolic signature suggests that high mitochondrial glycine-formate metabolism could play a crucial role in invasion. The observed production of serine in this context aligns with findings in glioblastoma multiforme cell lines, further supporting the significance of glycine-formate metabolism in tumorigenesis and invasiveness (Meiser et al., 2018).

Deep-phenotype analysis of ovarian cancer

Physical-chemical parameters of malignant ascites from OC patients were analyzed and quantified by the blood-gas analyzer. Additionally, we employed 1H-NMR spectroscopy-based metabolomics to analyze and quantify polar and lipid metabolites. Simultaneously, a 13-plex panel of cytokines and chemokines was analyzed using FACS. The comprehensive analysis revealed unique metabolic and cytokine/chemokine profiles for each ovarian cancer patient, providing further insights into their clinical stages and TNM classifications.

Conclusion and outlook

In our patients with peritoneal metastasis, the pH of ascites was alkaline and correlated with tumor progression. In functional experiments in-vitro, decreasing the pH of the cell culture medium suppressed the malignant phenotype of gastric and ovarian cancer cells. It reduced tumor growth, metabolism, adhesion, and migration but increased apoptosis. In this study, we have delivered the proof of principle that NMR spectroscopy-based metabolomics can further stratify OC patients according to their specific metabolic phenotypes.

The metabolomics approach must be confirmed on a larger prospective dataset with an adequate sample size. We expect that, shortly, metabolomics data will assist in

determining the prognosis of patients with OC, optimize their therapy by highlighting novel targets, and facilitate treatment response assessment based on metabolic markers of tumor activity. Manipulating the intraperitoneal pH might help prevent peritoneal metastasis in patients at risk.

Summary

Summary in English

Background

Gastric and ovarian cancer are two of the most common cancer worldwide, and peritoneal metastasis occurs in the advanced stage of those two cancers. The adverse prognosis patients with peritoneal carcinoma from gastric and ovarian cancers is closely tied to peritoneal metastasis and the development of malignant ascites. Nevertheless, the precise mechanisms through which ascites in the peritoneal cavity impact tumor metabolism and recurrence remain elusive. This study takes an exploratory approach, seeking to comprehensively analyze the molecular and physicochemical traits of malignant ascites triggered by gastric and ovarian cancers, and to examine their impacts on the in vitro proliferation of gastric and ovarian cancer cells.

Methods

We investigated how ascites affect cancer cells by measuring intraperitoneal pH and physical-chemical parameters distribution in cancer and benign control patients. MKN45 and OAW42 cell lines were cultured under different pH conditions, with subsequent assessment of tumor cell metabolic activity, adhesion, anti-apoptotic potential, and migratory capabilities via MTT assay, adhesion assay, flow cytometry, and scratch assay. Additionally, a three-dimensional spherical model was employed to examine the characteristics of gastric and ovarian cancer cells at different pH levels using scanning electron microscopy. Furthermore, 10% corresponding malignant ascites were introduced to MKN45 and OAW42 cell lines to evaluate their impact on tumor proliferation. Finally, a comprehensive phenotypic analysis of ovarian ascites samples was conducted, incorporating ^{1}H-NMR-based metabolomics, blood gas analyzer-based analysis, and flow cytometry with a 13-complex cytokine panel.

Results

Ascites pH was higher in cancer patients (7.60±0.38) than in control (6.99±0.19) and even more so in stage IV (7.69±0.20) than in stage III (7.45±0.27). Ovarian and gastric cancer cells within 3D spherical structures exhibit rapid proliferation in a slightly alkaline environment. Tumor characteristics, including metabolic activity, adhesion, resistance to apoptosis, and migratory ability, are susceptible to inhibition through pH reduction in the cell culture medium. However, malignant ascites demonstrate resilience against tumor cells exposed to acidic pH conditions. Metabolomics analysis of malignant ascites from ovarian cancer patients revealed notably higher concentrations of alanine, isoleucine, phenylalanine, and glutamine in stage IV ovarian cancer patients compared to those in stages II-III. In comparison, concentrations of 3-hydroxybutyrate were notably higher in the ascites of patients with ovarian cancer at lower stages. Increased ascites pH was positively correlated with lipid metabolites. IL-8 displayed a positive correlation with lipid metabolites and acetate, while glutathione and carnitine exhibited a negative correlation with cytokines IL-6 and chemokines IL-8 and MCP-1.

Conclusion

Malignant ascites play a role in advancing ovarian and gastric cancers, potentially linked to their alkaline nature. Furthermore, variances in metabolites and cytokines within ascites from advanced-stage patients could offer refined stratification for ovarian cancer patients. These discoveries deepen our comprehension of ovarian cancer ascites pathology. Controlling pH levels may prove to be an effective strategy in preventing and treating peritoneal metastases.

Deutsche Zusammenfassung

Hintergrund

Magengeschwüre und Eierstockkrebs gehören zu den häufigsten Krebsarten weltweit, und Peritonealmetastasen treten im fortgeschrittenen Stadium dieser beiden Krebsarten auf. Die ungünstige Prognose von Patienten mit Peritonealkarzinom bei Magen- und Eierstockkrebs hängt eng mit Peritonealmetastasen und der Entwicklung von malignem Aszites zusammen. Dennoch bleiben die genauen Mechanismen, durch die Aszites in der Bauchhöhle den Tumorstoffwechsel und das Wiederauftreten beeinflussen, unklar. Diese Studie verfolgt einen explorativen Ansatz, um die molekularen und physikochemischen Merkmale von malignem Aszites, der durch Magen- und Eierstockkrebs ausgelöst wird, umfassend zu analysieren und ihre Auswirkungen auf die in vitro Proliferation von Magen- und Eierstockkrebszellen zu untersuchen.

Methoden

Wir haben untersucht, wie Aszites Krebszellen beeinflusst, indem wir den intraperitonealen pH-Wert und die Verteilung physikochemischer Parameter bei Krebs- und benignen Kontrollpatienten gemessen haben. Die Zelllinien MKN45 und OAW42 wurden unter verschiedenen pH-Bedingungen kultiviert, und anschließend wurden die metabolische Aktivität der Tumorzellen, ihre Adhäsion, ihre antiapoptotischen Potenziale und ihre Wanderungsfähigkeiten mittels MTT-Assay, Adhäsionsassay, Durchflusszytometrie und Scratch-Assay bewertet. Darüber hinaus wurde ein dreidimensionales kugelförmiges Modell verwendet, um die Eigenschaften von Magen- und Eierstockkrebszellen bei verschiedenen pH-Werten mithilfe der Raster-Elektronenmikroskopie zu untersuchen. Darüber hinaus wurden MKN45- und OAW42-Zelllinien 10% entsprechendem malignem Aszites zugesetzt, um ihre Auswirkungen auf die Tumorproliferation zu bewerten. Schließlich wurde eine umfassende

phänotypische Analyse von Eierstockaszitesproben durchgeführt, die ^{1}H-NMR-basierte Metabolomik, die Analyse auf Basis eines Blutgasanalysators und die Durchflusszytometrie mit einem 13-komplexen Zytokinspektrum umfasste.

Ergebnisse

Der pH-Wert des Aszites war bei Krebspatienten (7,60 ± 0,38) höher als bei Kontrollpersonen (6,99 ± 0,19) und sogar noch höher bei Stadium-IV-Patienten (7,69 ± 0,20) als bei Stadium-III-Patienten (7,45 ± 0,27). Magen- und Eierstockkrebszellen innerhalb dreidimensionaler kugelförmiger Strukturen zeigen eine schnelle Proliferation in einer leicht alkalischen Umgebung. Tumorcharakteristika wie metabolische Aktivität, Adhäsion, Resistenz gegen Apoptose und Wanderungsfähigkeit sind durch eine Reduzierung des pH-Werts im Zellkulturmedium anfällig für Hemmung. Maligner Aszites zeigt jedoch eine Resistenz gegenüber Tumorzellen, die sauren pH-Bedingungen ausgesetzt sind. Die metabolomische Analyse von malignem Aszites bei Eierstockkrebspatienten ergab deutlich höhere Konzentrationen von Alanin, Isoleucin, Phenylalanin und Glutamin bei Patienten mit Stadium-IV-Eierstockkrebs im Vergleich zu denen in den Stadien II-III. Im Vergleich dazu waren die Konzentrationen von 3-Hydroxybutyrat im Aszites von Patienten mit Eierstockkrebs in niedrigeren Stadien deutlich höher. Ein erhöhter Aszites-pH-Wert korrelierte positiv mit Lipidmetaboliten. IL-8 zeigte eine positive Korrelation mit Lipidmetaboliten und Acetat, während Glutathion und Carnitin eine negative Korrelation mit Zytokinen IL-6 und Chemokinen IL-8 und MCP-1 aufwiesen.

Schlussfolgerung

Maligner Aszites spielt eine Rolle bei der Progression von Eierstock- und Magenkrebs, die möglicherweise mit ihrer alkalischen Natur verbunden ist. Darüber hinaus könnten Unterschiede in Metaboliten und Zytokinen innerhalb

von Aszites von Patienten im fortgeschrittenen Stadium eine verfeinerte Stratifikation für Eierstockkrebspatienten ermöglichen. Diese Erkenntnisse vertiefen unser Verständnis der Pathologie von Eierstockkrebs-Aszites. Die Kontrolle der pH-Werte könnte sich als wirksame Strategie zur Vorbeugung und Behandlung von Peritonealmetastasen erweisen.

References

ARCHID, R., SOLASS, W., TEMPFER, C., KONIGSRAINER, A., ADOLPH, M., REYMOND, M. A. & WILSON, R. B. 2019. Cachexia Anorexia Syndrome and Associated Metabolic Dysfunction in Peritoneal Metastasis. *Int J Mol Sci,* 20.

ARFIN, S., JHA, N. K., JHA, S. K., KESARI, K. K., RUOKOLAINEN, J., ROYCHOUDHURY, S., RATHI, B. & KUMAR, D. J. A. 2021. Oxidative stress in cancer cell metabolism. 10**,** 642.

AUGSTEN, M. J. F. I. O. 2014. Cancer-associated fibroblasts as another polarized cell type of the tumor microenvironment. 4**,** 62.

AYANTUNDE, A. & PARSONS, S. J. A. O. O. 2007. Pattern and prognostic factors in patients with malignant ascites: a retrospective study. 18**,** 945-949.

BHOWMICK, N. A., NEILSON, E. G. & MOSES, H. L. J. N. 2004. Stromal fibroblasts in cancer initiation and progression. 432**,** 332-337.

BOEDTKJER, E., BUNCH, L. & F PEDERSEN, S. J. C. P. D. 2012. Physiology, pharmacology and pathophysiology of the pH regulatory transport proteins NHE1 and NBCn1: similarities, differences, and implications for cancer therapy. 18**,** 1345-1371.

BOEDTKJER, E. & PEDERSEN, S. F. 2020. The Acidic Tumor Microenvironment as a Driver of Cancer. *Annu Rev Physiol,* 82**,** 103-126.

BORSI, L., BALZA, E., GAGGERO, B., ALLEMANNI, G. & ZARDI, L. J. J. O. B. C. 1995. The Alternative Splicing Pattern of the Tenascin-C Pre-mRNA Is Controlled by the Extracellular pH (*). 270**,** 6243-6245.

BOSE, S., RAMESH, V. & LOCASALE, J. W. J. T. I. C. B. 2019. Acetate metabolism in physiology, cancer, and beyond. 29**,** 695-703.

BRABLETZ, T. J. N. R. C. 2012. To differentiate or not—routes towards metastasis. 12**,** 425-436.

C SHENG, K., D WRIGHT, M. & APOSTOLOPOULOS, V. J. C. M. C. 2011. Inflammatory mediators hold the key to dendritic cell suppression and tumor progression. 18**,** 5507-5518.

CĂLINESCU, O., PAULINO, C., KüHLBRANDT, W. & FENDLER, K. J. J. O. B. C. 2014. Keeping it simple, transport mechanism and pH regulation in Na+/H+ exchangers. 289**,** 13168-13176.

CALVO, A. C., PEY, A. L., YING, M., LOER, C. M. & MARTINEZ, A. J. T. F. J. 2008. Anabolic function of phenylalanine hydroxylase in Caenorhabditis elegans. 22**,** 3046-3058.

CANEBA, C., YANG, L., BADDOUR, J., CURTIS, R., WIN, J., HARTIG, S., MARINI, J., NAGRATH, D. J. C. D. & DISEASE 2014. Nitric oxide is a positive regulator of the Warburg effect in ovarian cancer cells. 5**,** e1302-e1302.

CHEN, R. R., YUNG, M. M., XUAN, Y., ZHAN, S., LEUNG, L. L., LIANG, R. R., LEUNG, T. H., YANG, H., XU, D. & SHARMA, R. J. C. B. 2019. Targeting of lipid metabolism with a metabolic inhibitor cocktail eradicates peritoneal metastases in ovarian cancer cells. 2**,** 1-15.

CHEON, D.-J., TONG, Y., SIM, M.-S., DERING, J., BEREL, D., CUI, X., LESTER, J., BEACH, J. A., TIGHIOUART, M. & WALTS, A. E. J. C. C. R. 2014. A Collagen-Remodeling Gene Signature Regulated by TGF-β Signaling Is Associated with Metastasis and Poor Survival in Serous Ovarian CancerCollagen-Remodeling Gene Signature Predicts Poor Survival. 20**,** 711-723.

CHO, K. R. & SHIH, I.-M. J. A. R. O. P. M. O. D. 2009. Ovarian cancer. 4**,** 287-313.

CHOI, B.-H. & COLOFF, J. L. J. C. 2019. The diverse functions of non-essential amino acids in cancer. 11**,** 675.

CIPOLLETTA, D., COHEN, P., SPIEGELMAN, B. M., BENOIST, C. & MATHIS, D. J. P. O. T. N. A. O. S. 2015. Appearance and disappearance of the mRNA signature characteristic of Treg cells in visceral adipose tissue: age, diet, and PPARγ effects. 112**,** 482-487.

COOPER, G. M., HAUSMAN, R. E. & HAUSMAN, R. E. 2007. *The cell: a molecular approach*, ASM press Washington, DC.

CORDANI, M., SáNCHEZ-ÁLVAREZ, M., STRIPPOLI, R., BAZHIN, A. V., DONADELLI, M. J. O. M. & LONGEVITY, C. 2019. Sestrins at the interface of ROS control and autophagy regulation in health and disease. 2019.

COX, A. G., TSOMIDES, A., YIMLAMAI, D., HWANG, K. L., MIESFELD, J., GALLI, G. G., FOWL, B. H., FORT, M., MA, K. Y. & SULLIVAN, M. R. J. T. E. J. 2018. Yap regulates glucose utilization and sustains nucleotide synthesis to enable organ growth. 37**,** e100294.

DE CRAENE, B. & BERX, G. J. N. R. C. 2013. Regulatory networks defining EMT during cancer initiation and progression. 13**,** 97-110.

DENKER, S. P., HUANG, D. C., ORLOWSKI, J., FURTHMAYR, H. & BARBER, D. L. 2000. Direct binding of the Na--H exchanger NHE1 to ERM proteins regulates the cortical cytoskeleton and cell shape independently of H(+) translocation. *Mol Cell,* 6**,** 1425-36.

DIETL, K., RENNER, K., DETTMER, K., TIMISCHL, B., EBERHART, K., DORN, C., HELLERBRAND, C., KASTENBERGER, M., KUNZ-SCHUGHART, L. A. & OEFNER, P. J. J. T. J. O. I. 2010. Lactic acid and acidification inhibit TNF secretion and glycolysis of human monocytes. 184**,** 1200-1209.

DIOTALLEVI, M., CHECCONI, P., PALAMARA, A. T., CELESTINO, I., COPPO, L., HOLMGREN, A., ABBAS, K., PEYROT, F., MENGOZZI, M. & GHEZZI, P. J. F. I. I. 2017. Glutathione fine-tunes the innate immune response toward antiviral pathways in a macrophage cell line independently of its antioxidant properties. 1239.

ESTRELLA, V., CHEN, T., LLOYD, M., WOJTKOWIAK, J., CORNNELL, H. H., IBRAHIM-HASHIM, A., BAILEY, K., BALAGURUNATHAN, Y., ROTHBERG, J. M., SLOANE, B. F., JOHNSON, J., GATENBY, R. A. & GILLIES, R. J. 2013. Acidity generated by the tumor microenvironment drives local invasion. *Cancer Res,* 73**,** 1524-35.

FANG, J. S., GILLIES, R. D. & GATENBY, R. A. Adaptation to hypoxia and acidosis in carcinogenesis and tumor progression. Seminars in cancer biology, 2008. Elsevier, 330-337.

FENOUILLE, N., BASSIL, C. F., BEN-SAHRA, I., BENAJIBA, L., ALEXE, G., RAMOS, A., PIKMAN, Y., CONWAY, A. S., BURGESS, M. R. & LI, Q. J. N. M. 2017. The creatine kinase pathway is a metabolic vulnerability in EVI1-positive acute myeloid leukemia. 23**,** 301-313.

FIELDING, R., RIEDE, L., LUGO, J. P. & BELLAMINE, A. J. N. 2018. L-carnitine supplementation in recovery after exercise. 10**,** 349.

FOTIADIS, D., KANAI, Y. & PALACíN, M. J. M. A. O. M. 2013. The SLC3 and SLC7 families of amino acid transporters. 34**,** 139-158.

FREIDMAN, N., CHEN, I., WU, Q., BRIOT, C., HOLST, J., FONT, J., VANDENBERG, R. & RYAN, R. J. N. R. 2020. Amino acid transporters and exchangers from the SLC1A family: structure, mechanism and roles in physiology and cancer. 45**,** 1268-1286.

FUKAMACHI, T., CHIBA, Y., WANG, X., SAITO, H., TAGAWA, M. & KOBAYASHI, H. 2010. Tumor specific low pH environments enhance the cytotoxicity of lovastatin and cantharidin. *Cancer Letters,* 297**,** 182-189.

GALLAGHER, F. A., KETTUNEN, M. I., DAY, S. E., HU, D. E., ARDENKJAER-LARSEN, J. H., ZANDT, R.,

JENSEN, P. R., KARLSSON, M., GOLMAN, K., LERCHE, M. H. & BRINDLE, K. M. 2008. Magnetic resonance imaging of pH in vivo using hyperpolarized 13C-labelled bicarbonate. *Nature,* 453**,** 940-3.

GAO, P., TCHERNYSHYOV, I., CHANG, T.-C., LEE, Y.-S., KITA, K., OCHI, T., ZELLER, K. I., DE MARZO, A. M., VAN EYK, J. E. & MENDELL, J. T. J. N. 2009. c-Myc suppression of miR-23a/b enhances mitochondrial glutaminase expression and glutamine metabolism. 458**,** 762-765.

GAO, Q., YANG, Z., XU, S., LI, X., YANG, X., JIN, P., LIU, Y., ZHOU, X., ZHANG, T., GONG, C., WEI, X., LIU, D., SUN, C., CHEN, G., HU, J., MENG, L., ZHOU, J., SAWADA, K., FRUSCIO, R., GRUNT, T. W., WISCHHUSEN, J., VARGAS-HERNáNDEZ, V. M., POTHURI, B. & COLEMAN, R. L. 2019a. Heterotypic CAF-tumor spheroids promote early peritoneal metastatis of ovarian cancer. *J Exp Med,* 216**,** 688-703.

GAO, Q., YANG, Z., XU, S., LI, X., YANG, X., JIN, P., LIU, Y., ZHOU, X., ZHANG, T. & GONG, C. J. J. O. E. M. 2019b. Heterotypic CAF-tumor spheroids promote early peritoneal metastasis of ovarian cancer. 216**,** 688-703.

GARCIA, E., ANDREWS, C., HUA, J., KIM, H. L., SUKUMARAN, D. K., SZYPERSKI, T. & ODUNSI, K. J. J. O. P. R. 2011. Diagnosis of early stage ovarian cancer by 1H NMR metabonomics of serum explored by use of a microflow NMR probe. 10**,** 1765-1771.

GARRISON, R. N., KAELIN, L. D., GALLOWAY, R. & HEUSER, L. J. A. O. S. 1986. Malignant ascites. Clinical and experimental observations. 203**,** 644.

GEYEREGGER, R., ZEYDA, M., ZLABINGER, G. J., WALDHäUSL, W. & STULNIG, T. M. J. J. O. L. B. 2005. Polyunsaturated fatty acids interfere with formation of the immunological synapse. 77**,** 680-688.

GILLIES, R. J. 2001. The tumour microenvironment: causes and consequences of hypoxia and acidity. Introduction. *Novartis Found Symp,* 240**,** 1-6.

GILLIES, R. J., RAGHUNAND, N., KARCZMAR, G. S. & BHUJWALLA, Z. M. J. J. O. M. R. I. A. O. J. O. T. I. S. F. M. R. I. M. 2002. MRI of the tumor microenvironment. 16**,** 430-450.

GONG, W., CHEN, Y. & ZHANG, Y. J. T. C. R. 2021. Prognostic and clinical significance of Solute Carrier Family 7 Member 1 in ovarian cancer. 10**,** 602.

HANAHAN, D. J. C. D. 2022. Hallmarks of cancer: new dimensions. 12**,** 31-46.

HAO, G., XU, Z. P. & LI, L. J. R. A. 2018. Manipulating extracellular tumour pH: an effective target for cancer therapy. 8**,** 22182-22192.

HAWK, M. A. & SCHAFER, Z. T. 2018. Mechanisms of redox metabolism and cancer cell survival during extracellular matrix detachment. *J Biol Chem,* 293**,** 7531-7537.

HAY, N. J. N. R. C. 2016. Reprogramming glucose metabolism in cancer: can it be exploited for cancer therapy? 16**,** 635-649.

HILAL, Z., REZNICZEK, G. A., KLENKE, R., DOGAN, A. & TEMPFER, C. B. 2017. Nutritional status, cachexia, and anorexia in women with peritoneal metastasis and intraperitoneal chemotherapy: a longitudinal analysis. *J Gynecol Oncol,* 28**,** e80.

HINTON, A., SENNOUNE, S. R., BOND, S., FANG, M., REUVENI, M., SAHAGIAN, G. G., JAY, D., MARTINEZ-ZAGUILAN, R. & FORGAC, M. J. J. O. B. C. 2009. Function of a subunit isoforms of the V-ATPase in pH homeostasis and in vitro invasion of MDA-MB231 human breast cancer cells. 284**,** 16400-16408.

HJELMELAND, A. B., WU, Q., HEDDLESTON, J. M., CHOUDHARY, G. S., MACSWORDS, J., LATHIA,

J. D., MCLENDON, R., LINDNER, D., SLOAN, A. & RICH, J. N. 2011. Acidic stress promotes a glioma stem cell phenotype. *Cell Death Differ,* 18**,** 829-40.

HONG, R. & HAN, S. I. 2018. Extracellular acidity enhances tumor necrosis factor-related apoptosis-inducing ligand (TRAIL)-mediated apoptosis via DR5 in gastric cancer cells. *The Korean Journal of Physiology & Pharmacology,* 22.

HOSIOS, A. M., HECHT, V. C., DANAI, L. V., JOHNSON, M. O., RATHMELL, J. C., STEINHAUSER, M. L., MANALIS, S. R. & VANDER HEIDEN, M. G. J. D. C. 2016. Amino acids rather than glucose account for the majority of cell mass in proliferating mammalian cells. 36**,** 540-549.

HUBER, V., CAMISASCHI, C., BERZI, A., FERRO, S., LUGINI, L., TRIULZI, T., TUCCITTO, A., TAGLIABUE, E., CASTELLI, C. & RIVOLTINI, L. Cancer acidity: An ultimate frontier of tumor immune escape and a novel target of immunomodulation. Seminars in cancer biology, 2017. Elsevier, 74-89.

IWAGOI, Y., MOTOHARA, T., HWANG, S., FUJIMOTO, K., IKEDA, T. & KATABUCHI, H. J. I. J. O. C. O. 2021. Omental metastasis as a predictive risk factor for unfavorable prognosis in patients with stage III–IV epithelial ovarian cancer. 26**,** 995-1004.

JIN, L. & ZHOU, Y. J. O. L. 2019. Crucial role of the pentose phosphate pathway in malignant tumors. 17**,** 4213-4221.

KAWAUCHI, K., ARAKI, K., TOBIUME, K. & TANAKA, N. J. N. C. B. 2008. p53 regulates glucose metabolism through an IKK-NF-κB pathway and inhibits cell transformation. 10**,** 611-618.

KEIBLER, M. A., WASYLENKO, T. M., KELLEHER, J. K., ILIOPOULOS, O., VANDER HEIDEN, M. G., STEPHANOPOULOS, G. J. C. & METABOLISM 2016. Metabolic requirements for cancer cell proliferation. 4**,** 1-16.

KIM, S., KIM, B. & SONG, Y. S. J. C. S. 2016. Ascites modulates cancer cell behavior, contributing to tumor heterogeneity in ovarian cancer. 107**,** 1173-1178.

KIPPS, E., TAN, D. S. & KAYE, S. B. J. N. R. C. 2013. Meeting the challenge of ascites in ovarian cancer: new avenues for therapy and research. 13**,** 273-282.

KRUTILINA, R. I., PLAYA, H., BROOKS, D. L., SCHWAB, L. P., PARKE, D. N., OLUWALANA, D., LAYMAN, D. R., FAN, M., JOHNSON, D. L. & YUE, J. J. C. 2021. HIF-Dependent CKB Expression Promotes Breast Cancer Metastasis, Whereas Cyclocreatine Therapy Impairs Cellular Invasion and Improves Chemotherapy Efficacy. 14**,** 27.

KURMI, K., HITOSUGI, S., YU, J., BOAKYE-AGYEMAN, F., WIESE, E. K., LARSON, T. R., DAI, Q., MACHIDA, Y. J., LOU, Z. & WANG, L. J. C. M. 2018. Tyrosine phosphorylation of mitochondrial creatine kinase 1 enhances a druggable tumor energy shuttle pathway. 28**,** 833-847. e8.

LAGADIC-GOSSMANN, D., HUC, L. & LECUREUR, V. 2004. Alterations of intracellular pH homeostasis in apoptosis: origins and roles. *Cell Death Differ,* 11**,** 953-61.

LAWLER, J. Counter regulation of tumor angiogenesis by vascular endothelial growth factor and thrombospondin-1. Seminars in Cancer Biology, 2022. Elsevier.

LEE, S., MELE, M., VAHL, P., CHRISTIANSEN, P. M., JENSEN, V. E. D. & BOEDTKJER, E. 2014. Na+,HCO3−-cotransport is functionally upregulated during human breast carcinogenesis and required for the inverted pH gradient across the plasma membrane. *Pflügers Archiv - European Journal of Physiology,* 467**,** 367-377.

LENGYEL, E. J. T. A. J. O. P. 2010. Ovarian cancer development and metastasis. 177**,** 1053-1064.

LI, P., SHAN, B., JIA, K., HU, F., XIAO, Y., ZHENG, J., GAO, Y.-T., WANG, H. & GAO, Y. J. B. C. 2020.

Plasma omega-3 polyunsaturated fatty acids and recurrence of endometrial cancer. 20**,** 1-11.

LI, X.-H., CHEN, X.-J., OU, W.-B., ZHANG, Q., LV, Z.-R., ZHAN, Y., MA, L., HUANG, T., YAN, Y.-B., ZHOU, H.-M. J. T. I. J. O. B. & BIOLOGY, C. 2013. Knockdown of creatine kinase B inhibits ovarian cancer progression by decreasing glycolysis. 45**,** 979-986.

LIAO, Z., TAN, Z. W., ZHU, P. & TAN, N. S. J. C. I. 2019. Cancer-associated fibroblasts in tumor microenvironment–Accomplices in tumor malignancy. 343**,** 103729.

LIM, J. P., LEUNG, B. P., DING, Y. Y., TAY, L., ISMAIL, N. H., YEO, A., YEW, S. & CHONG, M. S. J. C. I. I. A. 2015. Monocyte chemoattractant protein-1: a proinflammatory cytokine elevated in sarcopenic obesity. 10**,** 605.

LIU, M., STARENKI, D., SCHARER, C. D., SILVA-SANCHEZ, A., MOLINA, P. A., POLLOCK, J. S., COOPER, S. J., AREND, R. C., ROSENBERG, A. F. & RANDALL, T. D. J. C. I. R. 2022. Circulating Tregs Accumulate in Omental Tumors and Acquire Adipose-Resident Features. 10**,** 641-655.

LIU, X., COOPER, D. E., CLUNTUN, A. A., WARMOES, M. O., ZHAO, S., REID, M. A., LIU, J., LUND, P. J., LOPES, M. & GARCIA, B. A. J. C. 2018. Acetate production from glucose and coupling to mitochondrial metabolism in mammals. 175**,** 502-513. e13.

LUO, X., CHENG, C., TAN, Z., LI, N., TANG, M., YANG, L. & CAO, Y. J. M. C. 2017. Emerging roles of lipid metabolism in cancer metastasis. 16**,** 1-10.

MACPHERSON, R. E., GAMU, D., FRENDO-CUMBO, S., CASTELLANI, L., KWON, F., TUPLING, A. R. & WRIGHT, D. C. J. O. 2016. Sarcolipin knockout mice fed a high-fat diet exhibit altered indices of adipose tissue inflammation and remodeling. 24**,** 1499-1505.

MAEDA, H., KOBAYASHI, M. & SAKAMOTO, J. J. W. J. O. G. W. 2015. Evaluation and treatment of malignant ascites secondary to gastric cancer. 21**,** 10936.

MAK, T. W., GRUSDAT, M., DUNCAN, G. S., DOSTERT, C., NONNENMACHER, Y., COX, M., BINSFELD, C., HAO, Z., BRüSTLE, A. & ITSUMI, M. J. I. 2017. Glutathione primes T cell metabolism for inflammation. 46**,** 675-689.

MARCHAN, R., BüTTNER, B., LAMBERT, J., EDLUND, K., GLAESER, I., BLASZKEWICZ, M., LEONHARDT, G., MARIENHOFF, L., KASZTA, D. & ANFT, M. J. C. R. 2017. Glycerol-3-phosphate Acyltransferase 1 Promotes Tumor Cell Migration and Poor Survival in Ovarian CarcinomaGPAM Mediates Tumor Cell Migration. 77**,** 4589-4601.

MASSONNEAU, J., OUELLET, C., LUCIEN, F., DUBOIS, C. M., TYLER, J. & BOISSONNEAULT, G. J. F. O. B. 2018. Suboptimal extracellular pH values alter DNA damage response to induced double-strand breaks. 8**,** 416-425.

MATSUYAMA, S., LLOPIS, J., DEVERAUX, Q. L., TSIEN, R. Y. & REED, J. C. 2000. Changes in intramitochondrial and cytosolic pH: early events that modulate caspase activation during apoptosis. *Nat Cell Biol,* 2**,** 318-25.

MATTE, I., LANE, D., LAPLANTE, C., RANCOURT, C. & PICHé, A. J. A. J. O. C. R. 2012. Profiling of cytokines in human epithelial ovarian cancer ascites. 2**,** 566.

MAURER, G. D., BRUCKER, D. P., BäHR, O., HARTER, P. N., HATTINGEN, E., WALENTA, S., MUELLER-KLIESER, W., STEINBACH, J. P. & RIEGER, J. J. B. C. 2011. Differential utilization of ketone bodies by neurons and glioma cell lines: a rationale for ketogenic diet as experimental glioma therapy. 11**,** 1-17.

MEISER, J., SCHUSTER, A., PIETZKE, M., VANDE VOORDE, J., ATHINEOS, D., OIZEL, K., BURGOS-

BARRAGAN, G., WIT, N., DHAYADE, S. & MORTON, J. P. J. N. C. 2018. Increased formate overflow is a hallmark of oxidative cancer. 9**,** 1-12.

MENENDEZ, J. A. J. B. E. B. A.-M. & LIPIDS, C. B. O. 2010. Fine-tuning the lipogenic/lipolytic balance to optimize the metabolic requirements of cancer cell growth: molecular mechanisms and therapeutic perspectives. 1801**,** 381-391.

MEYER, K. A., NEELEY, C. K., BAKER, N. A., WASHABAUGH, A. R., FLESHER, C. G., NELSON, B. S., FRANKEL, T. L., LUMENG, C. N., LYSSIOTIS, C. A., WYNN, M. L. J. B. & REPORTS, B. 2016. Adipocytes promote pancreatic cancer cell proliferation via glutamine transfer. 7**,** 144-149.

MIERZIAK, J., BURGBERGER, M. & WOJTASIK, W. J. B. 2021. 3-hydroxybutyrate as a metabolite and a signal molecule regulating processes of living organisms. 11**,** 402.

MIKA, A., KOBIELA, J., PAKIET, A., CZUMAJ, A., SOKOŁOWSKA, E., MAKAREWICZ, W., CHMIELEWSKI, M., STEPNOWSKI, P., MARINO-GAMMAZZA, A. & SLEDZINSKI, T. J. S. R. 2020. Preferential uptake of polyunsaturated fatty acids by colorectal cancer cells. 10**,** 1-8.

MIKUŁA-PIETRASIK, J., URUSKI, P., TYKARSKI, A., KSIĄŻEK, K. J. C. & SCIENCES, M. L. 2018. The peritoneal "soil" for a cancerous "seed": a comprehensive review of the pathogenesis of intraperitoneal cancer metastases. 75**,** 509-525.

MOELLERING, R. E., BLACK, K. C., KRISHNAMURTY, C., BAGGETT, B. K., STAFFORD, P., RAIN, M., GATENBY, R. A., GILLIES, R. J. J. C. & METASTASIS, E. 2008. Acid treatment of melanoma cells selects for invasive phenotypes. 25**,** 411-425.

MONTCOURRIER, P., SILVER, I., FARNOUD, R., BIRD, I., ROCHEFORT, H. J. C. & METASTASIS, E. 1997. Breast cancer cells have a high capacity to acidify extracellular milieu by a dual mechanism. 15**,** 382-392.

MOONEY, S. M., RAJAGOPALAN, K., WILLIAMS, B. H., ZENG, Y., CHRISTUDASS, C. S., LI, Y., YIN, B., KULKARNI, P. & GETZENBERG, R. H. J. J. O. C. B. 2011. Creatine kinase brain overexpression protects colorectal cells from various metabolic and non-metabolic stresses. 112**,** 1066-1075.

MOREADITH, R., AND & LEHNINGER, A. J. J. O. B. C. 1984. The pathways of glutamate and glutamine oxidation by tumor cell mitochondria. Role of mitochondrial NAD (P)+-dependent malic enzyme. 259**,** 6215-6221.

MORIGNY, P., BOUCHER, J., ARNER, P. & LANGIN, D. J. N. R. E. 2021. Lipid and glucose metabolism in white adipocytes: pathways, dysfunction and therapeutics. 17**,** 276-295.

MORITA, T., NAGAKI, T., FUKUDA, I., OKUMURA, K. J. M. R. F. & MUTAGENESIS, M. M. O. 1992. Clastogenicity of low pH to various cultured mammalian cells. 268**,** 297-305.

NAGY, J. A., HERZBERG, K. T., DVORAK, J. M. & DVORAK, H. F. J. C. R. 1993. Pathogenesis of malignant ascites formation: initiating events that lead to fluid accumulation. 53**,** 2631-2643.

NEELAKANTAN, D., DOGRA, S., DEVAPATLA, B., JAIPRASART, P., MUKASHYAKA, M. C., JANKNECHT, R., DWIVEDI, S. K. D., BHATTACHARYA, R., HUSAIN, S. & DING, K. J. M. C. R. 2019. Multifunctional APJ pathway promotes ovarian cancer progression and metastasis. 17**,** 1378-1390.

NEURAUTER, G., SCHROCKSNADEL, K., SCHOLL-BURGI, S., SPERNER-UNTERWEGER, B., SCHUBERT, C., LEDOCHOWSKI, M. & FUCHS, D. J. C. D. M. 2008. Chronic immune

stimulation correlates with reduced phenylalanine turnover. 9**,** 622-627.

NICKLIN, P., BERGMAN, P., ZHANG, B., TRIANTAFELLOW, E., WANG, H., NYFELER, B., YANG, H., HILD, M., KUNG, C. & WILSON, C. J. C. 2009. Bidirectional transport of amino acids regulates mTOR and autophagy. 136**,** 521-534.

NIEMAN, K. M., KENNY, H. A., PENICKA, C. V., LADANYI, A., BUELL-GUTBROD, R., ZILLHARDT, M. R., ROMERO, I. L., CAREY, M. S., MILLS, G. B. & HOTAMISLIGIL, G. S. J. N. M. 2011. Adipocytes promote ovarian cancer metastasis and provide energy for rapid tumor growth. 17**,** 1498-1503.

NIETO, M. A., HUANG, R. Y.-J., JACKSON, R. A. & THIERY, J. P. J. C. 2016. EMT: 2016. 166**,** 21-45.

NING, Y.-X., LUO, X., XU, M., FENG, X. & WANG, J. J. O. 2017. Let-7d increases ovarian cancer cell sensitivity to a genistein analog by targeting c-Myc. 8**,** 74836.

ORIMO, A. & WEINBERG, R. A. J. C. C. 2006. Stromal fibroblasts in cancer: a novel tumor-promoting cell type. 5**,** 1597-1601.

PAKUŁA, M., MIKUŁA-PIETRASIK, J., WITUCKA, A., KOSTKA-JEZIORNY, K., URUSKI, P., MOSZYŃSKI, R., NAUMOWICZ, E., SAJDAK, S., TYKARSKI, A. & KSIĄŻEK, K. J. I. J. O. M. S. 2019. The epithelial-mesenchymal transition initiated by malignant ascites underlies the transmesothelial invasion of ovarian cancer cells. 20**,** 137.

PAPALAZAROU, V., ZHANG, T., PAUL, N. R., JUIN, A., CANTINI, M., MADDOCKS, O. D., SALMERON-SANCHEZ, M. & MACHESKY, L. M. J. N. M. 2020. The creatine–phosphagen system is mechanoresponsive in pancreatic adenocarcinoma and fuels invasion and metastasis. 2**,** 62-80.

PAPE, K. A., KHORUTS, A., MONDINO, A. & JENKINS, M. K. J. T. J. O. I. 1997. Inflammatory cytokines enhance the in vivo clonal expansion and differentiation of antigen-activated CD4+ T cells. 159**,** 591-598.

PARSONS, S. L., LANG, M. W. & STEELE, R. J. J. E. J. O. S. O. 1996. Malignant ascites: a 2-year review from a teaching hospital. 22**,** 237-239.

PERILLO, B., DI DONATO, M., PEZONE, A., DI ZAZZO, E., GIOVANNELLI, P., GALASSO, G., CASTORIA, G., MIGLIACCIO, A. J. E. & MEDICINE, M. 2020. ROS in cancer therapy: The bright side of the moon. 52**,** 192-203.

POUYSSéGUR, J., FRANCHI, A. & PAGèS, G. 2001. pHi, aerobic glycolysis and vascular endothelial growth factor in tumour growth. *Novartis Found Symp,* 240**,** 186-96; discussion 196-8.

RAU, B., BRANDL, A., PISO, P., PELZ, J., BUSCH, P., DEMTRöDER, C., SCHüLE, S., SCHLITT, H.-J., ROITMAN, M. & TEPEL, J. J. G. C. 2020. Peritoneal metastasis in gastric cancer: results from the German database. 23**,** 11-22.

RAY, A. & DITTEL, B. N. J. J. 2010a. Isolation of mouse peritoneal cavity cells. e1488.

RAY, A. & DITTEL, B. N. J. J. O. V. E. J. 2010b. Isolation of mouse peritoneal cavity cells.

REN, P., YUE, M., XIAO, D., XIU, R., GAN, L., LIU, H. & QING, G. J. T. J. O. P. 2015. ATF4 and N-Myc coordinate glutamine metabolism in MYCN - amplified neuroblastoma cells through ASCT2 activation. 235**,** 90-100.

RICH, I. N., WORTHINGTON-WHITE, D., GARDEN, O. A. & MUSK, P. 2000. Apoptosis of leukemic cells accompanies reduction in intracellular pH after targeted inhibition of the Na(+)/H(+) exchanger. *Blood,* 95**,** 1427-34.

RIIHIMäKI, M., HEMMINKI, A., SUNDQUIST, K., SUNDQUIST, J. & HEMMINKI, K. J. O. 2016. Metastatic spread in patients with gastric cancer. 7**,** 52307.

SAITO, Y. & SOGA, T. J. C. S. 2021. Amino acid transporters as emerging therapeutic targets in cancer. 112**,** 2958-2965.

SANGISETTY, S. L. & MINER, T. J. J. W. J. O. G. S. 2012. Malignant ascites: a review of prognostic factors, pathophysiology and therapeutic measures. 4**,** 87.

SCHUG, Z. T., PECK, B., JONES, D. T., ZHANG, Q., GROSSKURTH, S., ALAM, I. S., GOODWIN, L. M., SMETHURST, E., MASON, S. & BLYTH, K. J. C. C. 2015. Acetyl-CoA synthetase 2 promotes acetate utilization and maintains cancer cell growth under metabolic stress. 27**,** 57-71.

SHAO, H., MOHAMED, E. M., XU, G. G., WATERS, M., JING, K., MA, Y., ZHANG, Y., SPIEGEL, S., IDOWU, M. O. & FANG, X. J. O. 2016. Carnitine palmitoyltransferase 1A functions to repress FoxO transcription factors to allow cell cycle progression in ovarian cancer. 7**,** 3832.

SHENDER, V. O., PAVLYUKOV, M. S., ZIGANSHIN, R. H., ARAPIDI, G. P., KOVALCHUK, S. I., ANIKANOV, N. A., ALTUKHOV, I. A., ALEXEEV, D. G., BUTENKO, I. O., SHAVARDA, A. L. J. M. & PROTEOMICS, C. 2014. Proteome–metabolome profiling of ovarian cancer ascites reveals novel components involved in intercellular communication. 13**,** 3558-3571.

SIKALIDIS, A. K. J. P. & RESEARCH, O. 2015. Amino acids and immune response: a role for cysteine, glutamine, phenylalanine, tryptophan and arginine in T-cell function and cancer? 21**,** 9-17.

SILVA, A. S., YUNES, J. A., GILLIES, R. J. & GATENBY, R. A. J. C. R. 2009. The potential role of systemic buffers in reducing intratumoral extracellular pH and acid-mediated invasion. 69**,** 2677-2684.

SIMPSON, C. D., ANYIWE, K. & SCHIMMER, A. D. 2008. Anoikis resistance and tumor metastasis. *Cancer Lett,* 272**,** 177-85.

SLUITER, N., DE CUBA, E., KWAKMAN, R., KAZEMIER, G., MEIJER, G. & TE VELDE, E. A. 2016. Adhesion molecules in peritoneal dissemination: function, prognostic relevance and therapeutic options. *Clin Exp Metastasis,* 33**,** 401-16.

STEINERT, R., HANTSCHICK, M., VIETH, M., GASTINGER, I., KüHNEL, F., LIPPERT, H. & REYMOND, M. A. J. A. O. S. 2008. Influence of subclinical tumor spreading on survival after curative surgery for colorectal cancer. 143**,** 122-128.

STOCK, C. & PEDERSEN, S. F. Roles of pH and the Na+/H+ exchanger NHE1 in cancer: From cell biology and animal models to an emerging translational perspective? Seminars in cancer biology, 2017. Elsevier, 5-16.

STRASSER, B., SPERNER-UNTERWEGER, B., FUCHS, D., GOSTNER, J. M. J. I.-A. D. E., MECHANISMS & IMPLICATIONS 2016. Mechanisms of inflammation-associated depression: immune influences on tryptophan and phenylalanine metabolisms. 95-115.

STüWE, L., MüLLER, M., FABIAN, A., WANING, J., MALLY, S., NOëL, J., SCHWAB, A. & STOCK, C. J. T. J. O. P. 2007. pH dependence of melanoma cell migration: protons extruded by NHE1 dominate protons of the bulk solution. 585**,** 351-360.

TANG, B., ZHANG, L., YU, J., PENG, M., CHENG, Y., HU, D., LIU, Y., GUO, Y. & ZHOU, H. 2021. SLC7A5 Promotes Colorectal Cancer Progression by Regulating Cell Cycle and Migration.

THEWS, O., GASSNER, B., KELLEHER, D. K., SCHWERDT, G. & GEKLE, M. 2006. Impact of extracellular acidity on the activity of P-glycoprotein and the cytotoxicity of chemotherapeutic drugs. *Neoplasia,* 8**,** 143-52.

THIBAULT, B., CASTELLS, M., DELORD, J.-P., COUDERC, B. J. C. & REVIEWS, M. 2014. Ovarian cancer microenvironment: implications for cancer dissemination and chemoresistance

acquisition. 33**,** 17-39.
TIAN, W., LEI, N., ZHOU, J., CHEN, M., GUO, R., QIN, B., LI, Y., CHANG, L. J. C. D. & DISEASE 2022. Extracellular vesicles in ovarian cancer chemoresistance, metastasis, and immune evasion. 13**,** 64.
URUSKI, P., MIKUŁA-PIETRASIK, J., PAKUŁA, M., BUDKIEWICZ, S., DRZEWIECKI, M., GAIDAY, A. N., WIERZOWIECKA, M., NAUMOWICZ, E., MOSZYŃSKI, R. & TYKARSKI, A. J. I. J. O. M. S. 2021. Malignant ascites promote adhesion of ovarian cancer cells to peritoneal mesothelium and fibroblasts. 22**,** 4222.
VALVONA, C. J., FILLMORE, H. L., NUNN, P. B. & PILKINGTON, G. J. J. B. P. 2016. The regulation and function of lactate dehydrogenase a: therapeutic potential in brain tumor. 26**,** 3-17.
VAN BAAL, J. O., VAN NOORDEN, C. J., NIEUWLAND, R., VAN DE VIJVER, K. K., STURK, A., VAN DRIEL, W. J., KENTER, G. G., LOK, C. A. J. J. O. H. & CYTOCHEMISTRY 2018. Development of peritoneal carcinomatosis in epithelial ovarian cancer: a review. 66**,** 67-83.
VANDER HEIDEN, M. G., CANTLEY, L. C. & THOMPSON, C. B. J. S. 2009. Understanding the Warburg effect: the metabolic requirements of cell proliferation. 324**,** 1029-1033.
VON STRANDMANN, E. P., REINARTZ, S., WAGER, U. & MüLLER, R. J. T. I. C. 2017. Tumor–host cell interactions in ovarian cancer: pathways to therapy failure. 3**,** 137-148.
WARBURG, O., WIND, F. & NEGELEIN, E. 1927a. THE METABOLISM OF TUMORS IN THE BODY. *J Gen Physiol,* 8**,** 519-30.
WARBURG, O., WIND, F. & NEGELEIN, E. J. T. J. O. G. P. 1927b. The metabolism of tumors in the body. 8**,** 519.
WEBB, B. A., CHIMENTI, M., JACOBSON, M. P. & BARBER, D. L. 2011. Dysregulated pH: a perfect storm for cancer progression. *Nat Rev Cancer,* 11**,** 671-7.
WELS, J., KAPLAN, R. N., RAFII, S., LYDEN, D. J. G. & DEVELOPMENT 2008. Migratory neighbors and distant invaders: tumor-associated niche cells. 22**,** 559-574.
WHEELER, M. L. & DEFRANCO, A. L. J. T. J. O. I. 2012. Prolonged production of reactive oxygen species in response to B cell receptor stimulation promotes B cell activation and proliferation. 189**,** 4405-4416.
WILSON, R. B., SOLASS, W., ARCHID, R., WEINREICH, F.-J., KöNIGSRAINER, A., REYMOND, M. A. J. P. & PERITONEUM 2019. Resistance to anoikis in transcoelomic shedding: The role of glycolytic enzymes. 4**,** 20190003.
WISE, D. R., DEBERARDINIS, R. J., MANCUSO, A., SAYED, N., ZHANG, X.-Y., PFEIFFER, H. K., NISSIM, I., DAIKHIN, E., YUDKOFF, M. & MCMAHON, S. B. J. P. O. T. N. A. O. S. 2008. Myc regulates a transcriptional program that stimulates mitochondrial glutaminolysis and leads to glutamine addiction. 105**,** 18782-18787.
WISE, D. R. & THOMPSON, C. B. J. T. I. B. S. 2010. Glutamine addiction: a new therapeutic target in cancer. 35**,** 427-433.
YANG, Q., BAE, G., NADIRADZE, G., CASTAGNA, A., BEREZHNOY, G., ZIZMARE, L., KULKARNI, A., SINGH, Y., WEINREICH, F. J. & KOMMOSS, S. J. J. O. T. M. 2022. Acidic ascites inhibits ovarian cancer cell proliferation and correlates with the metabolomic, lipidomic and inflammatory phenotype of human patients. 20**,** 1-19.
YAROSZ, E. L. & CHANG, C.-H. J. I. N. 2018. The role of reactive oxygen species in regulating T cell-mediated immunity and disease. 18.
YIGIT, R., MASSUGER, L. F., FIGDOR, C. G. & TORENSMA, R. J. G. O. 2010. Ovarian cancer creates

a suppressive microenvironment to escape immune elimination. 117**,** 366-372.
YONEMURA, Y., ENDOU, Y., SASAKI, T., HIRANO, M., MIZUMOTO, A., MATSUDA, T., TAKAO, N., ICHINOSE, M., MIURA, M. & LI, Y. J. E. J. O. S. O. 2010. Surgical treatment for peritoneal carcinomatosis from gastric cancer. 36**,** 1131-1138.
YOO, H.-C. & HAN, J.-M. J. C. 2022. Amino Acid Metabolism in Cancer Drug Resistance. 11**,** 140.
ZHOU, M., GUAN, W., WALKER, L. D., MEZENCEV, R., BENIGNO, B. B., GRAY, A., FERNáNDEZ, F. M., MCDONALD, J. F. J. C. E., BIOMARKERS & PREVENTION 2010. Rapid mass spectrometric metabolic profiling of blood sera detects ovarian cancer with high accuracy. 19**,** 2262-2271.

Own Contribution Statement

This work was performed in the Clinic for General, Visceral and Transplant Surgery (AVT) at the UKT under the direction of Prof. Dr. med. Alfred Königsreiner and under the supervision of Prof. Dr. med. Marc A. Reymond.

The study was designed together with:

- Prof. Marc Reymond, M.D., Ditector, National Center for Pleura and Peritoneum (NCPP), University Hospital Tübingen, Tübingen, Germany (supervisor of this thesis), and
- Christoph Trautwein, Ph.D., research group leader at the Department of Preclinical Imaging and Radiopharmacy, Werner Siemens Imaging Center, University Hospital Tübingen, Tübingen, Germany.

Sampling in the operating room was scheduled and performed by myself in close coordination and under the responsbility of Dr. Giorgi Nadiradze (Clinic for General, Visceral and Transplant Surgery) and Prof. Stefan Kommoss (Tübigen University's Women's Hospital), who collected the patient's informed consent.

All functional experiments were carried out by myself in the NCPP laboratories after thorough training and support from the head the laboratory, Dr. Jürgen Weinreich, Ph.D. The metabolomics measurements and analysis were performed at the Department of Preclinical Imaging and Radiopharmacy by Dr. Trautwein and the team of the Werner Siemens Imaging Center and I took part personally to these measurements.

The statistical evaluation was carried out independently by me following the instructions of Prof. Marc Reymond, M.D. and Dr. Trautwein, Ph.D.

Parts of this doctoral dissertation are published in: Yang Q, Bae G, Nadiradze G, Castagna A, Berezhnoy G, Zizmare L, Kulkarni A, Singh Y, Weinreich FJ, Kommoss S, Reymond MA, Trautwein C. Acidic ascites inhibits ovarian cancer cell proliferation and correlates with the metabolomic, lipidomic and inflammatory phenotype of human patients. J Transl Med. 2022 Dec 12;20(1):581. doi: 10.1186/s12967-022-03763-3. PMID: 36503580; PMCID: PMC9743551.

I certify that I wrote the manuscript myself using no others sources and aids than those specified by me. I did not use artificial intelligence tools such as Chat GPT for this redaction, with the exception of the ackowledgments.

Tübingen, Aug. 19th, 2023

_____

Qianlu Yang

Acknowledgments

I would like to express my sincere gratitude to Prof. Marc Reymond, my thesis director, for his invaluable guidance, unwavering support, and insightful feedback throughout the course of this research. His expertise and dedication have been instrumental in shaping the direction of this work. He has taught me more than just experimental research, but also many ways of thinking that have truly changed my understanding of medicine and life.

I am also indebted to Prof. Königsrainer, Dr. Weinreich, and Dr. Trautwein for their supervision; collaboration, enthusiasm, and shared commitment to advancing scientific knowledge. Their contributions have significantly enriched the quality of this work.

I am deeply appreciative of my husband, Jie Yan, for his constant encouragement, understanding, and patience during the demanding phases of this research journey. His steadfast belief in me has been a driving force behind my accomplishments.

I extend my heartfelt thanks to my parents and sister for their unconditional love, unending encouragement, and the sacrifices they have made to provide me with a solid foundation in education and life. Their unwavering support has been a cornerstone of my success.

Tis research would not have been possible without the collective efforts and support of these individuals and many others who have touched my life in meaningful ways in my home country, China, and during my privileged time in Europe. I am truly grateful for their presence in my journey.

Qianlu Yang